



National Library
of Canada

Bibliothèque nationale
du Canada

Canadian Theses Service Service des thèses canadiennes

Ottawa, Canada
K1A 0N4

NOTICE

The quality of this microform is heavily dependent upon the quality of the original thesis submitted for microfilming. Every effort has been made to ensure the highest quality of reproduction possible.

If pages are missing, contact the university which granted the degree.

Some pages may have indistinct print especially if the original pages were typed with a poor typewriter ribbon or if the university sent us an inferior photocopy.

Reproduction in full or in part of this microform is governed by the Canadian Copyright Act, R.S.C. 1970, c. C-30, and subsequent amendments.

AVIS

La qualité de cette microforme dépend grandement de la qualité de la thèse soumise au microfilmage. Nous avons tout fait pour assurer une qualité supérieure de reproduction.

S'il manque des pages, veuillez communiquer avec l'université qui a conféré le grade.

La qualité d'impression de certaines pages peut laisser à désirer, surtout si les pages originales ont été dactylographiées à l'aide d'un ruban usé ou si l'université nous a fait parvenir une photocopie de qualité inférieure.

La reproduction, même partielle, de cette microforme est soumise à la Loi canadienne sur le droit d'auteur, SRC 1970, c. C-30, et ses amendements subséquents.

THE UNIVERSITY OF ALBERTA

**ARENE AND HETEROARENE BRIDGED ORGANOIRON COMPLEXES:
MODEL COMPOUNDS FOR ORGANOMETALLIC POLYMERS.**

BY

ROXTON MONDAY CHUKWU

A THESIS

**SUBMITTED TO THE FACULTY OF GRADUATE STUDIES AND RESEARCH
IN PARTIAL FULFILLMENT OF THE REQUIREMENTS FOR THE DEGREE
OF MASTER OF SCIENCE**

DEPARTMENT OF CHEMISTRY

EDMONTON, ALBERTA

FALL, 1990



National Library
of Canada

Bibliothèque nationale
du Canada

Canadian Theses Service Service des thèses canadiennes

Ottawa, Canada
K1A 0N4

The author has granted an irrevocable non-exclusive licence allowing the National Library of Canada to reproduce, loan, distribute or sell copies of his/her thesis by any means and in any form or format, making this thesis available to interested persons.

The author retains ownership of the copyright in his/her thesis. Neither the thesis nor substantial extracts from it may be printed or otherwise reproduced without his/her permission.

L'auteur a accordé une licence irrévocable et non exclusive permettant à la Bibliothèque nationale du Canada de reproduire, prêter, distribuer ou vendre des copies de sa thèse de quelque manière et sous quelque forme que ce soit pour mettre des exemplaires de cette thèse à la disposition des personnes intéressées.

L'auteur conserve la propriété du droit d'auteur qui protège sa thèse. Ni la thèse ni des extraits substantiels de celle-ci ne doivent être imprimés ou autrement reproduits sans son autorisation.

ISBN 0-315-65094-X

THE UNIVERSITY OF ALBERTA

RELEASE FORM

NAME OF AUTHOR: ROXTON MONDAY CHUKWU
TITLE OF THESIS: ARENE AND HETEROARENE BRIDGED
ORGANOIRON COMPLEXES: MODEL
COMPOUNDS FOR ORGANOMETALLIC
POLYMERS.
DEGREE : MASTER OF SCIENCE
YEAR THIS DEGREE GRANTED: 1990

PERMISSION IS HEREBY GRANTED TO THE UNIVERSITY OF ALBERTA LIBRARY TO REPRODUCE SINGLE COPIES OF THIS THESIS AND TO LEND OR SELL SUCH COPIES FOR PRIVATE, SCHOLARLY OR SCIENTIFIC RESEARCH PURPOSES ONLY.

THE AUTHOR RESERVES OTHER PUBLICATION RIGHTS, AND NEITHER THE THESIS NOR EXTENSIVE EXTRACTS FROM IT MAY BE PRINTED OR OTHERWISE REPRODUCED WITHOUT THE AUTHOR'S WRITTEN PERMISSION.

Date: *Oct. 12th* '90

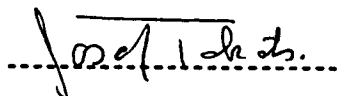
THE UNIVERSITY OF ALBERTA

FACULTY OF GRADUATE STUDIES AND RESEARCH

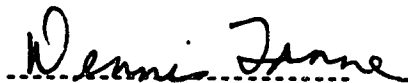
THE UNDERSIGNED CERTIFY THAT THEY HAVE READ, AND RECOMMEND TO THE FACULTY OF GRADUATE STUDIES AND RESEARCH FOR ACCEPTANCE, A THESIS ENTITLED ARENE AND HETEROARENE BRIDGED ORGANOIRON COMPLEXES: MODEL COMPOUNDS FOR ORGANOMETALLIC POLYMERS SUBMITTED BY ROXTON MONDAY CHUKWU IN PARTIAL FULFILLMENT OF THE REQUIREMENTS FOR THE DEGREE OF MASTER OF SCIENCE



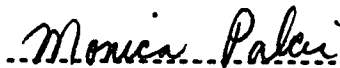
Allen D. Hunter.



Josef Takats.



Dennis D. Tanner.



Monica Palcic.

DATE: Oct. 12th '90

Dedicated to Maduabuchi

Abstract

The syntheses and characterization of a series of organometallic complexes wherein the organometallic fragment $(\eta^5\text{-Cp})\text{Fe}(\text{CO})_2$ (i.e. Fp) is σ -bonded to a ring carbon of an arene or heteroarene group is described.

Thus, various complexes containing pyridine, pyrimidine, pyrazine, pyridazine and quinoxaline, as either terminal or bridging ligands, including a sterically crowded quinoxaline complex have been synthesized *via* nucleophilic displacement of a halide group, bonded to the heteroarene, by the Fp⁻ nucleophile. The ease of displacement of the halide increased in the order Br < Cl < F. Likewise, the ease of substitution increased with number of aza (N) groups in the arene ring. Attempts to synthesize related phthalazine complexes (*via* the above route) and related furan and thiophene complexes *via* metathesis between a Fp-halide (i.e. FpCl or FpI) and metallated (Li or K) substrates yielded unstable products. The syntheses of Fp-C₆H₅ *via* thermal decarbonylation of the acyl precursor, and various fluorophenyl complexes including 1,3-C₆F₄Fp₂ and 1,4-C₆F₄Fp₂ *via* either metathesis or nucleophilic displacement was also achieved.

Results from spectroscopic characterization of the complexes indicate very strong electronic interaction between the Fp fragment and the arene/heteroarene ring. Evidence from electrochemical (cyclic voltammetric) oxidation studies shows that the stability of the complexes upon oxidation is greatly dependent upon the electronic properties of the arene/heteroarene ligands. Thus, increasing the number of electron withdrawing groups on the arene ring as well as substitution of a CH group with an N atom, not only results in an increase in the oxidation potential, but

also in the degree of reversibility of the oxidation process. Similarly, the extent of metal-metal interaction is shown to be directly related to substitution geometry. Thus the wave to wave separations of the two single-electron oxidation waves for the two geometric isomers were $\Delta E_{1/2} = 200\text{mV}$ for 1,3-C₆F₄Fp₂ and 280mV for the 1,4-isomer. This is evidence for a strong π interaction between the the metal centers in these species.

Structural studies on representative complexes suggest that the orientations of the arene/heteroarene rings towards the Fp groups differ from the orientation modes predicted by molecular orbital theory.

ACKNOWLEDGEMENTS

I wish to acknowledge my research supervisor Dr. Allen D. Hunter for his intellectual, financial and moral support throughout my program.

I am also grateful to Dr. George B. Richter-Addo, who patiently introduced myself and others in our research group to the technique of cyclic voltammetry, and to the members of the Hunter research group including Dusan Ristic-Petrovic, Vivian Mozol, Lonni Shilliday, Jin Li, Stan Cai, Xiuguang Guo and Michael Mikoluk for providing an exciting research atmosphere, and for refereeing this thesis.

The contributions of some staff of the Chemistry department including Dr. Tom Nakashima and the NMR staff, Darlene Mahlow and Andrea Dunn of the analytical determinations lab., Jackie Jorgenson, and Dr. B. D. Santasiero who carried out the structural determinations are gratefully acknowledged.

The Financial support of the university of Alberta is also highly appreciated.

Finally, I wish to thank members of my family and friends both here and overseas and the almighty God for encouragement and spiritual support.

Table of Contents

Abstract.	v
Acknowledgements.	vii
List of Tables.	x
List of Figures.	xi
List of Abbreviations.	xiii
Chapter one - Introduction.	
Organic Model Compounds and Polymers Containing Delocalized Backbones: Forerunners to Organometallic Polymers.	1
Inorganic and Organometallic Polymers and Model Compounds Containing Delocalized π -Systems.	3
References.	11
Chapter Two - Novel Organometallic Complexes Containing Aromatic Azines: Synthesis and X-Ray Crystal Structure of 4,6-bis$\{(\eta^5\text{-Cyclopentadienyl})\text{IronDicarbonyl}\}$ 2-(Methylthio)Pyrimidine.	
Introduction.	13
Experimental Section.	15
Results and Discussion.	26
References.	55
Chapter Three - Electrochemical and Spectroscopic Studies of Phenyl and Pyridyl Complexes of Iron and X-Ray Crystal Structure of $\{(\eta^5\text{-Cyclopentadienyl})\text{IronDicarbonyl}\}$ PentafluoroPhenyl.	

Introduction.	60
Experimental Section.	65
Results and Discussion.	73
References.	103
Chapter Four - (η^5-Cyclopentadienyl)IronDicarbonyl Containing Terminal and Bridging Fused Heterocyclic Ligands: Synthesis and X-Ray Crystal Structure of 2-(η^5-Cyclopentadienyl)IronDicarbonyl}-3-Chloro Quinoxaline.	
Introduction.	107
Experimental Section.	110
Characterization of the Complexes.	116
References.	143
Chapter Five - General Discussion and Projections.	146
References.	150

Figure 4.1	ORTEP plot of compound ICl.	123
Figure 4.2	ORTEP plot of compound ICl view down Fe-C3.	124
Figure 4.3	ORTEP plot of compound ICl showing twist in quinoxaline ring.	125
Figure 4.4	IR (ν_{CO}) spectra of compounds ICl and 2.	131
Figure 4.5	1H NMR spectrum of compound ICl showing the quinoxaline region.	133
Figure 4.6	1H NMR spectrum of compound 2 showing C_5H_5 and quinoxaline protons.	136
Figure 4.7	(a) 1H NMR spectrum of compound 2 showing the quinoxaline region (b) irradiating the signal at 7.8 signal at 7.8 ppm.	137
Figure 4.8	^{13}C NMR spectrum of compound 2.	138
Figure 4.9	Cyclic voltammograms of compound 2 showing (a) first oxidation wave.(b) higher scan potentials.	140

List of Abbreviations

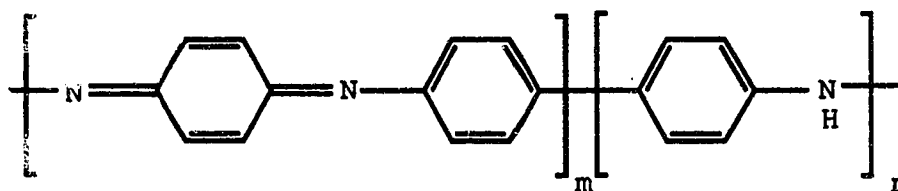
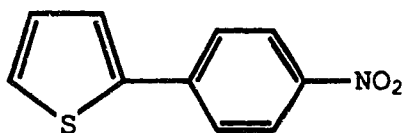
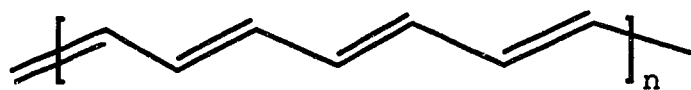
Cp	- η^5 -cyclopentadienyl, η^5 -C ₅ H ₅
Cp [#]	- η^5 -pentamethylcyclopentadienyl
Fp	-(η^5 -cyclopentadienyl)Iron dicarbonyl, (η^5 -C ₅ H ₅)Fe(CO) ₂
Et ₂ O	-diethyl ether
THF	-tetrahydrofuran
HMPA	-hexamethylphosphoramide
TMEDA	-tetramethylethylenediamine
bpy	-1,10-bipyridine
IR	-infrared
NMR	-nuclear magnetic resonance
MS	-mass spectrometry
m/z	-mass to charge ratio in the mass spectrum
P ⁺	-molecular ion (in the mass spectrum)
CV	-cyclic voltammetry
SCE	-saturated calomel electrode
V	-Volts
SET	-single electron transfer.
I	-inductive effect.
Bu	-butyl
s	-strong (IR signal), singlet (NMR signal)
w	-weak (IR signal)
sh	-shoulder (IR signal)
d	-doublet (NMR signal)
m	-multiplet (NMR signal)

CHAPTER ONE

GENERAL INTRODUCTION

Organic model compounds and polymers containing delocalized backbones: Forerunners to organometallic polymers.

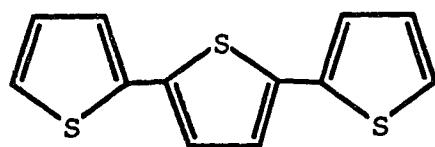
Organic polymers and oligomers whose backbones contain delocalized π -systems have been of increasing interest during the last decade. Examples of such delocalized π -systems include polyacetylene and materials containing aromatic rings, such as, 2-thienyl-*p*-nitrophenyl and poly(*p*-phenyleneamineimine), as illustrated below;



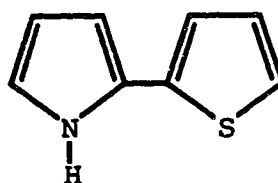
The π -electron delocalization in such species imparts several useful properties, such as, electrical conductivity and non-linear optical behaviour

on these materials.¹ Such delocalized repeating units are increasingly being used as bridging ligands in organometallic complexes, the results of which are novel oligomers and polymers. These materials, whose structures can be thought of as extensions of those of the organic compounds, have been receiving considerable attention as a result of their potentially advantageous properties. Indeed it has been noted² that with the exception of a few instances, introduction of a metal group into an organic polymer (in any of the forms mentioned in the next section) results in an enhanced conductivity. This may arise from an additional conduction route which the metal provides by virtue of its own electronic properties.

A thorough understanding of the electronic properties of well-defined and more easily processable lower molecular weight species (oligomers) of these organic materials often provides the basis for determining such structural properties as conjugation length of the more complex polymeric species. Most importantly, such studies provide a key to the development of a microscopic understanding of the electron transport properties of these materials. Recently reported examples of these studies include; a study of the lowest energy singlet excited states of terthiophene and thienylpyrrole (see structures below) for a better understanding of the optical and vibrational spectra of polythiophene and polythienylpyrrole respectively,^{1a} and the use of the redox properties (studied *via* cyclic voltammetry) of oligomeric *p*-phenylenes to predict the charge storage mechanism of conducting poly *p*-phenylenes.^{1c}



Terthiophene

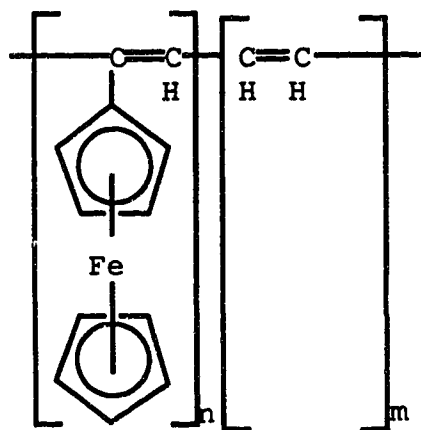


Thiénylpyrrole

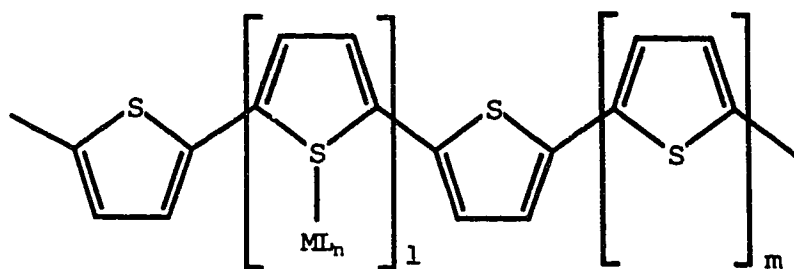
Gratifyingly, results from such studies often show qualitative correlations between the electronic behaviour of these model compounds and their higher molecular weight analogues.

Inorganic and organometallic polymers and model compounds containing delocalized π -systems.

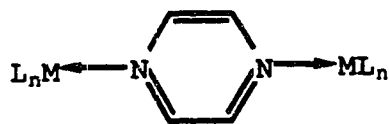
A novel and growing area of organotransition metal chemistry is the study of organometallic polymers. Earlier materials going by this nomenclature were generally comprised of organic polymer backbones, with the organometallic fragments incorporated as appendages as illustrated below.



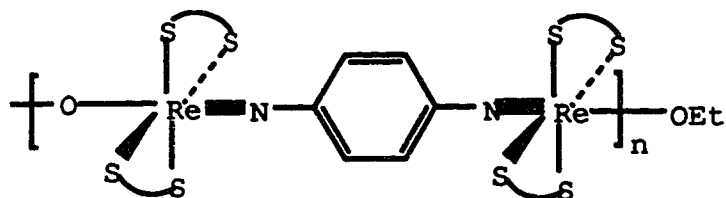
Interest in materials of this nature originally stemmed from the desire to use such species as catalysts.^{3,4} More recently, the magnetic and electrical properties of such species have become of interest.⁵ In these species, the organometallic fragment can be regarded as a dopant (acting as an electron donor or acceptor), thus serving as a charge storage centre during charging and discharging of the particular repeat unit. An example of such a system is illustrated below.⁵



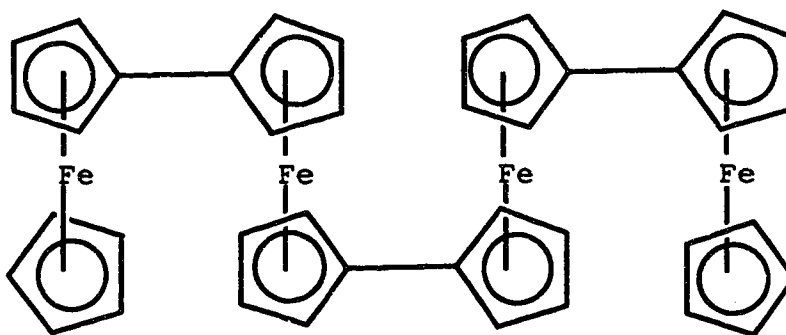
Polymers and model compounds in which the metal centre is contained in the main polymer chain backbone are relatively few. Most materials in this category contain bifunctional bridging ligands such as the N-heterocycles and the *p*-phenylenediimido functionality.⁶ Often, in such species the metal centres are bonded to the ligands through heteroatoms (e.g. N, O, S, etc.) hence such species can be regarded as coordination compounds. More recently, several examples of lower molecular weight species in which the ligands bonded to the metal centre are traditional organometallic ligands such as carbon monoxide and cyclopentadienyl group have been reported.⁶ Illustrative examples of compounds in these categories are shown below.



$ML_n = Ru(NH_3)_5^{2+}, Fe(CN)_5^{2-}, W(CO)_5, Cp(CO)_2Mn, \text{ etc.}$



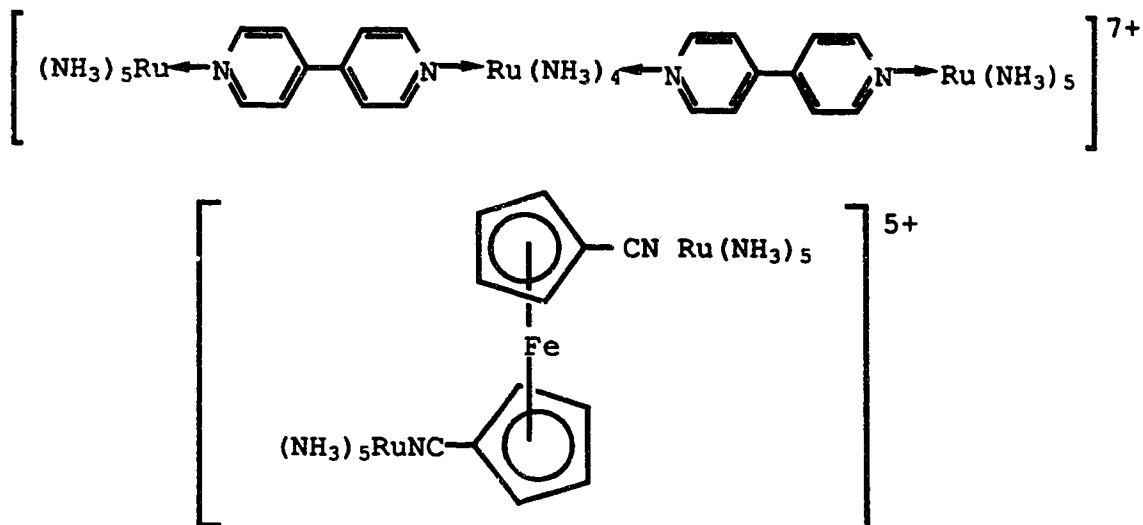
Another class of coordination polymers and model compounds in which the metal forms part of the main chain backbone are the metallocenyl complexes, an example of which is shown below.⁷



Results from electrochemical as well as spectroscopic studies on these last two

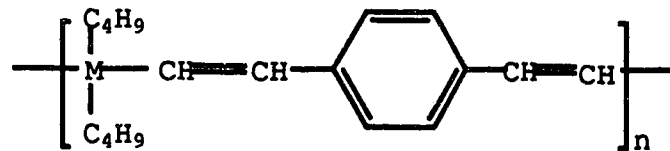
classes of compounds indicate that a reasonable correlation exists between the electron transfer behaviours of the model compounds and the higher molecular weight species. Both classes of materials have been shown to exhibit reasonable bulk electrical conductivities, especially when doped. A particularly well studied aspect of the low molecular weight materials in

these classes is their intervalence charge transfer properties involving the mixed valence species.⁸



Such species can be considered as prototype fragments of semiconductors, with two equivalent electron localization sites at the ends, and a third central localization site which could either be a ligand or another metal centre.

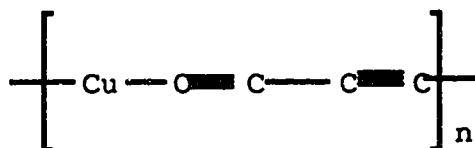
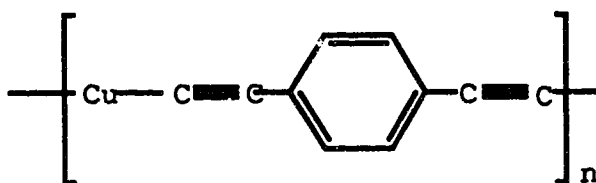
Polymers and oligomers in which the metals in the polymer backbone are linked to the chain carbon atoms through σ -bonds are few, even for the main group-metals.²



M = Sn, Ge, Si.

The introduction of such elements into the chain does not destroy the conjugative path because these elements contain d-orbitals which can act as

π -acceptors, thus leading to π - $d\pi$ overlap. Unfortunately, these materials are very poor conductors.² The first examples of transition-metal organometallic polymers containing such linkages were reported by Korshak and co-workers in 1960.² These polymers contain acetylide and phenylacetylide bridging ligands.

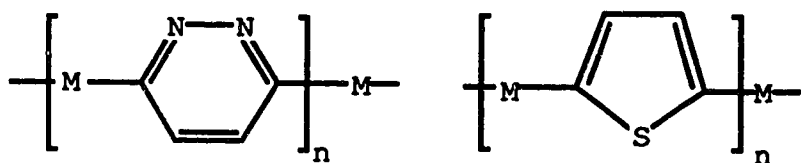


Conductivity as well as ESR studies on these polymers show² that they are semiconducting and photoconducting, and that there is a high degree of delocalization in the conjugated chain. Furthermore, the metal group has also been shown to act as an electron donor. More recently, other workers^{4,9} have extended this work to the syntheses and characterization of Ni, Pd and Pt containing species, with the same class of bridging ligands but with ligands of the type PR_3 completing the coordination sphere of the metal centre.

The central theme of the work underway in the Hunter group involves the syntheses and characterization of model compounds and polymers containing transition-metal-(arene)carbon σ -bonds. In this regard, the systematic synthesis and characterization of a variety of phenylene bridged

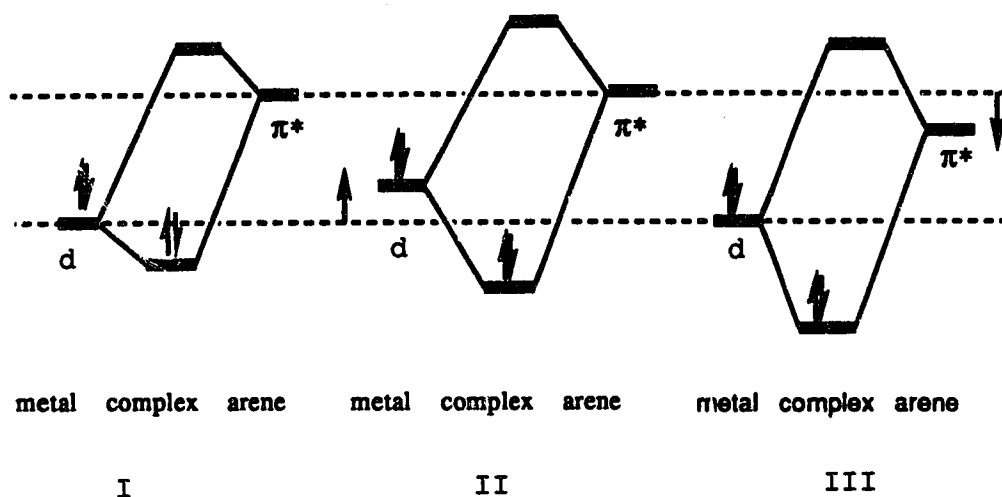
organometallic model complexes have been reported.¹⁰ As mentioned earlier, work on related organic and organometallic materials has naturally tended to be preceded by studies on lower molecular weight species since these are more readily studied, yet they can serve as excellent model compounds for the target higher molecular weight analogues. Moreover, some examples of such low molecular weight materials have been shown to exhibit unique properties which often lead to their being directly applied as semiconductors, liquid crystalline materials, etc. The electron transfer behaviour of these and other materials mentioned are increasingly being studied *via* cyclic voltammetry in addition to the more generally employed spectroscopic techniques.

Several organic polymers and oligomers containing heteroaromatic rings either as part of the polymer backbone, (e.g. polypyrrole, polythiophene) or as substituents are known to exhibit useful properties as earlier mentioned. As an extension of the study of model organometallic complexes in which the metal centre is directly attached to the ring carbon, the use of heteroaromatic compounds as bridging ligands seems a logical progression from the earlier work from our group.



Since the primary focus in the study of such materials is on the electron transfer between the electroactive centres, variation of the nature and type of the metal centres as well as variation of the bridging ligands is important.

Such systematic variation will ensure that one utilizes fragments which have proper orbital energy and symmetry match, thus leading to maximal interaction between the frontier orbitals of the metal and bridging ligand fragments (the highest occupied molecular orbitals (HOMO) and the lowest unoccupied molecular orbitals (LUMO), respectively). A simplified diagram of such orbital interactions is represented below.



It is evident from the above illustration that better interaction between the metal centre and the arene, and consequently between any two metal centres bonded to the arene, can be achieved by either destabilizing the metal centered HOMO, (e.g. by increasing the electron density around the metal centre) or by stabilizing the LUMO of the bridging ligand, (e.g. by switching to electron poor bridging ligands). The formal introduction of a heteroatom to a benzene ring is known to have substantial effects on the spectro-electronic properties of the arene ring.¹¹ Such heteroaromatic compounds are thus worthy of study as bridging ligands in the materials of interest. Moreover, such complexes might also be useful in bioinorganic

chemistry since such transition metal substituted complexes might mimic the organic molecules often encountered in living systems.

This thesis is an extension of work reported¹⁰ from our group on model compounds containing arene bridging ligands. The syntheses and characterization of both new arene and heteroarene bridged and terminally bonded complexes of iron are reported.

REFERENCES

1. See for example (a) Kuzmany, H.; Mehring, M.; Roth, S. *Electronic Properties of Conjugated Polymers III*, Springer-Verlag: Heidelberg; 1989. (b) Prasad, P.N.; Ulrich, D.R. *Non-linear Optical and Electroactive Polymers*, Plenum: New York; 1988. (c) Kuzmany, H.; Mehring, M.; Roth, S. *Electronic Properties of Conjugated Polymers*, Springer-Verlag: Heidelberg; 1987.
- 2 Keaton, J.E. *Organic Semiconducting Polymers*, Marcel Dekker: New York; 1968, p240-.
- 3 Paushkin, Y.M; Vishnykova, A.P.; Lunmin, A.F.; Nizova, S.A. *Organic Polymeric Semiconductors*, John Willey: Chichester; 1974, p173.
- 4 (a) Takahashi, S.; Kariya, M.; Yatake, T.; Kataoka, S. Sonogashira, K.; Hagihara, N. *J. Polym. Chem.* 1982, 20, 565. (b) Sonogashira, K.; Kataoka, S.; Takahashi, S.; Hagihara, N. *J. Organomet. Chem.* 1978, 319, 160. (c) Takahashi, S.; Ohyama, Y.; Murata, E.; Sonogashira, K.; Hagihara, N. *J. Polym. Sci.: Polym. Chem.* 1980, 18, 349. (d) Takahashi, S.; Murata, E.; Sonogashira, K.; Hagihara, N. *J. Polym. Sci.: Polym. Chem.* 1980, 18, 349. (e) Takahashi, S.; Morimoto, H.; Murata, E.; Kataoka, S.; Sonogashira, K.; Hagihara, N. *J. Polym. Sci.: Polym. Chem.* 1982, 20, 565.
- 5 For a recent study on such species, see Shaver, A.; Butler, I.S.; Cao, J.P. *Organometallics* 1989, 8, 2079.
- 6 For representative examples of such materials see (a) Kibel, W.; Hannack, M. *Inorg. Chem.* 1986, 25, 103. (b) Collman, J.P.; McDevitt, J.T.; Liedner, C.R.; Yee, G.T.; Torrance J.B.; Little, W.A. *J. Am.*

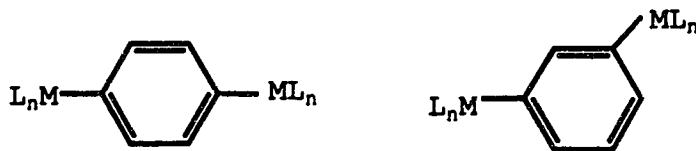
-
- Chem. Soc.* 1987, 109, 4606. (c) Gross, R.; Kaim, W. *Inorg. Chem.* 1986, 25, 498. (d) Woitellier, S.; Launay, J.P.; Spangler, C.W. *Inorg. Chem.* 1989, 28, 758. (e) Zulu, M.M.; Lees, A.J. *Organometallics* 1989, 8, 955. (f) Bruns, W.; Kiam, W. *J. Organomet. Chem.* 1990, 390, c45.
- 7 Gieger, W.E.; Connelly, N.G. *Adv. Organomet. Chem.* 1985, 24, 87.
- 8 Carter, F.L. *Molecular Electronic Devices II*, 2nd ed.; Marcel Dekker: New York; 1987.
- 9 (a) Amer, A.; Zimmer, H, Mulligan, K.J.; Mark, H.B *J. Polym. Sci.: Polym. Lett.* 1984, 22, 77. (b) Guenther, M.D.; Bezoari, M.D.; Kovacic, P. *J. Polym. Sci.: Polym. Lett.* 1984, 22, 65. (c) Ogawa, H.; Joh T.; Takahashi, S.; Sonogashira, K. *J. Chem. Soc. Chem. Commun.* 1985, 1220. (d) Ogawa, H.; Onitsuka, K.; Joh, T.; Takahashi, S.; Yamamoto, Y.; Yamazaki, H. *Organometallics* 1988, 7 2257.
- 10 (a) Richter-Addo, G.B.; Hunter, A.D. *Inorg. Chem.* 1989, 28, 4063, (b) Hunter A.D. *Organometallics* 1989, 8, 1118. (c) Hunter, A.D.; Szigety, A.B. *Organometallics* 1989, 8, 2670. (d) Hunter, A.D.; McLernon, J.C. *Organometallics* 1989, 8, 2679. (e) Richter-Addo, G.B.; Hunter, A.D.; Wichrowska, N. *Can. J. Chem.* 1990, 68, 41.
- 11 Schofield, H. *Heteroaromatic Nitrogen Compounds, Pyrroles and Pyridines*, ButerWorth: Norwich; 1967.

CHAPTER 2

NOVEL ORGANOMETALLIC COMPLEXES CONTAINING AROMATIC AZINES: SYNTHESIS AND X-RAY CRYSTAL STRUCTURE OF 4,6-bis{(η^5 - CYCLOPENTADIENYL)IRONDICARBONYL}-2-(METHYLTHIO)PYRIMIDINE¹

INTRODUCTION

Work in our laboratories has recently been directed towards the investigation of the nature and degree of the long range indirect metal-metal interaction in complexes in which two or more metal centres are bridged by arene rings.¹⁻² In these species both metals are directly σ -bonded to the arene-carbon, generally in either a 1,3 or 1,4 fashion, as shown below.



Other workers have reported related studies in which the phenylene bridges in these complexes are replaced by phenylacetelide^{3a} or phenylenediimido

groups^{3b} or by heteroaromatic ring(s)⁴ (e.g., pyrazine, 4,4' bipyridine, etc.) but with the metals bonded to the ring nitrogen atoms by formal nitrogen to metal dative bonds, e.g.,⁴



With the exception of substituted pyridyl complexes,⁵ comparatively few examples in which a metal fragment is σ -bonded to the ring carbon atom of a heterocyclic ligand have been reported.⁶ Still fewer bimetallic complexes with the σ -bonding mode have been reported.^{5f,7}

In the work reported in this thesis, these studies have been extended to the synthesis of novel complexes in which one or two organometallic fragments are bonded to the carbon atom(s) of a heteroarene ligand. In particular, a representative series of mono- and di-substituted azine derivatives have been prepared to investigate the effects of the energetics and/or geometric properties of these bridging ligands on the electronic behaviour of these model compounds. Since organic heterocyclic polymers are well known for their useful applications in materials science,⁸ it is expected that introducing organometallic centres to alternate with the heterocyclic rings will introduce new and interesting properties to these systems. Moreover, the heteroatoms can act as further coordination sites for new complexes which will further vary the properties of the polymers.⁹

In this chapter, the synthetic studies of various iron based model compounds and an X-ray crystallographic study of a representative example are reported.

EXPERIMENTAL SECTION

Unless otherwise noted, all reactions were carried out under anaerobic and anhydrous conditions using prepurified Ar or N₂ and conventional Schlenk techniques.¹⁰ Reagents were purchased from commercial suppliers or prepared according to standard procedures. Chemicals used were purified before use. Solvents were dried and deaerated by standard procedures and stored under N₂ or Ar.^{10,11} Thus, CH₂Cl₂ and Bu₂O were distilled from P₂O₅ and CaH₂ respectively, while THF, Et₂O, toluene and hexanes were distilled from sodium benzophenone ketal under an inert atmosphere¹² in all cases.

Infrared spectra were recorded on a PYE Unicam PU9522 infrared spectrometer and were calibrated with the 1601 cm⁻¹ band of polystyrene. Nuclear magnetic resonance spectra were recorded on Bruker WH-200, 300 or 400 spectrometers with reference to the deuterium signal of the solvent ((CD₃)₂SO) employed. The ¹H and ¹³C chemical shifts are reported in parts per million (ppm) downfield from external Me₄Si, ¹⁹F chemical shifts are reported in parts per million (ppm) downfield from external CFCl₃. Low resolution mass spectra were recorded at 16 or 70 eV on an AEI MS50 spectrometer at probe temperatures of 150-280°C, and assignments involving the most abundant naturally occurring isotopes. Positive ion fast atom bombardment mass spectra (FAB-MS) were recorded using Xe fast atoms on a customized¹³ AEI mass spectrometer. Data for nuclear magnetic resonance, mass spectra as well as elemental analysis were collected with the assistance of staff of the chemistry department.^{2c} The X-ray crystallographic study was carried out by Dr. B.D. Santarsiero of the chemistry department.

The analytical, mass spectral, infrared and nuclear magnetic resonance data for the complexes synthesized in this work are collected in Tables 2.1 and 2.2. The structural formulae of the compounds are shown in Figure 1.1. Synthetic procedures and non-optimized yields are summarized below.

CAUTION! MERCURY IS A VERY POISONOUS MATERIAL AND SHOULD BE HANDLED WITH EXTREME CARE.

Reactions of NaFp with chlorinated diazines A-H where Fp = $(\eta^5\text{-C}_5\text{H}_5)\text{Fe}(\text{CO})_2$ and the diazines are: A, 2,4-dichloropyrimidines; B, 4,6-dichloropyrimidine; C, 2,4-dichloro-6-methylpyrimidine; D, 2,4,6-trichloropyrimidine; E, 4,6-dichloro-2-methylthiopyrimidine; F, 2,4,5,6-tetrachloropyrimidine; G, 2,6-dichloropyrazine; H, 3,6-dichloropyridazine; 1,2,4,5-trichloropyridazine.

The purification procedures involving 2:1 mole ratio of nucleophile to substrate (i.e., Fp⁻ to haloazine) are slightly different from those involving a 1:1 mole ratio of reactants and are described separately.

(A) Reactions involving 1:1 reactant ratios.

The procedure for all of these reactions are similar, that of 2,4-dichloropyrimidine being described in detail as a representative example.

An excess of solid sodium amalgam¹⁴ (25.00 g, 25.0 mmol Na) was placed in a 200 mL three-neck flask equipped with a side arm and the flask was thoroughly flushed with N₂. The amalgam was liquified by addition of a few drops of mercury¹⁴ and then THF (75 mL) and Fp₂^{2a} (2.45 g, 6.7 mmol, where Fp₂ = $[(\eta^5\text{-C}_5\text{H}_5)\text{Fe}(\text{CO})_2]_2$) were added. The resultant dark red solution was stirred vigorously for 45 min to produce an orange solution containing

NaFp.¹⁵ Excess amalgam was drained through a side arm¹⁵ of the reaction flask and the solution was then filtered through Celite (2x3 cm) supported on a medium porosity frit, to remove any finely divided amalgam, and washed with THF (2x10 mL). The resulting orange solution of NaFp was cooled to $\sim -78^\circ\text{C}$ (solid CO_2 /acetone bath) and then 2,4-dichloropyrimidine (2.00 g, 13.5 mmol) was added. The orange solution was stirred at $\sim -78^\circ\text{C}$ for 2 h and then the cooling source was removed and the solution was allowed to warm up to ambient temperature and was stirred for a further 14 h. The reaction mixture was taken to dryness *in vacuo* and the resulting solid washed in air with distilled H_2O (2x15 mL) to remove NaCl and then with Et_2O ¹⁶ (3x10 mL) to remove Fp₂. (Alternatively, the solid is dissolved in CH_2Cl_2 and filtered to remove solid NaCl). The product was then crystallized from CH_2Cl_2 /hexane (5 mL/1 mL) to give 4-((cyclopentadienyl)iron dicarbonyl)-2-(chloro)pyrimidine, **1** (see Fig. 1.1), in 30% yield (1.11 g, 3.8 mmol) as yellow feathery crystals.

Similar reactions were carried out using substrates B-I to yield compounds **2**, **3**, **4a**, **5a**, **6a**, **7**, **8**, **9** (see Fig. 1.1) in 40, 44, 56, 42, 45, 31 and 95% yields, respectively. Compound **9** was shown by NMR to be a mixture of two isomers which were not successfully separated by column chromatography. Attempts to isolate the desired products from the original product mixture *via* column chromatography resulted in lower isolated yields (i.e., 12% for **1** and 16% for **6a**).

Reactions involving 2:1 (Fp⁻ to substrate) reactant ratios.

The reactions were carried out as above, but with two mole equivalents of nucleophile per mole equivalent of substrate. The procedure for isolating

the desired product in the reaction involving 2,4,5,6-tetrachloropyrimidine is described in detail as a representative example.

The substrate 2,4,5,6-tetrachloropyrimidine (3.00 g, 13.8 mmol) was reacted with NaFp (27.7 mmol, slight excess prepared as described above) in THF (80 mL) at -78°C . After 18 h the mixture was taken to dryness *in vacuo*. To the resulting "gummy" grey solid was added distilled H₂O (25 mL) in air and the mixture obtained was stirred thoroughly to dissolve the NaCl. The residual solid was then collected on a medium porosity fritted funnel and washed with H₂O (2x5 mL) then hexanes (2x3 mL).

Product isolation procedure A.

The resulting tan solid was then washed several times with Et₂O/hexanes¹⁶ (1:1) to eliminate all of the Fp₂ and the monosubstituted compounds (i.e., 5a, identified by comparison with an authentic sample). The remaining solid (light brown) was dissolved in a minimum of CH₂Cl₂ (~8 mL), filtered, and the filtrate cooled to obtain compound 5b in 25% yield (1.90 g, 3.8 mmol) as a yellow powder.

Product isolation procedure B.

Alternatively, the original solid mixture was dissolved in hexanes/benzene (1:1) and chromatographed in air on a Florisil (14x2.5 cm) packed column. The first bright yellow band (eluted with hexanes/benzene 4:1, 20 mL) showed no carbonyl absorption bands. The second tan band (eluted with hexanes/benzene 2:1, 50 mL) was shown to contain Fp₂, (by comparison with an authentic sample) with some amount of monosubstituted complex (no further attempts were made to separate this mixture). The third yellow band (eluted with hexanes/benzene, 2:1, 25 mL) contained the monosubstituted complex 5a. The column was then stripped with THF (40 mL)

to give a purple solution which was taken to dryness. This was then crystallized from CH_2Cl_2 (20 mL) to give 25% yield (1.80 g, 3.6 mmol) of the bimetallic product as yellow crystals. The purple coloration was later shown (by MS P^+ m/z at 324) to be due to the presence of a second monosubstituted compound in which one Cl group had been replaced by a hydrogen atom (i.e., $\text{C}_4\text{N}_2\text{HCl}_2\text{Fp}$).

Products from the reactions involving substrates D and E were purified by procedure B (*vide supra*) and yielded 20% of 4b and 22% of 5b, respectively. Reactions involving two mole equivalents of the anion Fp^- and substrates A, B, C, G and H yielded the monosubstituted compounds 1, 2, 3, 7, and 8, respectively, usually with large quantities of Fp_2 being formed as by-product. No evidence for the disubstituted product(s) were observed. A similar reaction with substrate I gave a mixture of compound 9 and a compound with the same mass as 8 (i.e., one Cl group had been replaced by a hydrogen atom).

Reactions of NaFp with halosubstituted pyridines: where the halopyridines are: R, 2,6-difluoropyridine; S, 2,3,4,5,6-pentafluoropyridine; T, 3-chloro-2,4,5,6-tetrafluoropyridine; U, 3,5-dichloro-2,4,6-trifluoropyridine).

Reactions involving 1:1 reactant mole ratios.

All of these reactions were performed in a similar manner, the reaction with 2,6-difluoropyridine being described in detail as a representative example.

A 200 mL three-neck flask (to which had been attached a Celite containing, medium porosity fritted funnel) was charged with 2,6-difluoro-

pyridine (1.00 g, 8.7 mmol). Then, THF (40 mL) was added and the solution was cooled to $\sim -78^\circ\text{C}$. A solution of NaFp (8.7 mmol Fp⁻) in THF (70 mL) prepared as usual, see above, was filtered slowly (over 10 min) into the substrate solution, with vigorous stirring. The frit was washed with THF (2x10 mL) and the red solution was stirred at $\sim -78^\circ\text{C}$ for 1 h. The cooling bath was then removed and the solution stirred for a further 2 h. The resulting mixture was taken to dryness *in vacuo* and the light brown powders remaining in the flask was partly dissolved in CH₂Cl₂ (20 mL). Filtration and washing with CH₂Cl₂ (2x5 mL) removed NaCl and other solid residues which were discarded. Pentane (5 mL) was added to the filtrate and then this mixture was concentrated *in vacuo* to ~ 12 mL. This solution was cooled to $\sim -9^\circ\text{C}$, and the product 2,6-C₅NH₃FFp, 10, was collected by filtration as a yellow powder in 41% yield (0.97 g, 3.6 mmol).

Similar reactions were carried out using substrates S, T, U, to produce compounds 11a, 12, and 13 in 78, 40 and 40% yields, respectively. Reactions carried out with 2,6-dibromopyrimidine, 2-chloropyridine and 2-fluoropyridine yielded Fp₂ almost quantitatively. Only in the case of 2,6-dibromopyridine was a significant peak at 2026 cm⁻¹ (THF) attributable to the desired product, (i.e., 2,6-C₅NH₃BrFp) observed.

¹⁹F NMR ((CD₃)₂SO) δ for 11a -100.05 (d, F2 & F6), -112.73 (d, F3 & F5). For 12, -77.95 (m, F2), -98.47 (m, F6), -105.94 (m, F5). For 13, -75.06 (s, F2 & F6).

Reactions involving 1:2 (substrate to Fp⁻) mole ratios.

These reactions were carried out as described for the diazines. However, only in the case of substrate S, C₅NF₅ was a disubstituted complex formed. This compound, 11b, was identified by MS m/z 457 (P⁺-CO) and IR, ν_{CO}

(CH₂Cl₂) 2033 (s) and 1982 cm⁻¹ (s) as C₅NF₃Fp₂. In these reactions, the predominant organometallic products were the monosubstituted species and the dimer Fp₂. Separation of the mono and disubstituted species from the reaction involving substrate S was difficult and the desired bimetallic product was not isolated as an analytically pure solid.

Preparation and attempted thermal decarbonylation of 2,5-C₅NH₃(COFp)₂, 14a and 2,6-C₅NH₃(COFp)₂, 14b.

The organic starting material, 2,5-pyridinedicarbonyldichloride, was synthesized by the published literature procedure.¹⁷ A solution of NaFp (9.0 mmol) in THF (75 mL) was prepared in the usual manner (see above) and the filtered solution was cooled to ~-78°C (solid CO₂/acetone). The substrate, 2,6-pyridinedicarbonyldichloride (0.95 g, 4.5 mmol), was added in one portion to the cooled Fp⁻ solution, and the resulting red mixture was stirred for 1 h at ~-78°C. The cooling bath was removed and the mixture was stirred for a further 2 h. The mixture was then taken to dryness *in vacuo* and the solid was washed with Et₂O¹⁶ (20 mL), distilled H₂O (50 mL) and then Et₂O (2x6 mL), and the washings (containing mostly Fp₂ and NaCl) were discarded. The yellow solid was dissolved in CH₂Cl₂ (10 mL) and then hexanes (5 mL) was added. This solution was concentrated to ~10 mL and kept at ~-9°C overnight to yield 65% (1.40 g, 2.9 mmol) of dull yellow, feathery crystals of C₅NH₃(COFp)₂, 14a.

Anal. Calcd for 2,6-C₅NH₃(COFp)₂: C, 51.77; H, 2.67; N, 2.87. Found: C, 51.49; H, 2.72; N, 2.75. IR (CH₂Cl₂) ν_{CO} 2024 (s), 1969 (s) and 1620 cm⁻¹ (s). Low resolution mass spectrum m/z 459 (P⁺ -CO).

The same procedure was used for the synthesis of complex **14b** from 2,5-pyridinedicarbonyldichloride but the product was not isolated in an analytically pure form. The approximate yield of **14b** was (35%).

Anal. Calcd for 2,5-C₅NH₃(COFp)₂: C, 51.77; H, 2.67; N, 2.87. Found: C, 50.71; H, 3.22; N, 2.71. IR (CH₂Cl₂) ν_{CO} 2024 (s), 1970 (s) and 1620 cm⁻¹ (s). Low resolution mass spectrum m/z 459 (P⁺ -CO)

Attempted thermal decarbonylation of 14a and 14b.¹⁸

Similar procedures were used for both compounds. The procedure for **14a** is described in detail.

A suspension of 2,6-C₅NH₃(COFp)₂ (0.50 g, 1.0 mmol) in Bu₂O (60 mL) was set to gently reflux with care being taken to avoid any local overheating or splashing of the diacyl compound on the sides of the flask. The progress of this reaction was monitored by occasionally allowing the reaction to cool to ambient temperature and recording the IR spectrum of the supernatant solution. The reflux was stopped after 2 h when the Fp₂ bands (most noticeably that at 1790 cm⁻¹) had become predominant, without any apparent shift/increase in the IR bands of the compound **14a** (in particular, the acyl band at 1608 cm⁻¹ had not decreased in intensity). The reaction was repeated using toluene and a second time using a toluene/Bu₂O (70:30) solvent mixture. These refluxes were stopped after 20 h and 14 h, respectively. No evidence for the formation of the desired product was obtained in any of these reactions.

Similar observations were made for thermal reactions using compound **14b**.

Reaction of FpX (X = Cl or I) with dimetallated (2,5) furans and thiophenes.

Dimetallation of thiophene to give 2,5-dilithiothiophene (2.0 mmol) was carried out by the published literature procedures.¹⁹ Thus, thiophene (0.16 g, 2.0 mmol) was placed into a 200 mL three-neck flask containing hexane (40 mL). Then TMEDA (0.37 mL, 4.6 mmol) and n-BuLi (in 2.5M hexanes 1.83 mL, 4.6 mmol) were added and the mixture was stirred for about 20 min during which time a white suspension formed. The mixture was warmed slowly to 40°C and then was refluxed for 30 min. The hexane was removed *in vacuo* and THF (60 mL) was added. The resulting yellowish solution was cooled to ~-78°C and FpI (2.34g, 7.8 mmol) was added over a 15 min period. The reaction mixture was then stirred for 17 h during which time it warmed up to room temperature. An IR spectrum of a sample of the solution in CH₂Cl₂ showed peaks at 2026 (s) 1992 (s) and 1780 (w) cm⁻¹ (N/B FpI has ν_{CO} at 2041 (s) and 1998 cm⁻¹(s) in CH₂Cl₂). The suspension was taken to dryness *in vacuo* and worked up by chromatography on a Florisil packed (14x2.5 cm) column with a hexane/benzene (4:1) mixture as eluting solvent. The first (yellow) band was collected (ν_{CO}= 2042, 1996, in CH₂Cl₂), and analysis by MS showed a major peak at m/z 386 consistent with the parent ion peak of a compound with the formulation Fp-S-Fp (peaks due to successive loss of four CO ligands were observed among others). Another major peak from the same sample at m/z 260 maybe due to the monosubstituted analogue of the desired product C₄SH₃Fp, (peaks due to loss of CO were also observed for this product). The second purple band was identified as Fp₂. No evidence for the desired disubstituted complex was obtained in this reaction.

A similar reaction was carried out using dimetallated furan¹⁹ which was obtained thus; to a 300 mL three-neck flask was added hexanes (50 mL) followed by KOBu^t (3.8 g 30 mmol). The suspension was cooled to $\sim -60^{\circ}\text{C}$. Then BuLi (11.9 mL, 30.0 mmol) was added and the suspension was stirred while maintaining the temperature below -40°C for about 20 min. TMEDA (5.3 mL, 4.80 g, 35.0 mmol) was added over 5 min followed by furan (0.85 g, 12.0 mmol, 1.21 mL). The solution was stirred while maintaining its temperature between -25°C and -40°C for 1 h. The solution was cooled to -78°C and THF (50 mL) was then added, followed after 5 min by FpCl (2.60g, 12.0 mmol) and the progress of the reaction was monitored by IR. After 10 min an IR spectrum of a sample of the mixture showed peaks at 2032 (s), 1992 (sh), 1974 (s), 1902 (w) and 1782 (w) cm^{-1} (note FpCl shows peaks at 2048 (s) and 2000 (s) cm^{-1}). The reaction mixture was then stirred for a further 5 h during which time it warmed to room temperature. A sample of the crude product analysed by MS showed signals attributable to Fp₂ as the only carbonyl containing material present. Likewise, an IR spectrum of the product at this stage showed only carbonyl signals attributable to Fp₂. The product was discarded. The reaction was repeated with similar results being obtained.

X-ray Crystal Structure Determination of C₁₉H₁₄Fe₂N₂O₄S, 5b.

The X-ray diffraction data collection and subsequent calculations were carried out by Dr. B.D. Santarsiero of the chemistry department. Thus, A red crystal of compound 5b (approximate dimensions 0.19x0.19x0.48 mm) was selected from a batch grown from CH₂Cl₂ (see above). Crystal data: C₁₉H₁₄Fe₂N₂O₄S, FW = 478.09, monoclinic space group P2₁/n, (alternative setting of P2₁/c of No. 14^{20a,20b}), a = 11.119(a)Å, b = 11.553(3)Å, c =

15.764(2)Å. $\beta = 104.49(1)^\circ$, $V = 1960 \text{ \AA}^3$, $Z = 4$, $D_c = 1.615 \text{ g cm}^{-3}$, MoK α radiation ($\lambda = 0.71073 \text{ \AA}$), $\mu(\text{MoK}\alpha) = 8.31 \text{ cm}^{-1}$. The X-ray diffraction data, 6189 reflections, were collected at room temperature on an Enraf-Nonius CAD4 diffractometer by the ω - 2θ scan method (ω scan width = $0.90 + 0.347 \tan\theta$). The structure was solved by examination of Patterson and Fourier maps and adjusted by full-matrix least-squares refinement. Hydrogen atoms were placed in idealized positions by assuming C-H bond length of 0.95Å and the appropriate sp^2 and sp^3 geometries. The coordinates of the hydrogen atoms on the methyl group were adjusted by the least squares refinement of positions indicated on a difference Fourier map. All hydrogen atoms were then refined in the calculations with fixed, isotropic Gaussian parameters, 1.2 times that of the attached atom and constrained to "ride" on that atom. The data were corrected for absorption using a scheme based on the absorption surface (Fourier filtering) method of Walker and Stuart.^{20d} The refinement converged to a final GOF of 2.56 and R of 0.076 with anisotropic Gaussian displacement parameter for all non-hydrogen atoms. The Enraf-Nonius SDP program package ^{20d} was used.

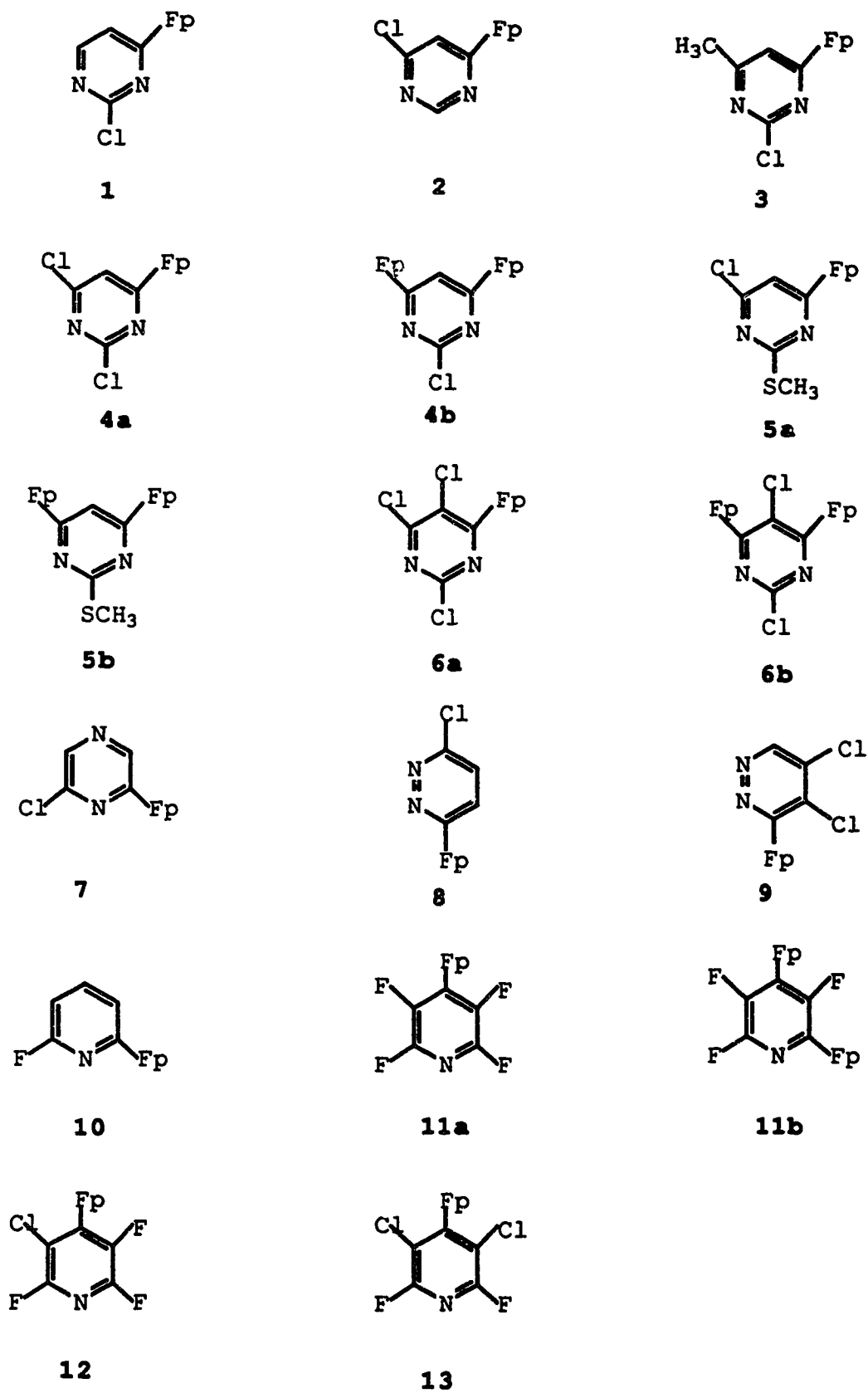
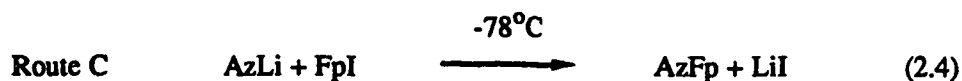
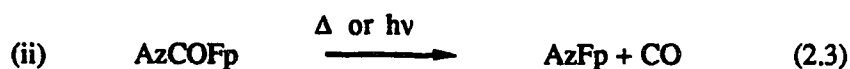
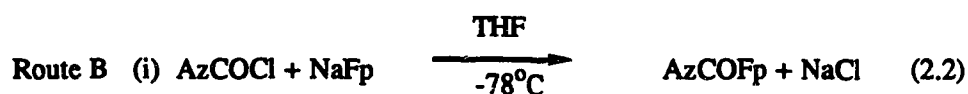
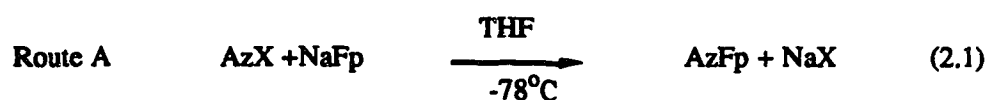


Figure 1.1 Isomeric forms of the complexes.

RESULTS AND DISCUSSION

Syntheses of Fp substituted heterocyclic compounds.

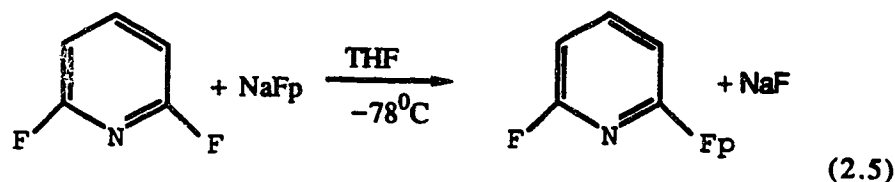
Given the synthetic utility^{1,2} and well developed chemistry of the $(\eta^5\text{-C}_5\text{H}_5)\text{Fe}(\text{CO})_2$, Fp, fragment, and considering the remarkable stability of earlier reported Fp-arene and Fp-azine complexes, this work was begun by investigating the syntheses of the Fp substituted heterocyclic complexes. We considered three routes, A, B and C, for the syntheses of our complexes viz:



(where Az = azine and X = F, Cl, Br). Each route has its limitations as described below.

Syntheses of monometallic complexes.

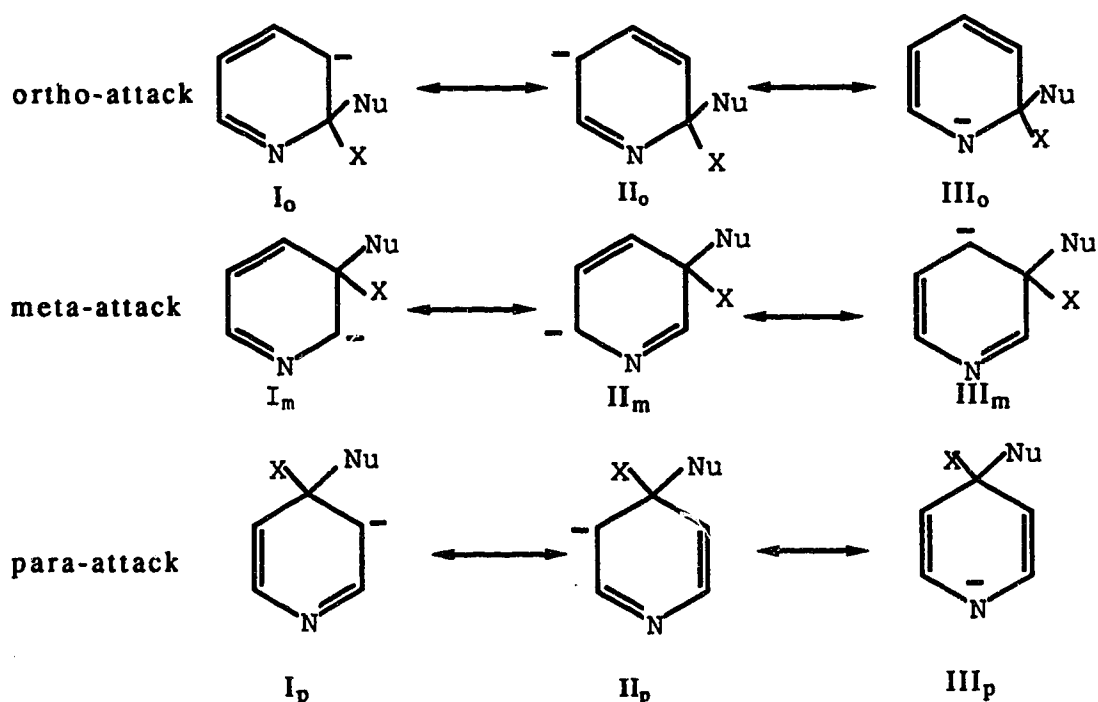
All the monosubstituted complexes reported were synthesized *via* a single route (namely route A above) involving the nucleophilic displacement of a halide by a Fp fragment, e.g.



These reactions generally proceeded smoothly with the desired products (see Fig. 1.1) being the major organometallic species isolated. A ubiquitous by-product of these reactions is the dimer, $Fp_2 = [(\eta^5-C_5H_5)Fe(CO)_2]_2$. However, with careful control of reaction conditions, the formation of this undesirable compound can be minimized. These reactions proceed most cleanly when the reagents are reacted and maintained at $\sim -78^{\circ}C$, for 1-2 h and then allowed to warm up slowly to room temperature over a few hours.

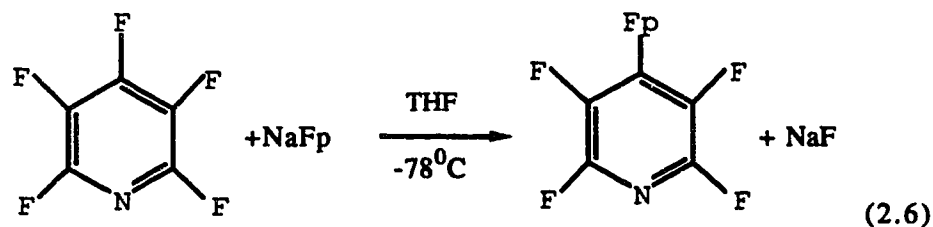
The (non-optimized) yields of products obtained from these reactions were dependent upon the degree and position of halogen substitution. Thus, those syntheses involving polyhalogenated azines usually displayed the highest yields (40-95%). This is consistent with previous observations that polyhalogenated azines and arenes are particularly well suited for organometallic nucleophilic substitution reactions.⁵ The yields of products obtained from those reactions involving dihalogenated azines, on the other hand, were generally lower (25-45%). As noted above, the halide plays a major role in activating the azine ring towards nucleophilic attack. Consistent with this, it has generally been assumed that only in polyhalogenated azines can such reactions proceed to give reasonable yields of products, the reactions of $Mn(CO)_5-C_3N_3F_2$ with Fp^- being a notable⁷ but expected (*vide infra*), exception. It is therefore interesting that with a nucleophile as strong as Fp^- ,²¹ a range of less activated azines does react to give moderate yields of products.

The influence of the aza group in activating the ring carbon towards nucleophilic attack can be rationalized by representing the intermediate formed from such processes using canonical structures. As an extension of the above, the preferred position of such attack can be predicted by assuming that the relative stabilities of these intermediates reflect the relative energies of the transition states which lead to them. In the pyridine reactions, for example, the preferred positions for nucleophilic attack are the *ortho* and *para* positions, i.e.

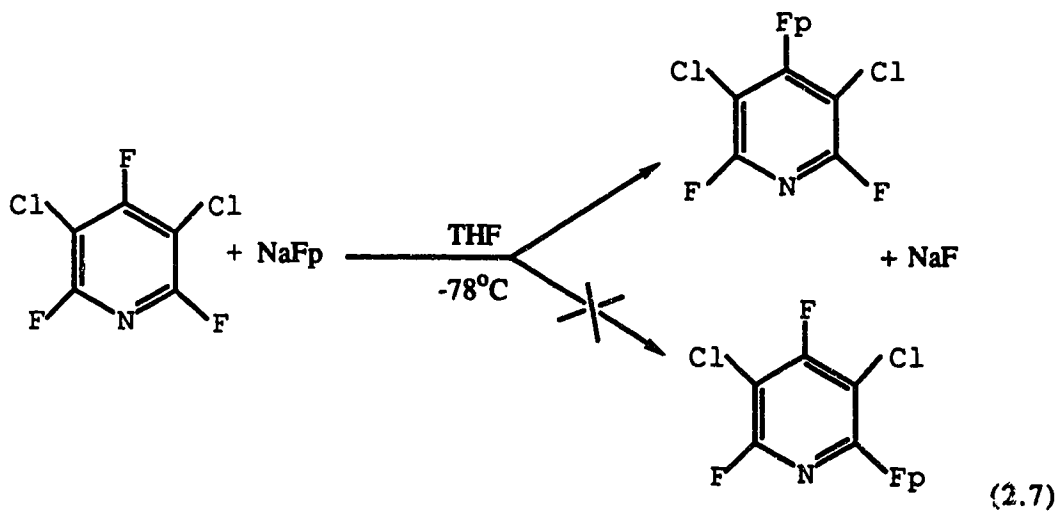


These two positions exhibit greater resonance stabilization because the greater electronegativity of the nitrogen atom results in favourable contributions from resonance forms III_o and III_p having charge localized on the nitrogen atom. In other words, the attack at the 2 and 4 positions will be

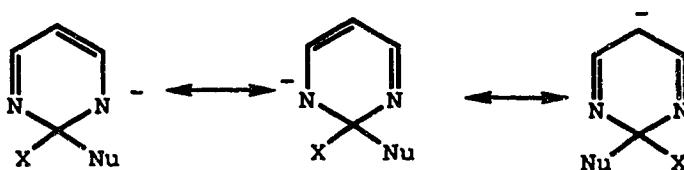
most favoured due to mesomeric withdrawal of electron density by the aza group, a phenomenon that has been previously established for organic nucleophiles,^{22,23} and which is not possible in the 3-position or in the analogous benzene derivatives. Hence, we observe that the 2, 4 and 6 positions are the positions of attachment of the Fp fragment (spectroscopic evidence for this is provided later). For example, we and others^{6c} have found that the reaction of pentafluoropyridine with Fp⁻ yielded the 4-substituted complex as the major organometallic product viz:



Indeed, we have observed that this remains the preferred position even when one or two bulky Cl groups replace the F group in the 3 or 3 and 5 positions, respectively.



Similar arguments can be made for the other azines and predict that the preferred sites of nucleophilic substitution are the 2 and 4(6)-positions for the pyrimidines, and the 3(6) positions for the pyridazines. This is in accord with the isomeric identities of the observed products (Fig. 1.1). The diazines are much more activated towards nucleophilic substitution than pyridines, having two aza groups in the ring.^{23,27} Thus, in the pyrimidines, substitution at the 2 and 4(6) positions gives intermediate complexes having two resonance forms with the negative charge residing on the more electronegative nitrogen atoms, viz;

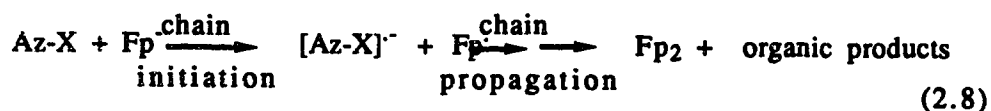


Consistent with the above, we observed that whereas the mono-chloro and fluoropyridines did not show any significant degree of substitution (by IR) with Fp^- , preliminary studies²⁸ indicate that the mono-chloro pyrimidines and quinolines undergo substitution.

The effect of the halide leaving group on the nucleophilic susceptibility of the azine is dominated by the electron withdrawing inductive effect ($-I$)²⁴ of these halides. Thus, even though the fluoride ion is a poorer leaving group than is the bromide ion, in aliphatic nucleophilic substitutions,²⁴ the fluoride ion being more electron withdrawing more readily polarizes the C-X bond in aromatic compounds. This leaves the ring carbon with a greater partial positive charge and hence renders the fluorinated species more susceptible to nucleophilic attack. As an example of

this effect, we observed that the reaction of Fp^- with 2,6-dibromopyridine substrate, S, yielded only a trace amount of substitution product (by IR) while the related reaction with the fluoro analogue gave *ca.* 45% isolated yield of the desired product. Thus, these reactions seem to proceed predominantly *via* an S_NAr pathway with the rate determining step being the formation of the charged Meisenheimer complex illustrated above.

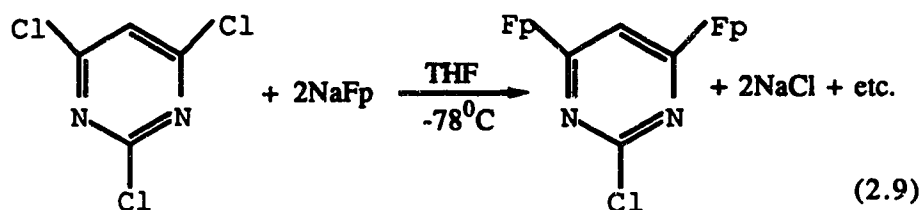
Although the exact origin of the Fp_2 by-product in these reactions is uncertain, it seems likely that it arises *via* a competitive single electron transfer, SET,²⁵ (i.e. $SRN1$) pathway. Such a process will be initiated by the formation of a free radical which then leads to the products *via* a chain process.²⁴ Thus, the readily oxidized Fp^- anion²⁶ reacts with the mildly oxidizing haloazines²⁴ to give Fp_2 as the predominant organometallic product,



when the nucleophilic substitution becomes slow or less favorable. Recent studies²⁹ on effects of substituents on the electron affinities of perfluorobenzenes C_6F_5X (where $X = I, Br, Cl, F, NO_2$, etc.) have shown that the electron affinities of the compounds decrease in the order $X = NO_2 > I > Br > Cl > F$. If as expected, increasing the electron affinity of the azine ring increases the oxidizing ability of the ring, and if the SET pathway is one of the routes followed by the reactants in these reactions, one can predict that bromo substituted azines being more oxidizing will more likely follow this SET pathway, thus leading to more Fp_2 by-product than the chloro and fluoro substituted azines. This is consistent with our observations.

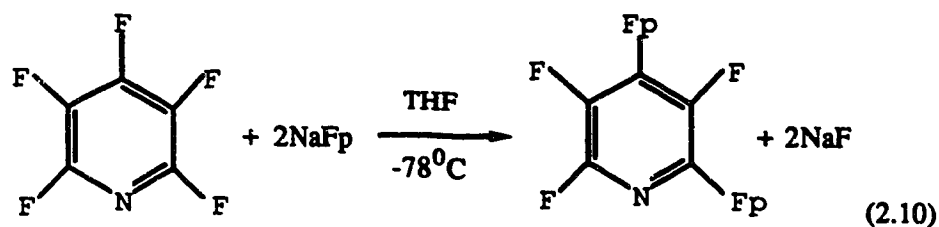
Syntheses of disubstituted complexes.

The syntheses of the disubstituted complexes were carried out in a similar fashion to that described for the monosubstituted analogues. However, two mole equivalents of Fp^- were used for each mole equivalent of precursor azine, e.g.

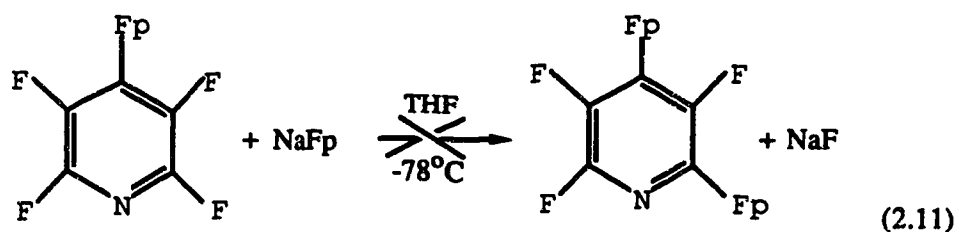


These reactions often yielded significant quantities of organometallic side products. These were mostly the Fp_2 dimer but some new monometallic compounds were also observed, *vide infra*. Although the bimetallic products formed had comparable air/moisture stabilities to their monometallic counterparts, they were isolated in comparatively low yields (20-28%) and the monometallic products were sometimes the dominant species. The low yields were not particularly surprising, on statistical grounds and may result from the deactivating property of a prior coordinated organometallic substituent *via* its steric bulk and the substantial transfer of electron density to the aromatic ring.^{2a} Similar observations have been made in previous studies of the reactions of Fp^- with $\text{C}_6\text{H}_4\text{Cl}_2\text{Cr}(\text{CO})_3$,^{2e} $(\text{C}_3\text{N}_3\text{Cl}_2)\text{Mn}(\text{CO})_5$,⁸ and $\text{C}_6\text{F}_5\text{NH}_2$.^{5e}

In addition to the disubstituted pyrimidine complexes, a disubstituted pyridine complex was obtained from the reaction of pentafluoropyridine with two equivalents of the Fp^- anion, thus,

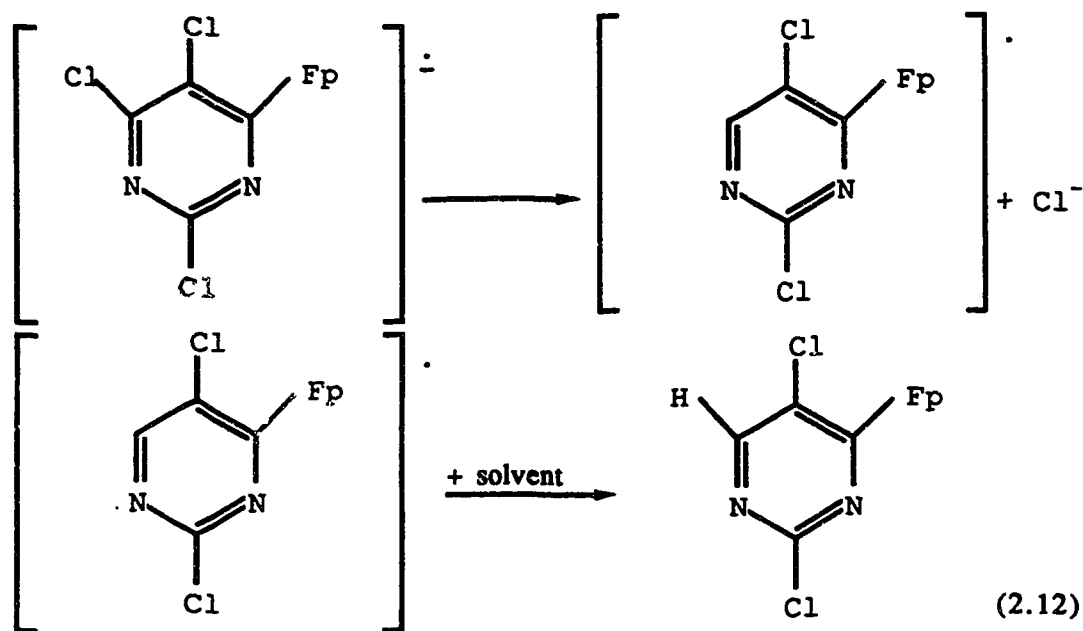


This material which was obtained in very low yields, was difficult to separate from the monosubstituted product (which was a coproduct of the reaction), and was thus not completely characterized. The observed low yields of this product relative to the pyrimidine analogues parallels the expected degrees of activation of the substrate compounds. Moreover, in contrast to the di- and tri-azines, attempts to synthesize this disubstituted pyridine compound by stepwise reaction of Fp^- anion on perfluoropyridine (via equations 2.6 and 2.11) were unsuccessful even under forcing reaction conditions.

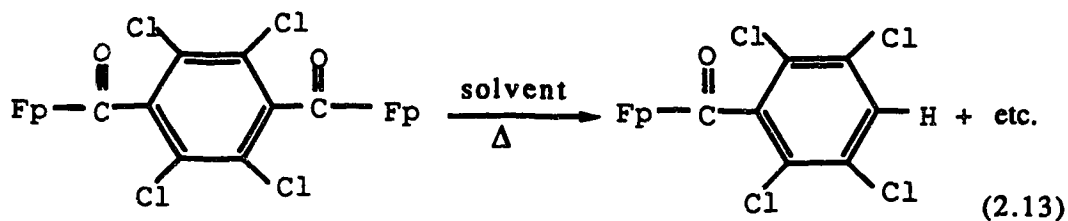


This again shows the influence of the aza group on the activation of the substrate especially towards multiple nucleophilic substitution.

Another class of products which were sometimes observed were the monosubstituted compounds in which a halide had been replaced by a hydrogen atom.³⁰ They may arise either from an SET process *vide supra*, during the course of the nucleophilic attack, or *via* thermal decomposition

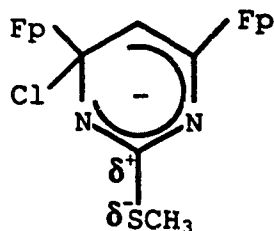


of the sterically crowded reaction product, as has been observed previously in related syntheses.^{2c}



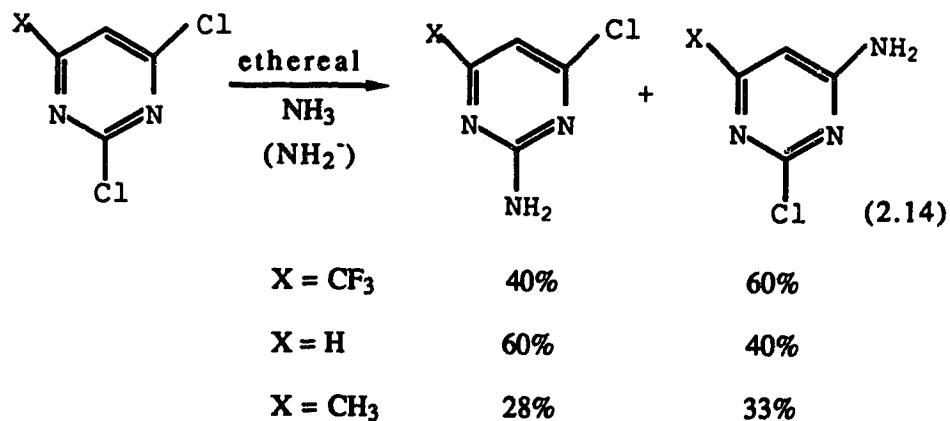
With the exception of 4,6-dichloro-2-methylthiopyrimidine, total substitution of all the halides was not achieved. Similar observations have been made earlier in the reactions involving the highly activated cyanuric chloride/fluoride substrates.^{6f,8} In the case of 4,6-dichloro-2-methylthiopyrimidine, the Cl groups are located on two of the most highly activated positions, *vide supra*, with the methylthio group (like the halides in

related compounds) stabilizing the Meisenheimer intermediate arising from the second nucleophilic attack, by polarization, i.e.



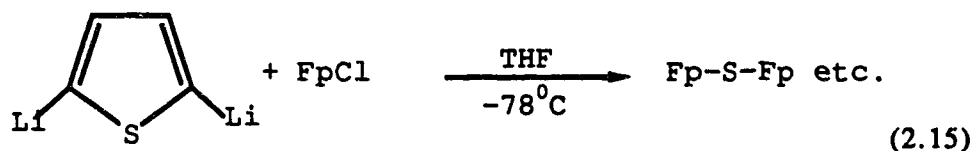
The importance of this polar effect is underscored by the fact that we could not achieve disubstitution in 4,6-dichloropyrimidine in which this electron withdrawing group is absent.

We observe one isomer for all our mono substituted Fp-pyrimidines, with the 4-position being favoured, and also one isomer for all the disubstituted pyrimidines, with the 4 and 6 positions being favoured. This observed regioselectivity of the Fp⁻ anion in substitution reactions with chlorinated pyrimidines is interesting, given that organic nucleophiles such as NH₂⁻, OEt⁻, OP(OR)₂⁻, etc.,³¹ have been shown to be non-specific between positions 2 and 4(6), i.e.



These observed isomer ratios have been attributed to the influence of the substituent X on the π electron distribution around the ring,^{31a} a phenomenon which apparently has no measurable effect in our reactions. These effects remain under investigation in our laboratory.

The reactions of FpI with metallated furans and thiophenes may have yielded the desired products as indicated by the IR spectra of the reaction mixtures, but as expected these were too unstable to be isolated.^{7b} Instead, we obtained the sulphur bridged compound (Fe-S-Fe) from the reaction with metallated thiophene.

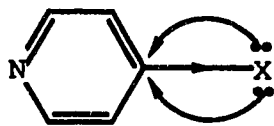


The mechanism of its formation would be interesting, and may be of relevance in the understanding of the desulphurization process.³²

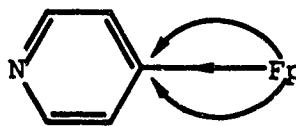
Characterization of the Complexes

All the fully characterized complexes showed remarkable air/moisture stability both as solids and in solution. Some of these complexes crystallize very readily from CH_2Cl_2 solutions. However, many of these compounds tend to at least partially desolvate when separated from the mother liquor especially when placed under vacuum or under N_2 for prolonged periods.

The η^1 -metal-arene bond in monometallic Fp-aryl complexes has been shown to have both σ and π components.³² The transition metal substituent in these and the Fp-azine complexes is less electronegative than carbon. The metal-carbon σ -bond in these species is therefore expected to be polarized towards the azine (arene) ring.³³ Moreover, the highest occupied molecular orbitals, HOMOs, on the metal centre are of the correct energy and symmetry to interact with the π^* antibonding orbitals on the azine.³⁴ Hence a significant π -donor component is expected in the M-C bond. Thus, in contrast to organic π -donors the Fp fragment acts as both a π -donor and a σ -donor of electron density to the azine ring³⁵, i.e.,



π -donor
 σ -acceptor
for X = F, OMe, NH_2 , etc



π -donor
 σ -donor

This description is confirmed by the observed spectroscopic properties of these complexes, (*vide infra*). Clearly, the extent of the σ bond polarization and the magnitude of the π -donor interaction is dependent on the

electronic properties of the azine ring. Thus, maximum electron transfer is expected where there are more electron withdrawing groups on the azine, as this will stabilize the azine's acceptor orbitals as mentioned in the introduction.

The IR and NMR spectral data for these complexes is listed in Tables 2.1 and 2.2 and can be compared with that of the analogous arene complexes reported earlier.^{3,4,30} Except for complex 9 (where a mixture of isomers is present but which showed peaks in the same region as related complexes), the ¹H and ¹³C NMR signals attributable to cyclopentadienyl rings and CO group are observed as singlets in regions previously reported for Fp-aryls (4.19 to 5.35 ppm and 86.8 to 87.6 ppm for the Cp's and 213.4 to 215.3 ppm for CO's respectively).^{2,6} In addition, the IR spectra for the carbonyl ligands in these complexes are composed of a pair of vibrations having the expected intensity ratios, with the symmetric stretching frequencies usually occurring above 2000 cm⁻¹ whereas the antisymmetric stretching frequencies occur below 2000 cm⁻¹.³⁶ These observations indicate that the Fp groups retain their three-legged piano stool structures, and that the Fp fragments in the disubstituted complexes are chemically equivalent (and thus in the 4,6 rather than the 2,4 positions for 4b, 5b and 6b), as was confirmed for compound 5b by its X-ray crystal structure, *vide infra*.

The carbonyl bands (IR) for a particular series of complexes having a common parent heteroarene ligand showed a consistent decrease of about 10 to 14 cm⁻¹ on going from the mono to the disubstituted complex (e.g 2034 and 1982 cm⁻¹ for C₄NHCl₂Fp, 5a, compared to 2020 and 1970 cm⁻¹ for C₄NHClFp₂, 5b). This is consistent with the increased electron density on the azine ring expected on replacing σ electron withdrawing substituents such as halides

Table 2.1. Analytical, Mass Spectra and Infrared data for the Complexes.

Complex #	Analytical Data						Low Resolution/FAB Mass Spectral Data		Infrared Data vCO(CH ₂ Cl ₂) cm ⁻¹
	C		H		N		P ⁺ , m/z		
	Calcd	Found	Calcd	Found	Calcd	Found			
1	45.46	45.54	2.43	2.40	9.68	9.42	290	2036(s),1982(s)	
2	45.46	45.32	2.43	2.46	9.68	9.63	290	2034(s),1981(s)	
3	47.30	47.31	2.96	3.15	9.20	8.59	304	2032(s),1978(s)	
4a	40.74	40.41	1.85	1.98	8.64	8.32	324	2036(s),1986(s)	
4b	44.21	44.61	2.38	2.66	6.01	6.02	466	2027(s),1975(s)	
5a	42.80	42.83	2.67	2.62	8.32	8.22	336	2034(s),1982(s)	
5b	47.70	47.14	2.93	3.23	5.86	5.47	478	2020(s),1970(s)	
6a	36.76	36.57	1.40	1.31	7.79	7.72	290	2041(s),1994(s)	
6b	43.16	43.69	2.01	2.08	5.59	5.47	500	2030(s),1980(s)	
7	45.46	45.58	2.43	2.73	9.68	9.47	290	2032(s),1978(s)	
8	45.46	45.51	2.43	2.42	9.68	9.29	291a	2030(s),1975(s)	
9	40.66	40.41	1.86	1.82	8.62	8.40	325	2044(s),1992(s)	
10	52.74	52.95	2.93	3.01	5.13	4.93	273	2026(s),1975(s)	
11a	44.07	43.83	1.54	1.57	4.25	4.28	327	2044(s),1997(s)	
12	41.96	42.00	1.49	1.44	4.08	4.04	359	2040(s),1994(s)	
13	40.11	40.03	1.39	1.32	3.90	3.79	359	2036(s),1990(s)	

a P⁺ obtained by FAB-MS **b** These complexes were not isolated in an analytically pure form, see text.

Table 2.2 ¹H and ¹³C NMR data for the Complexes in ppm ((CD₃)₂SO)

Complex #	¹ H NMR		¹³ C NMR							
	C ₅ H ₅	Azine-H	C ₅ H ₅	Fe-C	C ₂	C ₃	C ₄	C ₅	C ₆	Fe-CO
1	4.99	7.48, 7.6i	87.14	212.59	156.54	-	-	138.62	149.50	214.59
2	5.22	7.67	87.13	209.27	154.25	-	-	37.59	153.70	214.77
3	5.12	7.49	87.09	210.33	156.01	-	-	137.72	159.63	214.77
4a	5.31	7.80	87.21	216.76	154.41	-	-	136.07	153.57	214.08
4b	5.19	7.66	86.93	196.60	153.10	-	-	157.23	-	215.31
5a	5.14	7.33	87.00	210.06	166.67	-	-	132.25	153.16	214.56
5b	5.15	7.45	86.78	191.79	162.91	-	-	154.11	-	215.56
6a	5.15	7.30	87.20	214.75	152.76	-	-	142.54	150.54	213.55
6b	5.15	7.34	87.17	198.75	148.55	-	-	163.29	-	214.75
7	5.28	8.02, 8.41	86.88	187.63	-	156.2	-	135.80	147.54	214.95
8	5.35	8.00, 8.42	86.81	188.58	-	-	144.24	122.69	153.61	215.13
9*	-	-	87.21, 87.60	-	-	-	-	-	-	213.80, 213
10	5.15	6.42, 7.22, 7.38	86.80	184.55	-	135.81	138.92	100.99	160.43	215.74
				JCF=12.8		JCF=7	JCF=4	JCF=37.7	JCF=2.33	

*Contains two isomers.

with electron donating organometallic substituents (to give the disubstituted complex). Similarly, on going from complex 11, to 12 to 13 (i.e., progressively replacing F groups with Cl which have a lesser -I effect) we observe a consistent decrease in the CO stretching frequencies (by 4 cm^{-1} on each peak) for each F group which is replaced. This indicates that, as expected, the σ -component of the azine-substituent bond has a more pronounced effect on the net electron transfer from Fe to azine than does the π -component (which would yield the opposite effect).

The ^{13}C NMR spectra of the azine ring carbons in these complexes are particularly important in determining the substitution positions³⁷ and may also be useful in elucidating the nature of the azine-substituent bonding and electronic interactions. The effects of non-transition metal substituents, as well as some transition metal substituents, on the chemical shifts of arene carbons in substituted arenes have been shown to be linearly additive to a first approximation, where there are no substantial substituent-substituent interactions.^{2,3} Substituent effects have also been studied for azines, with the substituted pyridines being most thoroughly investigated.³⁸ To the best of our knowledge, however, no such studies have been reported for Fp substituted azines (or for other organometallic substituted azines).

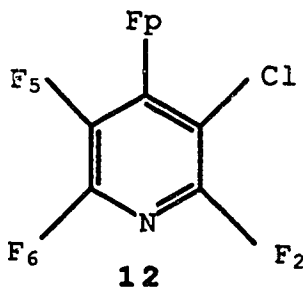
Assignment of the various ^{13}C NMR frequencies was established using the previously assigned substituent parameters for arenes^{2,37} and heteroarenes^{37,38} and on the basis of our systematic NMR studies of a series of substituted azines (including starting materials and their organometallic derivatives). These studies produced a consistent set of substituent constants for the Fp substituent in the substituted pyrimidines. Thus, the change in the observed chemical shift of C_x (Δ) on replacing a Cl group with a Fp group at

the 4/6 position was found to be $\Delta C_4(\text{ipso}) = +50$, $\Delta C_2(\text{meta}) = -12$, $\Delta C_5(\text{ortho}) = +17$, $\Delta C_6(\text{para}) = -3$ ppm. These values, in addition to some previously published values for organic substituents,^{2c} were used to predict the ^{13}C NMR spectra of the organometallic derivatives and those of the starting materials. These assignments were consistent with those made on the basis of peak areas and multiplicities (expected from number of equivalent nuclei, C-F coupling constants and/or NOE effects) and by direct comparison to related complexes. Indeed, the average difference between predicted and observed ^{13}C NMR chemical shifts was about 2 ppm. Thus, we find that, to a first approximation, the substituent parameters of the Fp groups (in the 4 and 6 positions) on pyrimidine derivatives are linearly additive as they are for *meta* substituted arenes.^{2c-d,37}

As our results show, the Fp substituent has a very large effect on the *ipso* carbon. This is consistent with previous results on Fp-aryl and [Fp-aryl]M(CO)₃ type complexes (e.g., 1,3-C₆H₄Fp₂^{2c} and 1,3,5-C₆H₃Fp₃Cr(CO)₃^{2d}) and reflects the dominant contributions from the paramagnetic screening terms of the iron centre.³⁹ Indeed, the magnitudes of these various Δ values are more consistent with [Fp-aryl]Cr(CO)₃ complexes^{2c} where the Cr(CO)₃ group reduces the electron density on the ring carbons in a manner comparable to the effect expected from aza groups in azines than with the uncomplexed arenes. Such electron withdrawing effects in these compounds are expected to sensitize the ring carbons to changes in electron density. The ^{13}C chemical shift assignments for the pyridazine and pyrazine complexes are somewhat less certain. They were based on the derived substituent constants of the pyrimidines and by taking into consideration the chemical shifts of the starting materials and the

expected NOE effects. For these compounds, we are confident of the assignments for the *ipso*-C(Fe), Cp and CO carbons, while the other assignments are more tentative.

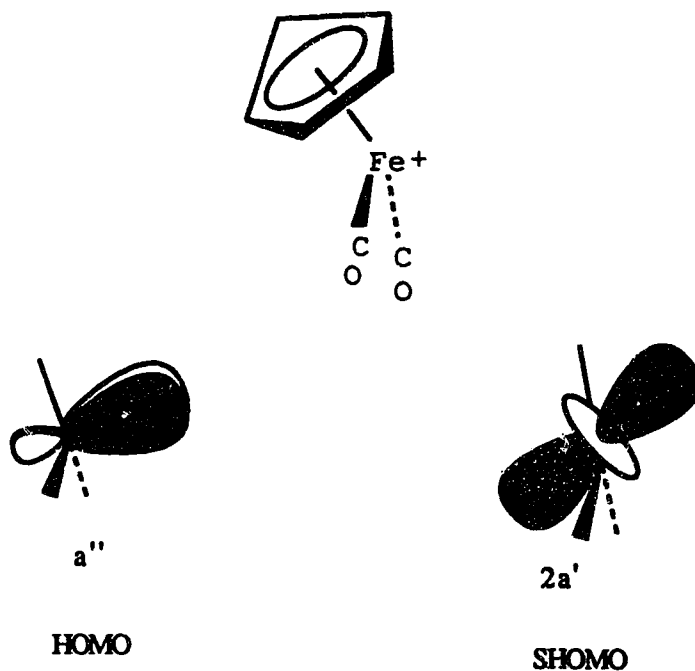
The ^{19}F NMR spectra were used to establish the isomeric forms of the polyfluorinated pyridine complexes. Thus, the presence of two resonances of equal intensity at -100.05 ppm ($\text{F}_{2,6}$) and -112.73 ($\text{F}_{3,5}$) ppm displaying a characteristic AA'XX' spin pattern for compound 11a confirms the earlier established^{5c} 4-substitution geometry for this compound (note : the Fp group in complex 11a has thus deshielded the *ortho* fluorines $\text{F}_{3,5}$, by about 30 ppm with respect to where they would be found in perfluoropyridine). Complex 13 showed a single absorption at -75.06 ppm, consistent with a symmetric isomeric form with two equivalent F nuclei. Compound 12 showed three absorptions at -77.95 ppm (quartet), -98.49 ppm (quartet), -105.94 ppm (pseudo triplet), with an AMX type pattern. Band assignment was made on the following basis (a) comparison of the chemical shift values to those of 11a and 13, (b) on the basis of the expected C-F coupling constants.^{5c} The illustrated 4-substitution geometry is consistent with this assignment.



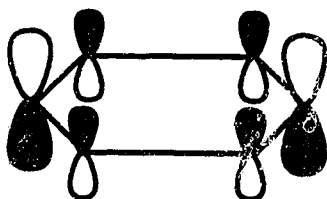
$\text{F}_2 = -77.95$	$\text{J}_{2-5} = 27.0$
$\text{F}_5 = -105.94$	$\text{J}_{2-6} = 11$
$\text{F}_6 = -98.47$	$\text{J}_{5-6} = 27.9$

We have also confirmed the identity of one of the complexes, $C_{19}H_{14}Fe_2N_2O_4S$, **5b**, by determining its structure by X-ray diffraction methods. The ORTEP drawings of selected views of this complex are reproduced in Figures 2.2 and 2.3. Selected bond lengths and angles, torsion angles and least squares planes are reported in Tables 2.3 to 2.6. The structures of the $CpFe(CO)_2$ fragments are as expected. Thus, each iron carries a symmetrically bonded $\eta^5-C_5H_5$ group as well as two linear CO groups having Fe-C and C-O bonds (1.756(8)Å, 1.755(7)Å, 1.755(8)Å, and 1.739(7)Å, and 1.135(10)Å, 1.147(8)Å, 1.133(10)Å and 1.153(9)Å respectively) in the expected ranges for the Fe-C (1.71 to 1.82Å)^{41,42} and C-O (1.12-1.17Å)^{41,42} bonds of Fe-carbonyls. As predicted from the spectroscopic data, the Fp fragments are substituted at the 4 and 6 positions of the pyrimidyl ring and each of these Fe-C bonds completes the third leg of the piano stool arrangement around each iron centre. The Fe-C(pyrimidine) bond lengths are 1.986(7)Å and 1.973(6)Å. These bond distances are within the range reported for other complexes having *formal* Fe-C(sp²) single bonds (1.94-2.03Å) and are close to those reported for cationic Fp-carbene complexes having *formal* Fe-C double bonds (1.91-2.03Å).⁴² Thus, partial double bond character (as expected for any Fe to azine π -bonding) cannot be completely ruled out for these linkages.

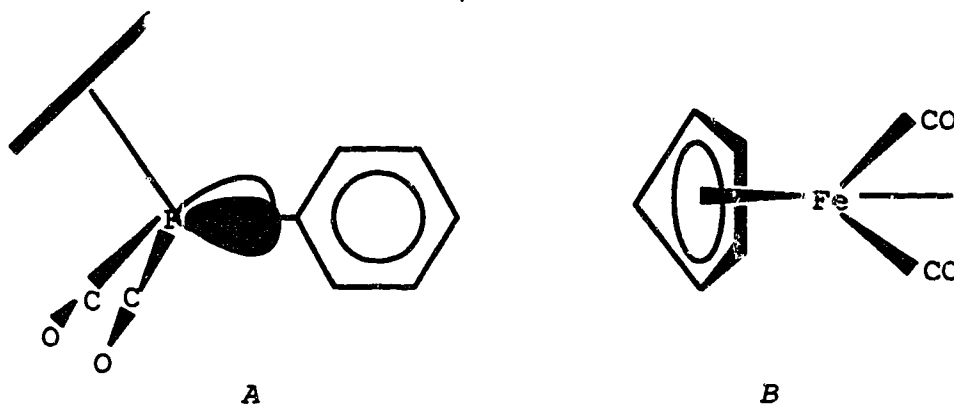
The most interesting observation about the structure is the orientation of the pyrimidine ring with respect to the mirror planes of the Fp groups. According to the model developed by Hoffmann *et al.*,^{34a,43} the $CpFe(CO)_2^+$ fragment, generated from $CpFe(CO)_3^+$, contains one symmetric and one antisymmetric orbitals as its highest occupied molecular orbitals.



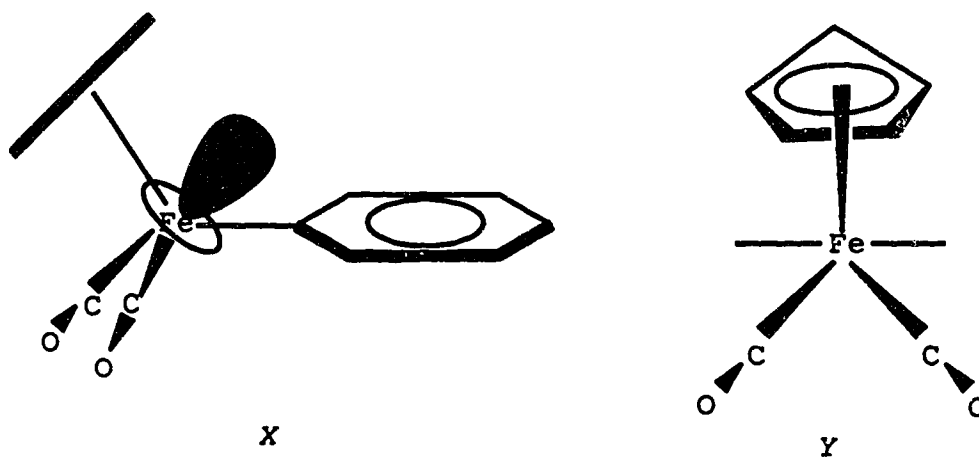
The a'' orbital is particularly well suited for π -interaction with ligands capable of acting as π -acceptors. Thus, in bonding with such ligands (e.g., C_6H_5^- , CH_2 , etc.), the Fp^+ fragment is expected to π -donate to the organic ligands' LUMO primarily through the a'' orbitals which are of higher energy.⁴³ A contribution to π -donation from the SHOMO (second highest occupied molecular orbital) $2a'$, is expected to be less favourable because of the lower energy of this orbital.⁴³ As mentioned earlier, we have shown that in phenylene bridged complexes, the Fp fragment is a π -donor to the arene. A typical LUMO for an arene is illustrated below:



To be consistent with the above calculations, the bonding will favour the geometry in which the arene ring is parallel to the mirror plane of the Fp fragment as in pictures A and B below.



Surprisingly, in this and related arene and azine complexes reported in this thesis, (see also Chapters 3 and 4) the arene ring is oriented perpendicular to the Fp mirror plane as in pictures X and Y below.



Our observations suggest that, at least in the solid state, the predominant π -interaction involves the Fp^+ $2a'$ orbitals donating to the

pyrimidine LUMO, since this will result in maximum overlap for the observed orientation. Since the 2a' orbital is of lower energy than a", and is therefore presumably a poorer π -donor, we cannot fully explain why the orientation of the pyrimidine ring is as observed. We are currently attempting to answer this question by studying the X-ray crystal structures of a number of Fp-azine and Fp-phenyl complexes and by modeling their structures with molecular mechanics calculations to determine the approximate steric component to the orientational preferences.

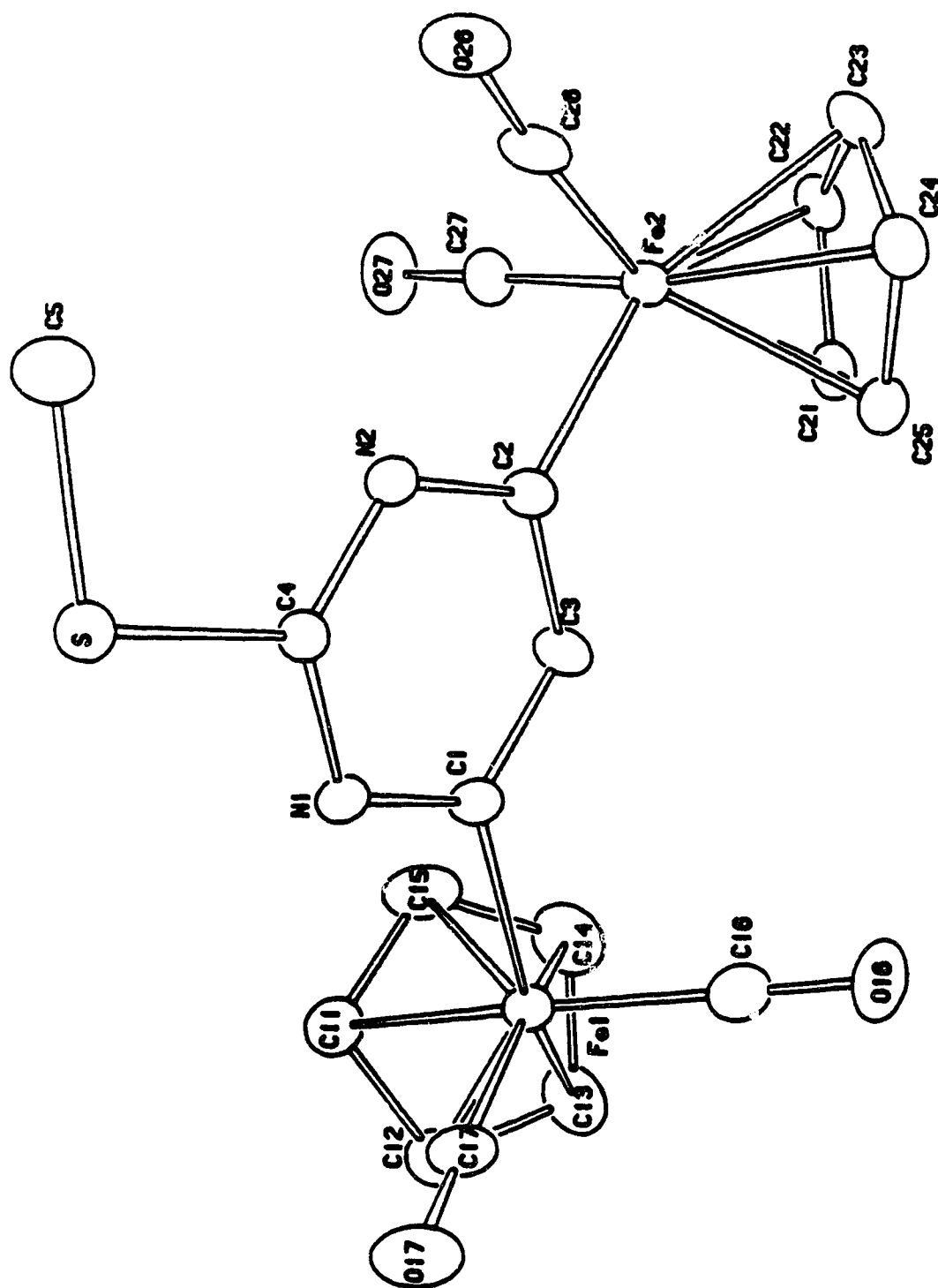


Figure 2.2 ORTEP plot of the complex $[\text{CpFe}(\text{CO})_2]_2\text{C}_4\text{HNSCH}_3$, 5b.

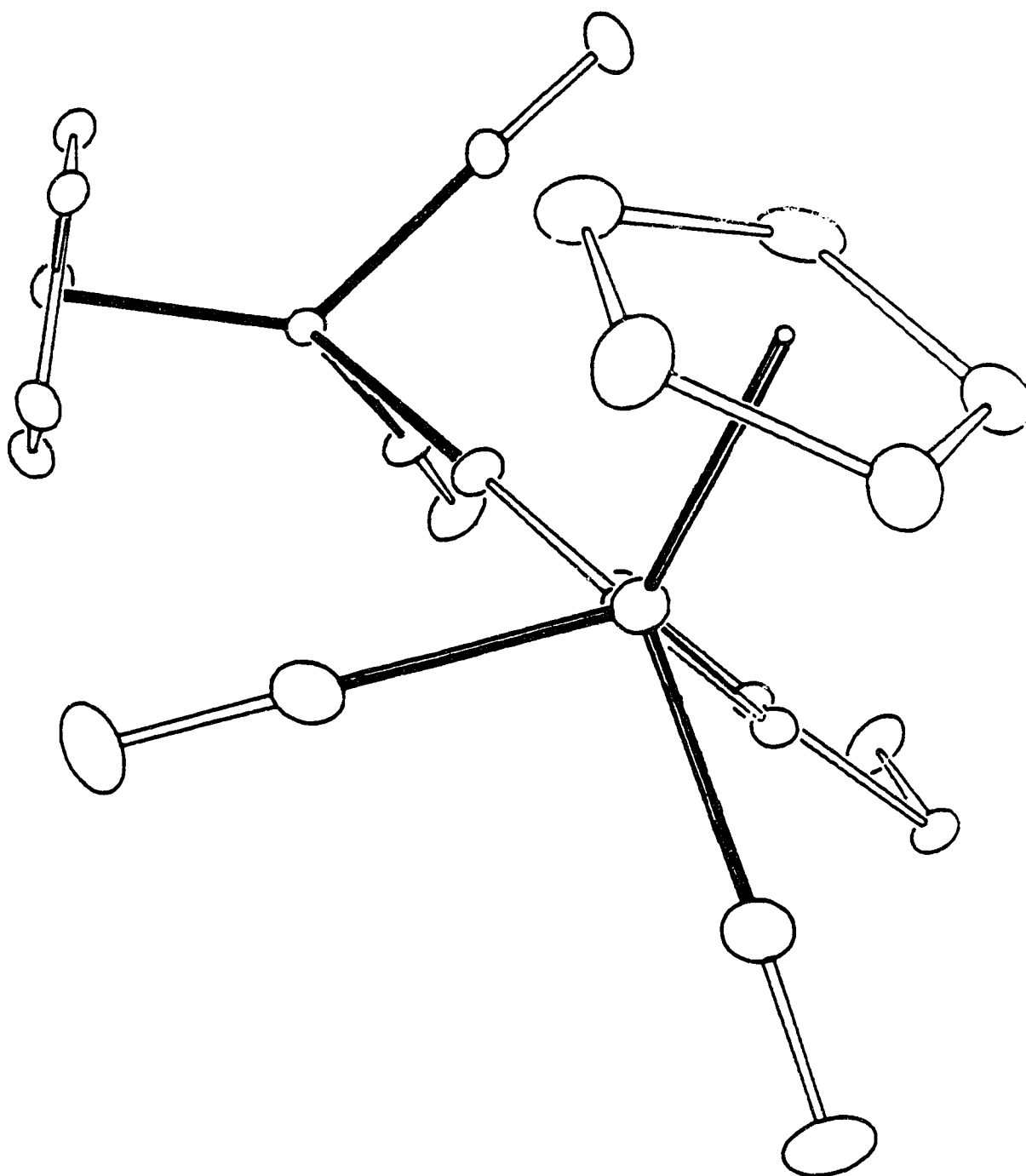


Figure 2.3 ORTEP plot of the complex $[\text{CpFe}(\text{CO})_2]_2\text{C}_4\text{HN}_2\text{SCH}_3$, **5b**, view down Fe1-C1.

Table 3.3 Selected bond lengths in [CpFe(CO)₂]₂C₄H_N2SCH₃, 5b.

Atom1	Atom2	Length	Atom1	Atom2	Length	Atom1	Atom2	Length
Fe1	C11	2.066 (8)	C16	O16	1.136 (10)	C23	C24	1.433 (9)
Fe1	C12	2.101 (8)	C17	O17	1.147 (8)	C24	C25	1.408 (11)
Fe1	C13	2.111 (8)	Fe2	C21	2.107 (7)	C26	O26	1.133 (10)
Fe1	C14	2.094 (8)	Fe2	C22	2.093 (7)	C27	O27	1.153 (9)
Fe1	C15	2.107 (7)	Fe2	C23	2.100 (8)	S	C4	1.776 (6)
Fe1	C16	1.756 (8)	Fe2	C24	2.112 (7)	S	C5	1.789 (9)
Fe1	C17	1.755 (7)	Fe2	C25	2.111 (7)	N1	C1	1.336 (8)
Fe1	C1	1.996 (7)	Fe2	C26	1.756 (8)	N1	C4	1.329 (8)
C11	C12	1.423 (11)	Fe2	C27	1.739 (7)	C1	C3	1.399 (9)
C11	C15	1.411 (12)	Fe2	C2	1.973 (6)	N2	C2	1.351 (8)
C12	C13	1.362 (12)	C21	C22	1.418 (10)	N2	C4	1.325 (8)
C13	C14	1.396 (13)	C21	C25	1.405 (9)	C2	C3	1.385 (10)
C14	C15	1.406 (14)	C22	C23	1.391 (10)			

*In Angstroms. Numbers in parentheses are estimated standard deviations in the least significant digit.

Table 2.4 Selected interatomic angles in [CpFe(CO)2]2C4HN2SCH3, 5b.

Atom1	Atom2	Atom3	Angle	Atom1	Atom2	Atom3	Angle	Atom1	Atom2	Atom3	Angle
C11	Fe1	C16	169.9 (3)	C11	C16	H15	126.8 (9)	C23	C24	H24	127.1
C11	Fe1	C17	100.4 (3)	C14	C16	H15	126.9 (9)	C26	C24	H24	126.1
C11	Fe1	C1	103.7 (3)	Fe1	C16	O16	178.9 (8)	Fe2	C26	H26	126.3
C12	Fe1	C16	127.1 (3)	Fe1	C17	O17	178.6 (7)	C21	C26	C24	109.9 (6)
C12	Fe1	C1	143.0 (3)	C21	Fe2	C26	158.6 (3)	C21	C26	H26	126.4
C13	Fe1	C17	120.3 (3)	C21	Fe2	C27	102.1 (3)	C24	C26	H26	126.6
C13	Fe1	C1	149.4 (3)	C21	Fe2	C2	104.9 (3)	Fe2	C26	O26	176.9 (7)
C14	Fe1	C17	167.5 (4)	C22	Fe2	C26	126.5 (3)	Fe2	C27	O27	177.8 (7)
C14	Fe1	C1	109.8 (3)	C22	Fe2	C2	143.6 (3)	C4	S	C6	102.1 (3)
C15	Fe1	C16	128.1 (3)	C23	Fe2	C27	122.1 (3)	C1	H1	C4	116.2 (6)
C15	Fe1	C17	136.6 (4)	C23	Fe2	C2	161.7 (2)	Fe1	C1	H1	120.5 (6)
Fe1	C11	H11	122.0	C24	Fe2	C27	160.4 (3)	Fe1	C1	C3	120.8 (6)
C12	C11	C16	107.0 (7)	C24	Fe2	C2	112.0 (3)	H1	C1	C3	116.7 (6)
C12	C11	H11	126.7	C25	Fe2	C26	129.6 (3)	C2	H2	C4	117.2 (6)
C16	C11	H11	126.2	C26	Fe2	C27	137.6 (3)	Fe2	C2	H2	117.7 (6)
Fe1	C12	H12	126.4	Fe2	C21	H21	122.7	Fe2	C2	C3	124.8 (6)
C11	C12	C13	108.5 (7)	C22	C21	C26	107.1 (6)	H2	C2	C3	117.3 (6)
C11	C12	H12	126.4	C22	C21	H21	126.7	C1	C3	C2	122.0 (6)
C13	C12	H12	126.1	C25	C21	H21	126.2	C1	C3	H3	119.0
C13	C13	H13	124.1	Fe2	C22	H22	126.9	C2	C3	C2	119.0
C12	C13	C14	109.0 (8)	C21	C22	C23	109.1 (6)	S	C4	H4	113.1 (6)
C12	C13	H13	124.6	C21	C22	H22	126.4	S	C4	H2	118.4 (6)
C14	C13	H13	126.4	C23	C22	H22	126.6	H1	C4	H2	128.6 (6)
Fe1	C14	H14	122.4	Fe2	C23	H23	124.9	S	C6	H61	110.0
C13	C14	C15	109.2 (8)	C22	C23	C24	108.1 (7)	S	C6	H62	108.6
C13	C14	H14	126.9	C22	C23	H23	126.9	S	C6	H63	109.6
C14	C14	H14	126.4	C24	C23	H23	126.0	H61	C6	H62	109.5
Fe1	C15	H15	127.7	Fe2	C24	H24	123.7	H61	C6	H63	109.6
C11	C15	C14	107.3 (8)	C23	C24	C25	106.8 (6)	H62	C6	H63	109.5

*In degrees. Numbers in parentheses are estimated standard deviations in the least significant digit.

Table 2.5 Least squares planes in [CpFe(CO)₂]2C₄H₉N₂SCH₃, 5b.

Plane	Coefficients ^a			Defining Atoms with Deviations ^c				
1	-0.1053	-0.1076	15.2964	5.7491	C11 C13 C15 <u>Fe1</u>	-0.003(7) 0.006(7) 0.008(7) -1.733	C12 C14	-0.001(7) -0.009(8)
2	1.8272	11.2002	-3.4287	8.6770	C21 C23 C25 <u>Fe2</u>	-0.001(8) 0.001(7) 0.002(7) -1.730	C22 C24	0.000(7) -0.002(8)
3	3.3180	-5.0122	11.7986	1.6661	C4 C1 C2 <u>Fe1</u> <u>S</u> <u>C16</u> <u>C2A</u>	0.011(8) 0.005(8) -0.023(8) 0.081 0.124 -1.363 -0.214	W1 C3 W2 <u>Fe2</u> <u>C5</u> <u>C17</u> <u>C2Z</u>	-0.012(5) 0.017(6) 0.006(5) -0.007 0.299 -0.799 1.723

Dihedral Angles^d

Planes	Angle	Planes	Angle	Planes	Angle
1 - 2	101.1	1 - 3	31.6	2 - 3	121.6

^aWeights are derived from the atomic coordinate and using the method of Hamilton, *Acta Cryst.*, 14, 185 (1961).

^bCoefficients are for the form $ax + by + cz - d = 0$ where $x, y,$ and z are fractional crystallographic coordinates.

^cDisplacements from the least-squares plane are given in Angstroms. Those atoms underlined were not included in the definition of the plane.

^dIn degrees.

Table 2.6 Torsional angles in [CpFe(CO)₂]₂C₄HN₂SCH₃, 5b.

Atom 1	Atom 2	Atom 3	Atom 4	Angle
C1	Fe1	C16	O16	-6.53 (35.69)
C2	Fe2	C27	O27	49.58 (17.51)
C16	C11	C12	C13	0.21 (0.80)
C11	C12	C13	C14	0.78 (0.85)
C12	C13	C14	C15	-1.48 (0.85)
C13	C14	C15	C11	1.58 (0.84)
C12	C11	C15	C14	-1.10 (0.80)
C25	C21	C22	C23	- .13 (1.04)
C21	C22	C23	C24	- .07 (1.13)
C22	C23	C24	C25	0.25 (0.92)
C23	C24	C25	C21	- .33 (0.88)
C22	C21	C25	C24	0.29 (0.84)
C5	S	C4	H1	-174.56 (0.48)
C5	S	C4	H2	3.23 (0.58)
C4	H1	C1	C3	1.25 (0.82)
C1	H1	C4	S	175.19 (0.44)
C1	H1	C4	H2	-2.33 (0.91)
C4	H2	C2	C3	2.92 (0.81)
C2	H2	C4	S	-177.26 (0.43)
C2	H2	C4	H1	0.15 (1.38)
H2	C2	C3	C1	-3.92 (0.91)

REFERENCES

1. Some of the work described in this Chapter has been presented in a poster and an oral format, (a) 72nd Canadian Chemical Conference, 1989, Victoria, B.C. *Abstr.* 348. (b) 73rd Canadian Chemical Conference, 1990, Halifax, Nova Scotia *Abstr.* 623IN-F14.
2. (a) Richter-Addo, G.B.; Hunter, A.D. *Inorg. Chem.* 1989, 28, 4063. (b) Hunter A.D. *Organometallics* 1989, 8, 1118. (c) Hunter, A.D.; Szigerty, A.B. *Organometallics* 1989, 8, 2670. (d) Hunter, A.D.; McLernon, J.C. *Organometallics* 1989, 8, 2679. (e) Richter-Addo, G.B.; Hunter, A.D.; Wichrowska, N. *Can. J. Chem.* 1990, 68, 41.
3. (a) See Ogawa, H.; Onitsuka, K.; Joh, T.; Takahashi, S.; Yamamoto, Y.; Yamazaki, H. *Organometallics* 1988, 7, 2257, and references cited therein. (b) Maata, E.A.; Changmin, K. *Inorg. Chem.* 1989, 28, 624.
4. See for example, (a) Woitellier, S.; Launay, J.P.; Spangler, C.W. *Inorg. Chem.* 1989, 28, 758. (b) Gross, R.; Kiam, W. *Inorg. Chem.* 1986, 25, 498. (c) Woitellier, S.; Launay, J.P.; Spangler, C.W. *Inorg. Chem.* 1989, 28, 758; (d) Zulu, M.M.; Lees, A.J. *Organometallics* 1989, 8, 955.
5. (a) Farizzi, F.; Sunley, G.J.; Wheeler, J.A.; Adams, H.; Bailey, N.A.; Montlis, P.M. *Organometallics* 1990, 9, 131. (b) Booth, B.L.; Haszeldin, R.N.; Taylor, M.B. *J. Chem. Soc. (A)* 1970, 1974. (c) Green, M.; Tauton-Rigby, A.; Stone, F.G.A. *J. Chem. Soc. (A)* 1968, 173. (d) Booth, B.L.; Haszeldine, R.N.; Taylor, M.B. *J. Organomet. Chem.* 1966, 6, 570. (e) Cooke, J.; Green, M.; Stone, F.G.A. *Inorg. Nucl. Chem. Lett.* 1967, 347. (f) King, R.G. *Inorg. Chem.* 1963, 2, 531. (g) Crociani, B.; DiBianca, F.; Giovenco, A.; Berton, A.; Bertani, R. *J. Organomet. Chem.* 1989, 361, 255.

6. (a) Rausch, M.D.; Criswell, T.R.; Ignatowicz, A.K. *J. Organomet. Chem.* **1968**, *13*, 419. (b) Nesmeyanov, A.N.; Kolobova, N.E.; Goncharenko, L.V.; Ansimov, K.N. *Izv. Akad. Nauk SSSR, Ser. Khim.* **1976**, *1*, 153, (Engl. translation, 142). (c) Nesmeyanov, A.N.; Ansimov, K.N.; Kolobova, N.E. *Izv. Akad. Nauk SSSR, Ser. Khim.* **1964**, *12*, 2247, (Engl. translation, 21153).
7. Artamkiya, G.A.; Milchenko, Y.A.; Beletskaya, I.P.; and Reutov, O.A. *J. Organomet. Chem.* **1987**, *321*, 371.
8. (a) Mort, J.; Pfister, G. *Electronic Properties of Polymers*; John Wiley & Sons: New York, **1982**. (b) Parasad, P.N.; Ulrich, D.R. *Non Linear Optical and Electroactive Polymers*; Plenum: New York; **1988**.
9. Shaver, A.; Butler, I.S.; Gao, J.-P. *Organometallics* **1989**, *8*, 2079.
10. Shriver, D.F.; Drezdson, M.A. *The Manipulation of Air Sensitive Compounds*, 2nd ed.; John Wiley & Sons: New York; **1986**.
11. Perrin, D.D.; Armarego, W.L.F.; Perrin, D.R.; *Purification of Laboratory Chemicals*, 3rd ed.; Pergamon: New York; **1987**.
12. See reference 10 and 11 for techniques on how to avoid organic peroxide build up.
13. Hogg, A.M. *Int. J. Mass Spectrom. Ion Phys.* **1983**, *49*, 25.
14. Caution: see reference 2c p.2671 for synthesis of sodium amalgam.
15. King, R.G. *Organomet. Synth.*; Academic Press: New York; **1965**, Vol. 1, p.114.
16. Wash solvent grade.
17. Matsuzaka, M.; Okabe, H.; Tanaka, S. *Chem. Abs.* **87**:135079, *Japan Kokai* **1977**, *33*, 677.

18. We recently reported^{2c} the successful thermal decarbonylation of related metal acyl complexes under these conditions.
19. (a) Feringa, B.L.; Hulst, R.; Rikers, R.; Brandsma, L. *Communications*, 1987, 316. (b) Brandsma, L. *Preparative Polar Organometallic Chemistry* Springer-Verlag: Berlin, Heidelberg; 1987, Vol. I.
20. (a) *International Tables of X-ray Crystallography* Kynoch: Birmingham; 1969, 1. (b) *ibid*, 1974, 4. (c) Walker, N.; Stuart, D. *Acta Crystallogr.* 1969, A39, 158. (d) *Enraf-Nonius Structure Determination Package, Version 3*, 1985, Delft, The Netherlands.
21. (a) Dessy, R.E.; Pohl, R.L.; King, R.B. *J. Am. Chem. Soc.* 1966, 88, 5121. (b) Henderson, S.; Henderson, R.A. *Adv. in Phys. Org. Chem.* 1987, 23, 7. (c) Artamskina, G.A.; Mil'Chenko, A.Y.; Beletskaya, I.P.; Reutow, D.A. *J. Organomet. Chem.* 1986, 311, 199.
22. Comins, D.L.; O'Connor, S. *Adv. in Heterocycl. Chem.* 1988, 44, 199 and work cited therein.
23. Joule, J.A.; Smith, G.F. *Heterocycl. Chem.* Van Nostrand Reinhold: Berkshire; 1978.
24. (a) Lowry, T.H.; Richardson, K.S. *Mechanism and Theory in Organic Chemistry* Harper & Row: New York; 1987, p.374, p.645. (b) Norman, R.O.C. *Principles of Organic Synthesis*, 2nd ed. Chaucer: Norfolk; 1978, p427. (c) Bunnett, J.F. *Acc. Chem. Res.* 1978, 11, 413.
25. (a) Kochi, J.K. *Angew. Chem. Int. Ed. Engl.* 1988, 27, 1227. (b) Heppert, J.A.; Morgenstern, M.A.; Schernbel, D.M.; Takusagawa, F.; Shaker, M.R. *Organometallics*, 1988, 7, 1715.
26. (a) Miholova, D.; Vlcek, A.A. *Inorg. Chim. Acta*, 1980, 41, 119. (b) Gresova, D.; Vlcek, A.A. *Inorg. Chim. Acta*, 1967, 1, 482.

27. Stock, L.M. *Aromatic Substitution Reactions*, Prentice-Hall Foundations of Modern Organic Chemistry Series, Prentice-Hall: Englewood; 1968.
28. Guo, X. G.; Chukwu, R.; Hunter, A.D. *Unpublished observations*.
29. (a) Dillow, G.W.; Karbale, P. *J. Am. Chem. Soc.* 1989, 111, 5592;
(b) Chowdhury, S.; Kishi, H.; Dillow, G.W.; Karbale, P. *Can. J. Chem.* 1989, 67, 603.
30. Bruce, M.I.; Stone, F.G.A. *J. Chem. Soc. (A)* 1966, 1837.
31. (a) Gershon, H.; Grefig, A.T.; Scala, A.A. *J. Heterocycl. Chem.* 1983, 20, 219. (b) Haas, A.; Lieb, M. *J. Heterocycl. Chem.* 1986, 23, 1079.
32. Thiophene and thiophene like compounds are the most prevalent sulphur containing contaminants in crude petroleum and are most difficult to desulphurize, see for example (a) Hockett, S.C.; Angelici, R.J. *Organometallics* 1988, 7, 1491. (b) Schuman, S.C.; Schalit, H. in *Cat. Rev.* Heinemann, H.; Ed.; Marcel Dekker: New York, 1971, p.246.
33. Stewart, R.P.; Treichel, P.M. *J. Am. Chem. Soc.* 1970, 92, 2710.
34. For calculations on related systems, see (a) Schilling, B.E.R.; Hoffmann, R.; Lichtenberger, D.L. *J. Am. Chem. Soc.* 1979, 101, 585.
(b) Seeman, J.I.; Davies, S.G. *J. Am. Chem. Soc.* 1985, 107, 6522.
(c) Crocco, G.L.; Gladysz, J.A. *J. Am. Chem. Soc.* 1988, 110, 6110.
35. Ewing, D.F. *Org. Magn. Reson.* 1979, 12, 499.
36. Lukehart, C.M. *Fundamental Transition Metal Organometallic Chemistry*, Brooks/Lee: Monterey; 1985, p79.
37. (a) Levy, G.C.; Lichter, R.L.; Nelson, G.L. *Carbon-13 Nuclear Magnetic Resonance Spectroscopy*, John Wiley & Sons: New York; 1980.
(b) Sothers, J.B. *Carbon-13 NMR Spectroscopy*; Academic: New York; 1972. (c) Memory, J.D.J.; Wilson, N.K. *NMR of Aromatic Compounds*;

- John Wiley & Sons: New York; 1982. (d) Ernst, L.; Wray, V.; Chertkov, V.A.; Sergeyev, N.M. *J. Magn. Reson.* 1975, 25, 123.
38. See for example Lichter, R.L.; Wasylshen R.E. *J. Am. Chem. Soc.* 1975, 97, 1808 and work cited therein.
39. (a) Brown, D.A.; Chester, J.P.; Fitzpatrick, N.J.; King, I.J. *Inorg. Chem.* 1977, 16, 2497. (b) Gansow, O.A.; Schexnayder, D.A.; Kimura, B.Y. *J. Am. Chem. Soc.* 1972, 94, 10. (c) Karplus, M.; Pople, J.A. *J. Chem. Phys.* 1963, 38, 2804.
40. (a) Bruce, M.I. *J. Chem. Soc. (A)* 1968, 1459. (b) Buckingham, A.D.; Pitcher, E.; Stone, F.G.A. *J. Chem. Phys.* 1962, 36, 124.
41. For structures of CpFe(CO)L aryls see (a) Adrianov, V.G.; Sergeeva, G.N.; Streuchkov, Y.T.; Aninov, K.N.; Kolobova, N.E.; Beechastnov, A.S. *Zh. Strukt. Kim.* 1970, 11, (Engl. translation, 168). (b) Lehmukuhi, H.; Mehler, G.; Benn, R.; Rufinska, A.; Schroth, G.; Kruger, C.; Raabe, E. *Chem. Ber.* 1987, 120, 1987. (c) Semion, V.A.; Struchkov, Y.T. *Zh. Strukt. Khim.* 1969, 10, (Engl. translation, 80).
42. For structures of Fp-R (where R is sp² hybridized) see: (a) Churchill, M.R.; Wormald J. *Inorg. Chem.* 1969, 8, 1936. (b) Ferede, R.; Noble, M.; Cordes, A.W.; Allison, N.T.; Lay, J. Jr. *J. Organomet. Chem.* 1988, 399, 1. (c) Bruce, M.I.; Liddell, J.J.; Snow, M.R.; Tickink, E.R.T. *J. Organomet. Chem.* 1988, 354, 103. (d) Dhal, L.F.; Doedena, R.J.; Huble, W.; Nielson, J. *J. Am. Chem. Soc.* 1966, 88, 446. (e) Kolobova, N.E.; Rozaantava, T.V.; Structov, Y.T.; Betaanov, A.S.; Bakmutov, V.I. *J. Organomet. Chem.* 1985, 292, 247.
43. Schilling, B. E. R.; Hoffmann, R. and Faller, J. W. *J. Am. Chem. Soc.* 1979, 101, 592.

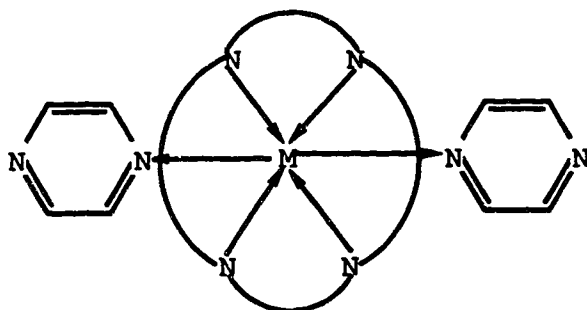
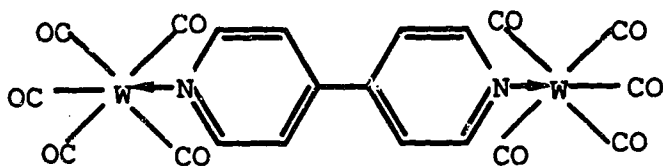
CHAPTER 3

ELECTROCHEMICAL AND SPECTROSCOPIC STUDIES OF PHENYL AND PYRIDINE COMPLEXES OF IRON AND X-RAY CRYSTAL STRUCTURE OF ((η^5 -CYCLOPENTADIENYL)IRONDICARBONYL)-PENTAFLUOROPHENYL.¹

INTRODUCTION

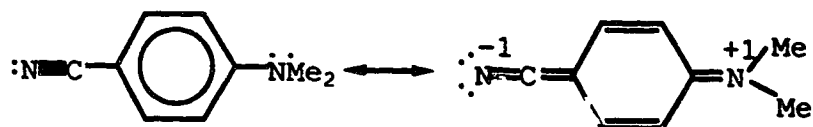
A wide variety of transition metal coordination and organometallic complexes are known to exhibit long range electron transfer properties.² This phenomenon is of considerable interest especially with regards to their potential applications in molecular electronics, photovoltaic devices, and non-linear optical materials.³ Among the most studied of such complexes are those in which the bridging ligands are composed of highly polarizable, conjugated π -systems which act as relay centres for the metal-metal communication in these species.

The study of the redox behaviour of these complexes has been shown to be a particularly useful means towards understanding this phenomenon of electron transfer.^{2c,4} In particular, the technique of cyclic voltammetry has been widely employed for such studies. Considering such problems as solubility which often hamper rigorous studies on polymers with related compositions, attention has been directed towards the study of monomeric and oligomeric model compounds e.g.

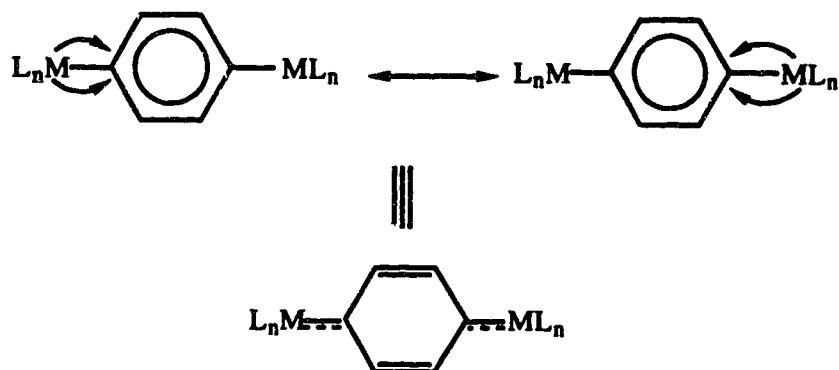


The spherical structure represents a porphyrin
 M = Fe, Ru, Os, Ni etc.

As reported in the previous Chapters of this thesis, we have synthesized a range of phenylene and azine bridged complexes, including terminal phenyl and azine bonded complexes. Spectroscopic evidence from these synthetic studies shows that the Fp fragment [$\text{Fp} = (\eta^5\text{-C}_5\text{H}_5)\text{Fe}(\text{CO})_2$] is a strong π -donor and interacts strongly with the π -systems of the bridging ligands. This factor should be favourable for the electronic interactions of the metal centres in bimetallic and polymetallic systems. We also have ^{13}C NMR evidence^{5a} to show that in the phenylene bridged complexes, the strongest interaction occurs when the organometallic groups are arranged *para* to one another (e.g., 1,4- $\text{C}_6\text{H}_4\text{Fp}_2$). Similar observations have generally been made in organic compounds in which a π donor group is substituted *para* to a π acceptor group. In Valence Bond terms such strong coupling is generally rationalized as being due in part to the contribution from a zwitterionic resonance form (see diagram below), which arises from a *through-resonance* interaction between the donor and acceptor groups, i.e.

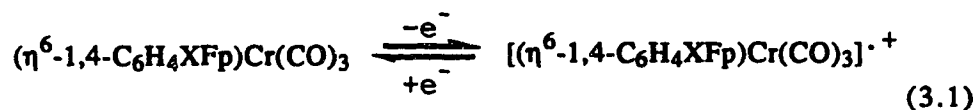
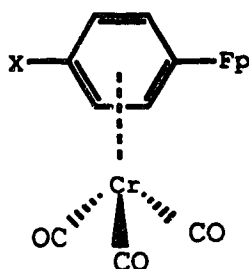


In the case of compounds with transition metal substituents, the presence of partially filled d orbitals on the transition metal fragments imparts to these metal fragments the ability to act as both donor and acceptor groups. Since the metal to arene π donation (from essentially non-bonding filled d orbitals on the metal to the arene π^*) seems to be maximized by *para*-substitution geometries, it appears that significant contributions from resonance structures which have quinone type features (dimetalloquinone) with partial metal to arene double bond character exists. Such resonance contributions can be represented as shown below.

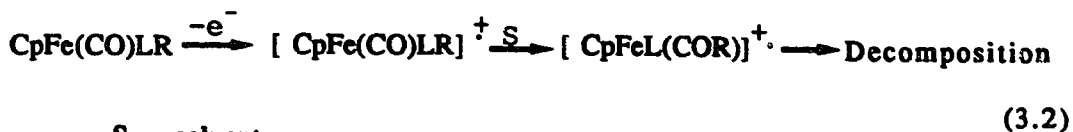


Since the arene ring is a poor donor ligand, the result will be a net transfer of electron density from iron to the arene ring and thus a greater degree of shielding of the *ipso* carbons should occur for the *para* substituted species as was previously reported.^{5a}

Work in our laboratories on phenylene-bridged polymetallic σ -, π -complexes containing iron and chromium^{5b,c} has shown that such complexes undergo reversible one electron oxidations, with the oxidation taking place at HOMOS which seem to be centered at the π -bonded metal centre.



Electrochemical reduction studies on complexes of type $(\eta^5\text{-C}_5\text{R}'_5)\text{FeL}_2\text{X}$ (where $\text{R}' = \text{H}, \text{CH}_3$; $\text{L} = \text{CO}, \text{PPh}_3, 1/2 \text{ dppe}$; $\text{X} = \text{halide, alkyl, aryl, etc.}$) are numerous.⁶ Similar complexes have also been subjected to electrochemical oxidation studies, including those in which the σ -bonded X ligand is an alkenyl⁷ or an alkynyl⁸ group. These later studies show that the oxidation takes place at the metal centre, usually with single electron transfer. The seventeen electron radical cation intermediates formed are generally labile, resulting in irreversible electrochemical oxidations



S = solvent

R = alkyl, benzyl, alkenyl, alkynyl, etc.

Fine tuning of the steric or electronic properties of the complexes *via* changing of the substituents on the ligands has sometimes led to stabilization of the radical cation. Work carried out by Whiteley *et al.*,⁸ shows that at scan rates of 0.1 V/s, the oxidation of complexes $[(\text{dppe})(\eta^5\text{-Cp})\text{Fe}(\text{CCPh})]$ and $[(\text{dppe})(\eta^5\text{-Cp})\text{Fe}(\text{CCBu}^t)]$ are completely reversible ($i_{p,c}/i_{p,a} = 1.0$, where this represents the ratio of the cathodic peak current over the anodic peak current, and is used to establish chemical reversibility, *vide infra*) whereas the complexes $[(\text{CO})(\text{PPh}_3)(\eta^5\text{-Cp})\text{Fe}(\text{CCPh})]$ and $[(\text{CO})(\text{PPh}_3)\eta^5\text{-CpFeCCBu}^n]$ exhibit electrochemical reversibility but not *formal* chemical reversibility ($i_{p,c}/i_{p,a} = 0.95$, for chemical reversibility, $i_{p,c}/i_{p,a} = 0.96^9$). To the best of our knowledge, the electrochemical oxidation studies of related complexes wherein the σ bonded X ligand is an aryl or an azinyl group and where L are both CO groups (e.g., $\text{C}_5\text{NF}_2\text{Cl}_2\text{Fp}$, $\text{C}_6\text{F}_4\text{Fp}_2$, etc.) have not been reported. We have therefore extended our studies on phenyl/pyridyl σ -bonded organoiron complexes to their electrochemical oxidations, with a view to elucidating the effects of the steric/electronic demands of the arene ring on the extent of metal-arene electron transfer and consequently the metal-arene-metal electronic interaction. We were also interested in elucidating the influence of the substitution geometry of the Fp group on the ring on such metal-arene-metal communications.

In this Chapter, the characterization of these complexes by cyclic voltammetry, spectroscopy and X-ray crystallography is reported.

EXPERIMENTAL SECTION

Unless otherwise noted, all reactions and subsequent manipulations were performed under anaerobic and anhydrous conditions. Reagents and chemicals used were handled by conventional techniques.¹⁰ The Fp_2 and $FpCl/FpI$ used were synthesized and purified by standard procedures.¹¹ General procedures routinely employed in the synthetic and spectroscopic studies have been described in the previous Chapter. The analytical, mass spectral, and IR data for the complexes synthesized during this work are collected in Table 3.1. Synthetic procedures and non-optimized yields are recorded below.

Preparation of C_6H_5Fp (1) and 1,3- $C_6H_4Fp_2$ (2).

The synthesis of 1,3- $C_6H_4Fp_2$ via synthesis of the acyl complex followed by thermal decarbonylation has earlier been reported.^{5a} The synthesis of C_6H_5Fp via the same route is reported below.

Synthesis of $C_6H_5C(O)Fp$.

In a three-neck flask equipped with a side arm was placed an excess of sodium amalgam, (25.20 g, 25.0 mmol Na). The amalgam was liquified by addition of a few drops of mercury and then THF (75 mL) was added followed by Fp_2 (2.50 g, 7.1 mmol). The resulting dark red solution was stirred vigorously for 45 min to produce an orange solution containing $NaFp$ (see Chapter 2). Excess amalgam was drained through the side arm on the reaction flask and the solution was then filtered through Celite (2x3 cm) supported on a medium porosity fritted funnel to remove any finely divided amalgam and

washed with THF (2x10 mL). The NaFp solution was cooled to $\sim -78^{\circ}\text{C}$ (solid CO_2 /acetone bath) and then benzoyl chloride (2.00 g, 14.3 mmol) was added. The solution was stirred at $\sim -78^{\circ}\text{C}$ for 1 h and then the cooling source was removed. The solution was then allowed to warm up to ambient temperature over a period of 1 h. The reaction mixture was taken to dryness *in vacuo* and the resulting solid was washed in air with distilled H_2O (2x15 mL) and then heptane¹² (3x10 mL). The yellow powder remaining was dried under vacuum to give a 90% yield (3.60 g, 12.8 mmol) of desired product, $\text{C}_6\text{H}_5\text{C}(\text{O})\text{Fp}$

Thermal decarbonylation of $\text{C}_6\text{H}_5\text{C}(\text{O})\text{Fp}$.

A 300 mL three-neck flask fitted with an air condenser was flushed with dinitrogen. Then the acyl compound synthesized above (1.00g, 3.6 mmol) was placed in the flask followed by a toluene/ Bu_2O (30:70) mixture (75 mL) and the mixture was set to reflux (care being taken to avoid any local overheating or splashing of the acyl on the sides of the flask). The progress of the reaction was monitored by occasionally cooling a sample in a vial, drying with dinitrogen and then obtaining the IR spectrum in CH_2Cl_2 . The reflux was stopped after 4 h, when the acyl peak at 1620 cm^{-1} had almost completely disappeared while a Fp_2 dimer peak at 1790 cm^{-1} began to appear. The heating source was removed and the flask and its contents were allowed to cool to room temperature. The mixture was taken to dryness *in vacuo* and the desired compound was purified by column chromatography. The first band eluted with pentane ($\sim 60\text{ mL}$) in a Florisil packed (14x2.5 cm) column was the desired product. This compound was crystallized in minimum CH_2Cl_2 ($\sim 8\text{ mL}$) at -9°C to give an 80% yield (0.72 g, 2.9 mmol) of orange crystals of $\text{C}_6\text{H}_5\text{Fp}$, (1).

Syntheses of C₆F₅Fp (6) and C₆F₃H₂Fp (4).

The syntheses of these two compounds were carried out by a procedure analogous to that described in the literature.¹³ Thus, to a solution of NaFp (16.8 mmol) in THF (90 mL), prepared as above, was added C₆F₆ (2.0 g 16.8 mmol) at -78°C , and the solution was stirred at this temperature for about 1 h. The cooling source was then removed and the solution was stirred for 2 h, during which time its contents warmed up to room temperature. The solution was then taken to dryness *in vacuo* and the product was isolated as the second band from a Florisil packed column, with pentane as eluting solvent. The product was crystallized in minimum CH₂Cl₂ (10 mL) to give a 60% yield (2.22 g, 6.4 mmol) of C₆F₅Fp, (6) as yellow crystals. A similar reaction carried out with 1,2,3,5-C₆F₄H₂ yielded 48% of compound 4 C₆F₃H₂Fp (for isomeric form, see page 77) as a yellow powder.

¹⁹F NMR ((CD₃)₂SO) Compound 4 -112.1 (m, F6), -119.5 (m, F2), -135.9 (m, F5).

Syntheses of 1,4-C₆FH₄Fp (3), 1,3-C₆F₄HFp (5), 1,3-C₆F₄Fp₂ (8), and 1,4-C₆F₄Fp₂ (7).

All these compounds were synthesized in a similar manner, the synthesis of 1,4-C₆FH₄Fp being described in detail.

In a 300 mL three-neck flask fitted with an addition funnel was placed n-BuLi (2.5 M solution in hexanes, 2 mL, 5.0 mmol) followed by an Et₂O/hexane (50:50) mixture (40 mL). The solution was cooled to -78°C . The compound 1,4-C₆H₄FBr (2.00 g, 11.4 mmol) was placed in the addition funnel and Et₂O (20 mL) was added. This solution was added to the cold (-78°C) mixture in the flask over 10 min. The cooling source was removed and the

mixture warmed up to room temperature and was stirred for an additional 20 min at 10-15°C. The mixture was again cooled to -78°C and THF (50 mL) was added. To the resulting greenish solution was added solid FpI (3.47 g, 11.4 mmol) over 5 min. The mixture was then stirred at -78°C for 1 h and the cooling source was removed. After 2 h, the solution was taken to dryness *in vacuo*, and the resulting solid dissolved in heptane/toluene (50:50, 15 mL). This solution was eluted on a Florisil packed (14x5 cm) column with pentane. The first bright yellow column had ν_{CO} at 2003 (vs), 1942 (vs) cm^{-1} (in CH_2Cl_2). The compound was identified by MS to be FpBu, but was not further studied. The second yellow band was shown to be the desired product. This yellow solution was taken to dryness to give a 63% yield (1.90 g, 7.0 mmol) of the desired product as a bright yellow powder.

Compounds 5, 7 and 8 were synthesized in an analogous manner in yields of 42%, 74% and 8%, respectively.

^{19}F NMR ($(\text{CD}_3)_2\text{SO}$) δ for Compound 3 -124.04 (m, F1). For Compound 5 - 81.82 (m, F2), -100.3 (m, F4), -141.6 (m, F6), -167.6 (m, F5). Compound 7 -108.27 (S). Compound 8 -45.3 (m, F2), -108.1 (m, F4/F6), -166.0 (m, F5).

Synthesis of 2,6- $\text{C}_5\text{NH}_3\text{FFp}$ (9), $\text{C}_5\text{NF}_4\text{Fp}$ (10), $\text{C}_5\text{NF}_3\text{ClFp}$ (11) and $\text{C}_5\text{NF}_2\text{Cl}_2\text{Fp}$ (12).

The syntheses and characterization of these compounds have been described in the previous Chapter.

Reaction of $\text{C}_5\text{NF}_4\text{Fp}$ (10) with Ag^+PF_6^- .

A 100 mL three-neck flask was charged with the complex $\text{C}_5\text{NF}_4\text{Fp}$ (0.51g, 1.6 mmol). To this was added CH_2Cl_2 (50 mL) followed by Ag^+PF_6^- (0.40 g, 1.6

mmol). The resulting bright yellow mixture was stirred and the reaction monitored by IR. After about 30 min, the mixture became light orange in colour. An IR spectrum of the reaction mixture at this stage showed peaks at 2005 and 2050 cm^{-1} . The reaction mixture was stirred for a further 4 h but there was no noticeable change in either the colour or the IR spectrum. The reaction mixture was taken to dryness, and a sample of the product mixture was analyzed by mass spectroscopy. to show a peak at m/z 435, attributable to a new complex in which the Ag^+ had become attached to the Fp containing starting material i.e. $[\text{C}_5\text{NF}_4\text{FpAg}]^+\text{PF}_6^-$. No further purification was performed on the product.

Electrochemical analysis of the products.

A standard three-electrode cell¹⁴ of approximately 40 mL volume was used for the cyclic voltammetric experiments. The working electrode was a small (~1 mm diameter) Pt bead sealed in soft glass. A coiled Pt wire (~15 cm in length) was used as the auxiliary electrode. The aqueous SCE reference electrode was separated from the working electrode compartment by a fine frit and a Luggin probe. The $[\text{n-Bu}_4\text{N}]\text{PF}_6$ support electrolyte was prepared by metathesis of $[\text{n-Bu}_4\text{N}]\text{I}$ with NH_4PF_6 in hot acetone and was recrystallized three times from ethanol. The $[\text{n-Bu}_4\text{N}]\text{PF}_6$ and the cell parts were dried in an oven at 130°C overnight just prior to use. The working electrode was cleaned by placing the electrode tip over boiling HNO_3 (reagent grade) for 1h, rinsing with distilled water (1 L), and then soaking it in a saturated ferrous ammonium sulphate solution (made up in 1 M H_2SO_4) for 30 min. Finally, it was rinsed with distilled water (1 L) and acetone (0.5 L reagent grade, Analar) and then was dried with a hot air gun just prior to use.

Dichloromethane (Spectrograde, BDH) was stirred over alumina (5 g, Woelm neutral, W200 Super 1) while simultaneously being purged with prepurified dinitrogen for 30 min. The solvent with some entrained alumina (~0.5 g) was then transferred by cannula to the electrochemical cell, which had been previously set up on a vacuum line under argon. The solutions employed during cyclic voltammetry (CV) were typically 5 to 7 X 10⁻⁴M in organometallic complex and 0.1M in [n-Bu₄N]PF₆].

The potentials were generated by a BAS CV27 voltammograph, and the resulting cyclic voltammograms were recorded on a Hewlett Packard 7090A X-Y recorder. The formal oxidation potential (E°) for reversible couples is defined as the average of the anodic ($E_{p,a}$) and cathodic ($E_{p,c}$) peak potentials. The separation of the cathodic and anodic potentials ΔE is defined by $|E_{p,c} - E_{p,a}|$, and the cathodic to anodic peak current ratio is defined by $i_{p,c}/i_{p,a}$.¹¹ Diffusion control was established for redox processes by the observation of a linear plot of $i_{p,c}$ vs the square root of scan rate ($v^{1/2}$) over at least one order of magnitude of scan rate. The oxidation of ferrocene is reported to be highly reversible in many solvents.¹⁵ After each experiment, ferrocene was added as an internal reference.¹⁶ Under our experimental conditions, ferrocene is reversibly oxidized $E^{\circ} = +0.47$ V vs SCE. ($i_{p,c}/i_{p,a} = 1.0$; $\Delta E = 60-70$ mV at 0.1 Vs⁻¹). The ratio $i_{p,c}/i_{p,a}$ is used throughout the text to establish chemical reversibility for the complexes studied. The electrochemical reversibility was established by comparison of the scan rate dependence of ΔE of the analyte to that of ferrocene recorded under identical conditions. In general, reversible first oxidations were exhausted before the second oxidations were studied, usually with a fresh electrode. Electrochemical data for the complexes are collected in Table 3.2.

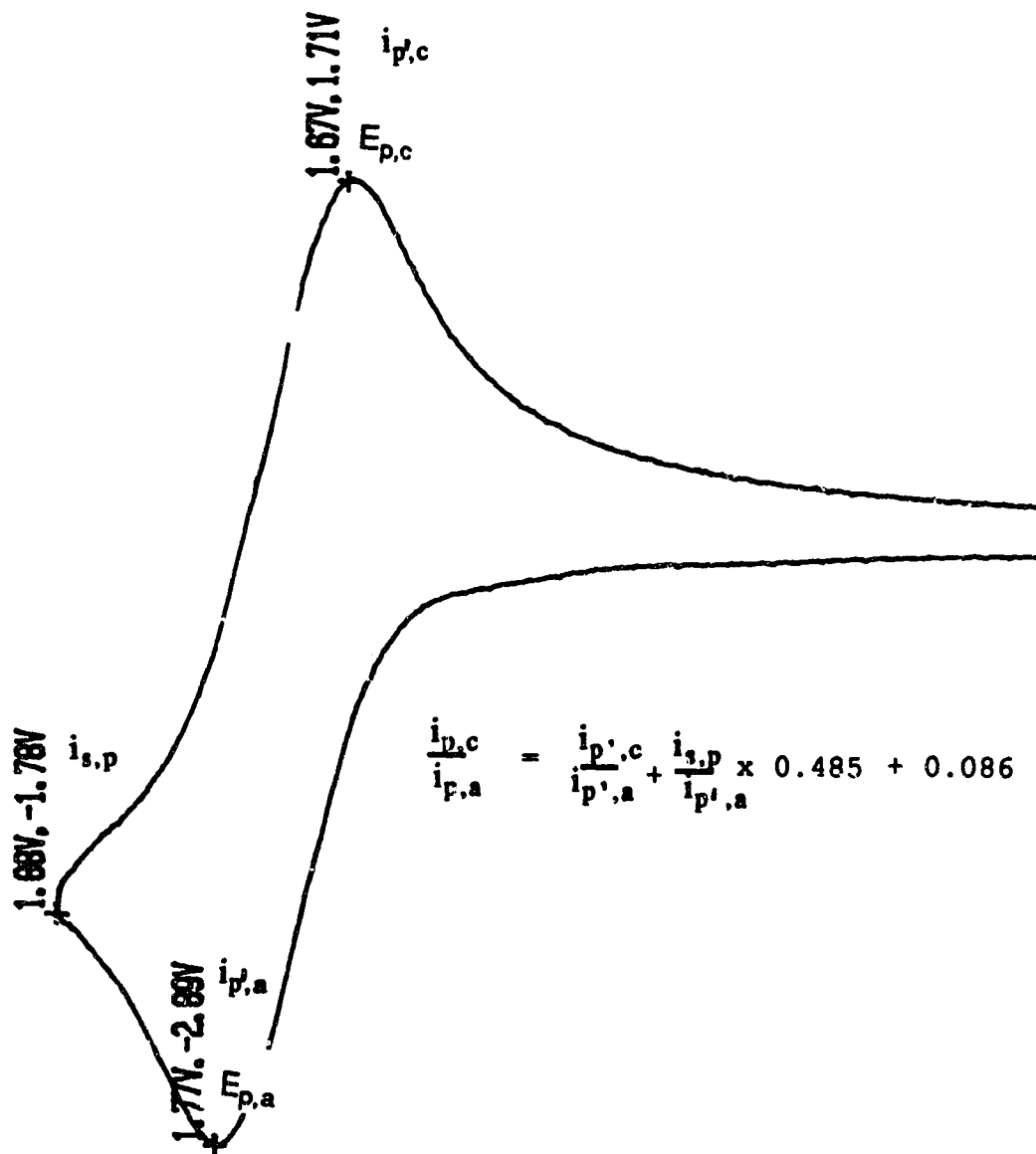


Figure 3.1 Cyclic voltammogram of a representative compound, showing some important features.

X-ray Crystal Structure Determination of C₁₃H₅F₅FeO₂.

All data collection and analysis was done by Dr. B.D. Santarsiero of this department. A clear brown crystal of C₁₃H₅F₄FeO₂ (approximate dimensions 0.258x0.262x0.528 mm) was mounted on a glass fiber with epoxy, and optically centered in the X-ray beam of a diffractometer. Crystal data: FW = 325.02, orthorhombic space group *Pnma* (No. 62),^{17a} $a = 6.993(2)$, $b = 12.774(4)$, $c = 13.649(3)$ Å, $V = 1219.2$ Å³, $z = 4$, $D_c = 1.771$ g cm⁻³, MoK α radiation ($\lambda = 0.71073$ Å) $\mu(\text{MoK}\alpha) = 12.80$ cm⁻¹. The X-ray diffraction data (5959 reflections) were collected at $\sim -50^\circ\text{C}$ on an Enraf-Nonius CAD4 diffractometer by the ω - 2θ scan method (ω scan width = $0.90 + 0.347 \tan \theta$).

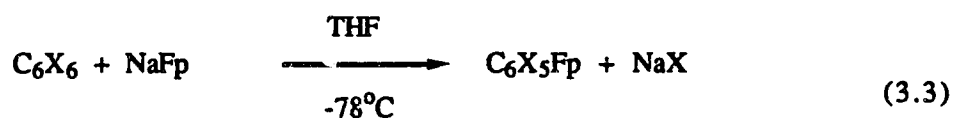
The structure was solved by examination of Patterson and Fourier maps, and adjusted by full-matrix least squares refinement. The hydrogen atoms were generated at idealized calculated positions by assuming a C-H bond length of 0.95 Å and the appropriate sp² geometry. These atoms were then included in the calculations with fixed, isotropic Gaussian parameters 1.2 times that of the attached atom and constrained to ride on the attached atom. The data were corrected for absorption (and other systematic errors) using a scheme based on the absorption surface (Fourier filtering) method of Walker and Stuart.^{17b} The refinement converged to a final GOF of 1.64 and R of 0.047, with anisotropic Gaussian displacement parameter for all non-hydrogen atoms. The Enraf-Nonius SDP Program Package^{17c} was used.

Results and Discussion

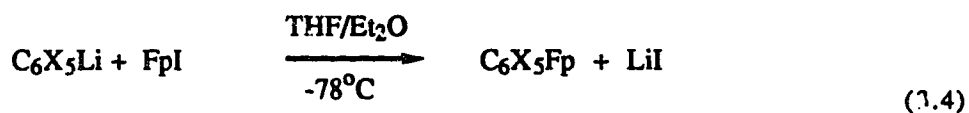
Syntheses of the Complexes

The syntheses of the required complexes were approached using the three widely applied routes to such species namely:

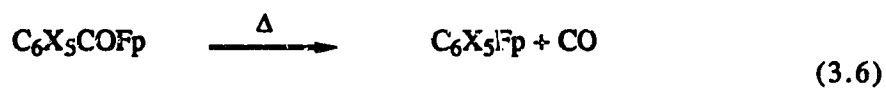
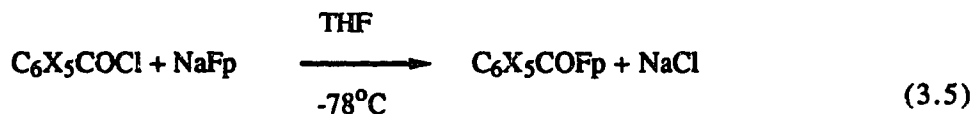
- (a) Direct nucleophilic displacement of a halide on the benzene/pyridine ring, e.g.



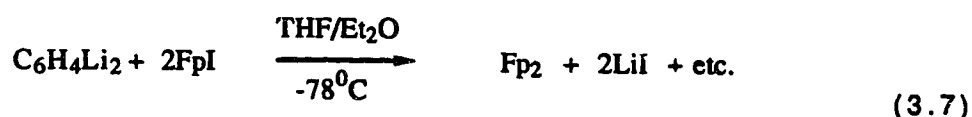
- (b) Metallation of the benzene/azine, *via* bromine lithium exchange, or deprotonation followed by metathesis reaction with FpI/FpCl.



- (c) Synthesis of the acyl complex *via* nucleophilic attack of the Fp⁻ anion on an acid chloride, followed by thermal decarbonylation of the acyl complex, e.g.



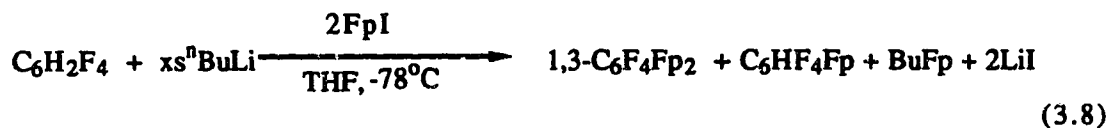
Each complex was synthesized *via* the most direct route (from convenient commercial starting materials) which avoided undesirable side reactions. The yields are non-optimized (the formulae of the compounds studied and their identification numbers are collected in Table 3.2). Route A could not be applied to the syntheses of compounds 1 and 2 since the litho and dilitho-benzenes from which these compounds will be formed are highly reducing^{6c-f,18} and have been shown to lead to the iron-containing dimer Fp₂,¹³ i.e.,



Compounds 4, 6, 9, 10, 11 and 12 were also not prepared *via* this route, since a more direct route involving nucleophilic attack on the polyhalogenated (and thus highly activated) precursor ligand has been shown to result in very high yields of desired products (see Chapter 2 of this thesis). The only compounds prepared *via* route A were therefore compounds 3, 5, 7, and 8. Indeed the presence of one F group on the benzene ring greatly reduces the electron transfer reaction of the lithiated complex. Thus in the synthesis of compound 3, only a trace of Fp₂ was observed in the IR spectrum of the crude product.

Among the compounds synthesized *via* route B, compound 8 was isolated in the lowest yields. Due to the unavailability of 1,3-dibromotetrafluorobenzene, the compound 2,4,5,6-tetrafluorobenzene was used as the starting material for this synthesis. It has been shown¹⁹ that under strongly basic conditions, the F group can moderately activate the

deprotonation of an *ortho*-proton. This activation was apparently successful for the monolithiation of the starting compound, but was incomplete for the dilithiation process, and this accounts for the occurrence of the mono-substituted compound, **5**, in large amounts in the final product of the reaction. Addition of strongly basic reagents such as TMEDA/HMPA which have been shown¹⁹ to result in increased activation of the H atoms in an arene ring towards deprotonation only complicated our work-up procedure and did not result in any observed increase in yields. Similarly, addition of a large excess of ⁿBuLi resulted in competition between the excess ⁿBuLi and 1,3-C₆F₄Li₂ for the FpI, thus,



Furthermore, the purification procedure for the disubstituted compound **8** was more difficult than for the others, for unlike the 1,4 isomer, **7**, which is only sparingly soluble in common solvents,^{5a} compound **8** is highly soluble in these solvents and is very difficult to separate from the Fp₂ dimer on a chromatographic column.

Compounds **1** and **2** were synthesized *via* route C as we have recently reported¹² that thermal decarbonylation of Fp acyl complexes results in high yields of products. In fact we have recently discovered that using toluene/Bu₂O mixture usually results in very smooth reactions with even less decomposition of the end products than with the initially reported Bu₂O solvent.

Spectroscopic Characterization of the Complexes

Some of the complexes synthesized in this study (2, 3, 5 and 7) were not isolated in a completely analytically pure state (perhaps because they have a tendency to absorb CH_2Cl_2 of solvation and then to desolvate under vacuum or upon standing for prolonged periods under N_2). The purity of these complexes was established by spectroscopic characterization (in particular, no evidence for the presence of other organometallic products).

As mentioned in the previous Chapter, the metal arene bond in mono and polymetallic Fp-aryl complexes has both σ and π components, with the σ components being the primary contributor to the bonding. We have also observed that the Fp fragment acts as both a π - and σ -donor, unlike organic π -donors which act as σ -acceptors. This observation is confirmed by the spectroscopic data in Table 3.1.

As expected, the position of the carbonyl stretching frequencies ν_{CO} vary with varying electron demand on the Fp group by the aryl ligand. Thus, on going from Fp-phenyl, 1, to Fp-pentafluorophenyl, 6, (with a more electron withdrawing perfluorophenyl ligand), an increase in the ν_{CO} for both symmetric and antisymmetric stretch of about 23 cm^{-1} is observed, (i.e., from 2016(s) and 1962(s) cm^{-1} for compound 1, $\text{C}_6\text{H}_5\text{Fp}$, to 2038(s) and 1989(s) cm^{-1} for compound 6, $\text{C}_6\text{F}_5\text{Fp}$).

The ^1H and ^{13}C chemical shifts of the cyclopentadienyl ring for all these complexes were found in the expected regions, namely; ~ 5 ppm for ^1H and ~ 87 ppm for ^{13}C . The isomeric forms for compounds 3, 4, 5, 7 and 8 were established by their ^{19}F NMR spectra, see experimental section (as well as ^1H NMR for 3). Thus, compound 3 showed three ^1H signals at 7.3(t), 6.8(t) and 5.2(s,Cp) and one ^{19}F signal at -124.02. Compound 4 showed ^{19}F signals at

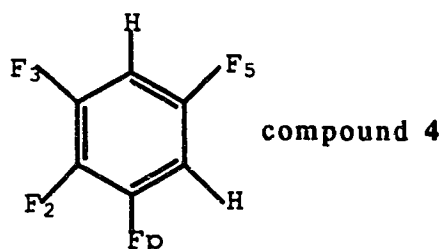
Table 3.1. Analytical, Mass Spectral and Infrared Data for the Complexes

Complex #	#	Analytical Data				Low resolution mass spectral data		Infrared Data (C ₆ F ₆ Cl ₂ cm ⁻¹)
		C Calcd	C Found	H Calcd	H Found	P+	P+	
C ₆ H ₅ Fp	1	61.47	61.36	3.96	3.90	254	2016(s),1962(s)	
1,3-C ₆ H ₄ Fp2	2 ^b	55.86	55.43	3.26	3.30	430	2016(s),1963(s)	
1,4-C ₆ H ₄ Fp	3 ^b	57.39	57.44	3.33	3.84	272	2020(s),1965(s)	
C ₆ H ₂ F ₃ Fp ^a	4	50.69	50.48	2.29	2.29	308	2040(s),1982(s)	
1,3-C ₆ H ₄ Fp	5 ^b	48.78	48.24	1.88	2.05	326	2037(s),1986(s)	
C ₆ F ₅ Fp	6	45.39	45.55	1.47	1.43	344	2039(s),1989(s)	
1,4-C ₆ F ₄ Fp2	7 ^b	47.85	47.10	2.01	2.49	502	2027(s),1981(s)	
1,3-C ₆ F ₄ Fp2	8	47.85	47.66	2.01	2.20	502	2028(s),1981(s)	

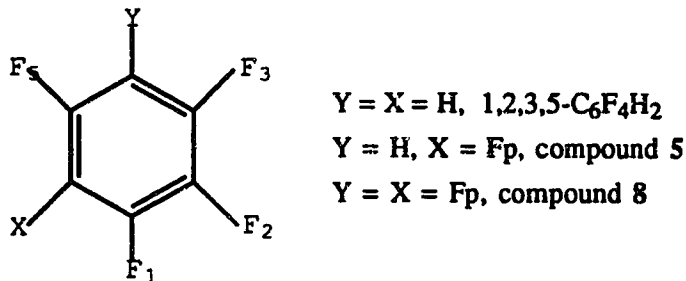
^aFor isomeric form, see text.

^b These complexes were not isolated in an analytically pure form, see text.

-112.1 (F2), -119.5 F(5), -135.9 (F3) with large couplings between F2 and F3 and between F2 and F5. Thus, as has been reported,^{20a} the Fp group displaces a F group opposite to one of the ring protons of the 1,2,3,5 tetrafluorobenzene starting material to form the product below.



Compound 5 showed four ¹⁹F signals at -81.2 (F5), -100.3 (F1), -141.6 (F3) and -167.61 (F2).



[The numbering of the above three compounds has been chosen for internal consistency rather than being based on the priority of groups]. The assignment of the above signals was made on the basis of the expected deshielding of the F atoms adjacent to Fp groups due to paramagnetic effects of the Fe.^{20b} Thus, from 1,2,3,5-tetrafluorobenzene (with chemical shift values at -114.15 (F5), -132.2 (F1/F3) and -166.6 (F2))^{20a} the F1 and F5 atoms of the complex are deshielded by about 33 ppm and F3 is shielded by about 10 ppm, while the F2 is almost unaffected.^{20a} Similar observations have been made by other workers.²⁰ Using the same argument to assign the F on

compound 8, F3 and F5 are expected to be deshielded by about 33 ppm while F1 will be shielded by about 10 ppm. Thus the three observed signals of compound 8 can be assigned as -45.3 (F5) -108.1 (F1/F3) and -166.0 (F2). These assignments are consistent with those made by Bruce *et al.*^{20a}

As expected, the electron richness of the arene ligand has direct bearing on the spectroscopic properties of the complexes. Thus, a correlation between the carbonyl stretching force constant k_{CO} and number of F groups on the phenyl ring is observed in Fig. 3.2, where k_{CO} is calculated assuming a C_{2v} symmetry for these complexes.²¹

$$k_1 \text{ or } k_2 = 4.038 \times 10^{-4} \nu^2$$

$$k_{CO} (\text{cm}^{-1}) = \frac{k_1 + k_2}{2}$$

Again, we observe that, as expected, the position of the ^{13}C signal in these complex is dependent on the electron demand on the transition metal centre. Thus, a linear correlation exists between the number of F groups on the phenyl ring (for mono substituted complexes) and the ^{13}C chemical shift values, see Fig. 3.3.

These correlations reflect the reduced electron density at the metal centre and consequently reduced back bonding to the CO π^* orbitals, arising from greater electron donation by the metal centre to the arene ring on increasing the number of electron withdrawing substituents (F) on the arene ring, and indicates facile electronic interaction between the metal centre and the arene ring.

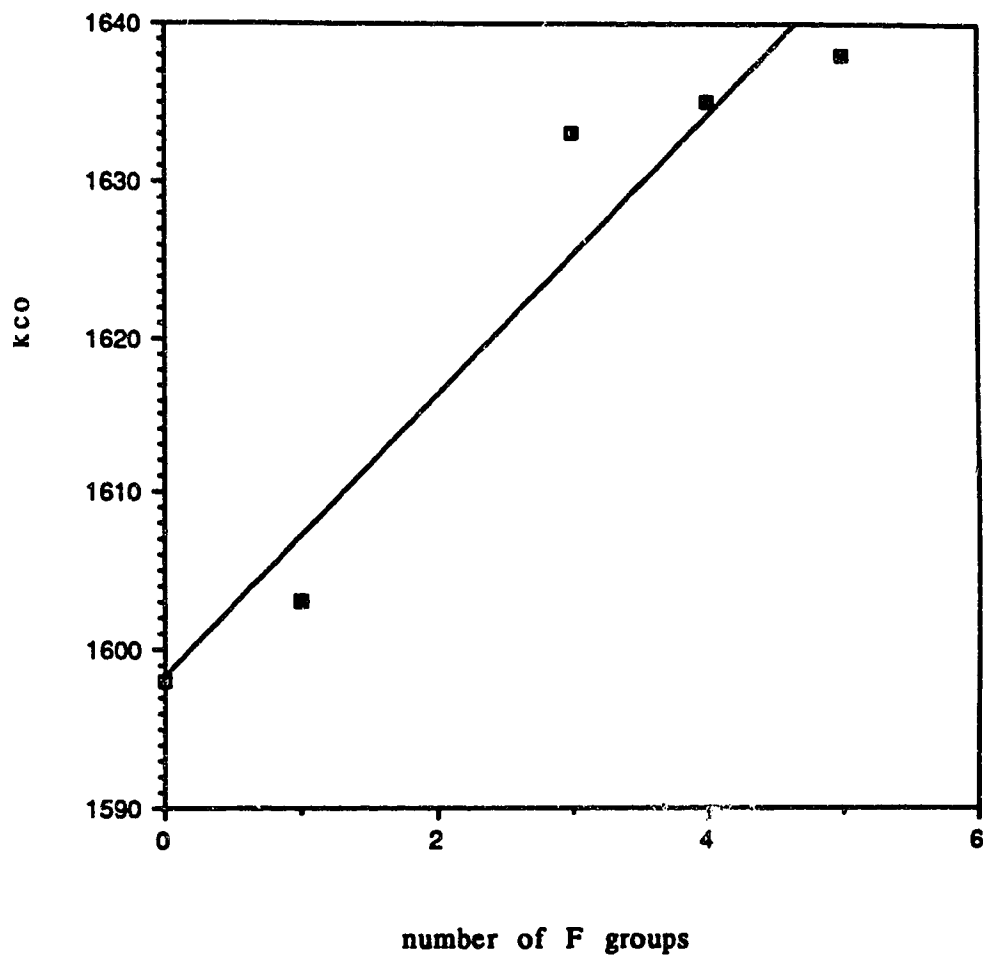


Figure 3.2 Carbonyl stretching force constant vs number of F groups on the arene ring.

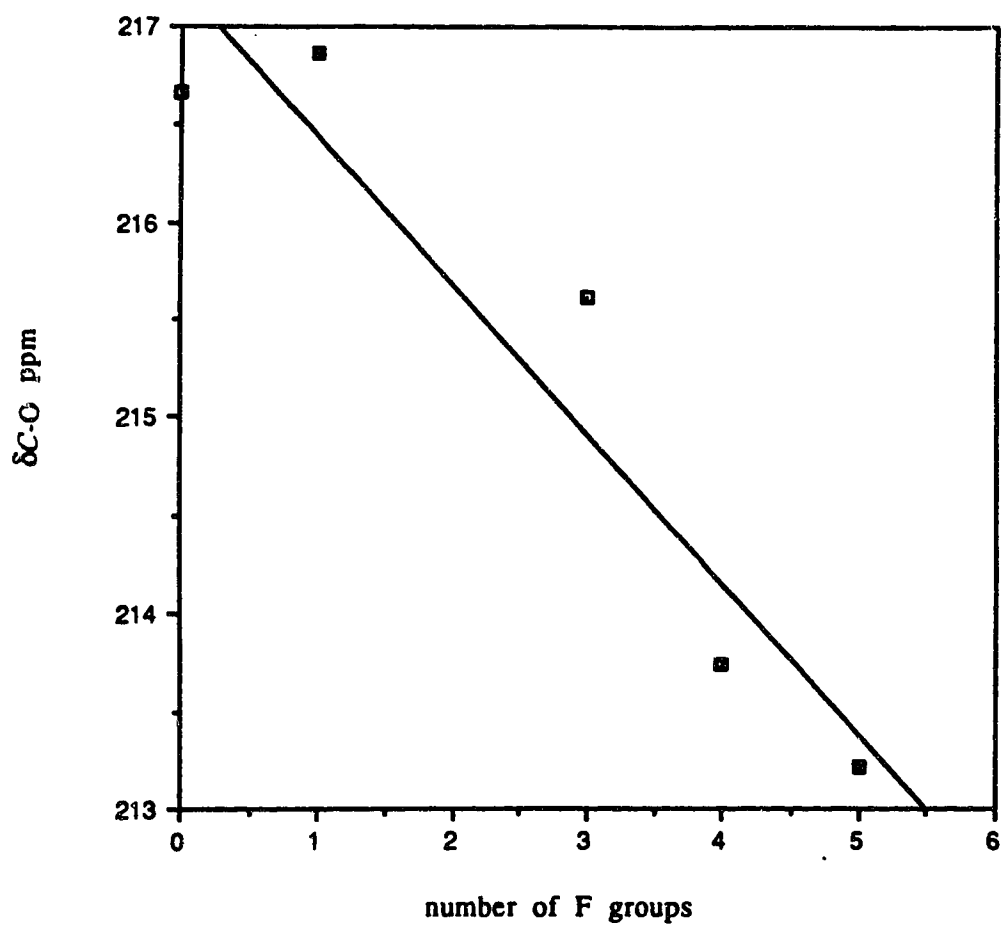


Figure 3.3 Chemical shift of C-O vs number of F groups on the arene ring.

Electrochemical Characterization of the Complexes.

The observed cyclic voltammetric data for the twelve complexes studied is summarized in Table 3.2. It is generally accepted that the electrons involved in the oxidation process of compounds of this nature, are located in orbitals which are primarily metal centered.⁶⁻⁸ As was mentioned in Chapter one, decreasing the electron density on an arene ring results in the stabilization of the arene LUMO and subsequently the stabilization of the metal centered bonding orbitals from which the oxidation takes place in the complex. Thus, we observed that the ease of oxidation of these complexes was linearly dependent on the number of electron withdrawing F substituents on the arene ring. A graph of $E_{p,a}$ vs the number of F groups on the arene ring (Fig 3.4) for the mono-Fp substituted phenyl complexes shows a linear correlation, with higher potentials observed with increasing number of F groups. Similarly, introduction of an aza group on the ring resulted in higher oxidation potentials, thus, compound 5 (C_6F_4HFp) has an $E^{0'}$ value of 1.56V whereas compound 10 (C_5NF_4Fp) has an $E^{0'}$ value of 1.76V. These observations are consistent with the spectroscopic data, *vide infra*, and indicates increased metal to arene electron transfer with decreasing electron richness of the arene ring.

The degree of reversibility upon oxidation exhibited by compounds of this type is usually associated with the stability of the oxidized forms. Thus, the more stable the oxidized species of a compound, the more chemically reversible the oxidation process for the particular compound will be. We generally observed that increasing the number of electron withdrawing F

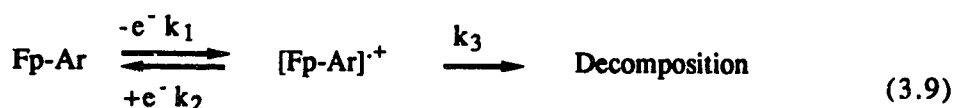
Table 3.2. Electrochemical data for the complexes

Compound	#	Scan rate V s ⁻¹	E°,(E _{p,a})V	ΔE,V	i _{p,c} /i _{p,a}
C ₆ H ₅ Fp	1	0.10	(1.16) ^b	-	-
1,3-C ₆ H ₄ Fp ₂	2	0.10	1.05 (1.09)	0.096	0.50 (0.68 at 1V/sec)
1,4-C ₆ H ₄ FFp	3	0.10	(1.22) ^b	-	-
C ₆ H ₂ F ₃ Fp*	4	0.10	(1.54) ^b	-	-
1,3-C ₆ HF ₄ Fp	5	0.10	1.56 (1.60)	0.090	0.83 (0.83 at 1V/sec)
C ₆ F ₅ Fp	6	0.10	1.64 (1.70)	0.100	0.64 (0.81 at 1V/sec)
1,4-C ₆ F ₄ Fp ₂	7	0.10	1.34 (1.35)	0.070	0.78 (0.97 at 1V/sec)
1,3-C ₆ F ₄ Fp ₂	8	0.10	1.37 (1.42)	0.090	0.54 (0.74 at 1V/sec)
2,6-C ₅ NH ₃ FFp	9	0.14	(1.25) ^b	-	-
C ₅ NF ₄ Fp	10	0.10	1.76 (1.80)	0.080	0.86 (0.98 at 1V/sec)
C ₅ NCIF ₃ Fp	11	0.10	1.71 (1.75)	0.090	0.85 (0.99 at 1V/sec)
C ₅ NCI ₂ F ₂ Fp	12	0.10	1.66 (1.70)	0.100	0.94 (0.97 at 1V/sec)

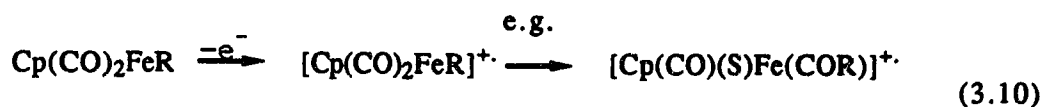
* For isomeric form, see text.

b No return peak observed.

groups on the phenyl or pyridyl ring resulted in an increase in the degree of reversibility for related compounds. Furthermore, introduction of an aza group (N) also resulted in an increase in the degree of reversibility for related complexes. Thus, all of the mono-Fp substituted aryl complexes with four or more F groups (or a combination of F and Cl groups for the pyridyl complexes) exhibited some degree of reversibility (i.e. with return peaks in the cyclic voltammogram, see Figure 3.5), whereas all other complexes with three or less F groups showed complete chemical irreversibility (ie. no return peaks observed, see Figure 3.6). Furthermore, the ratio of the cathodic peak current to the anodic peak current (i.e., $i_{p,c}/i_{p,a}$) for the Fp-phenyl complexes with four or more F groups on the phenyl ring was generally observed to be less than 0.96 at all scan rates studied (between and 2V/sec.), whereas the value of this ratio for the analogous pyridyl complexes were generally >0.96 at scan rates of 0.5V/sec. and above indicating that they were chemically reversible at these scan rates (see experimental section). These results indicate that for those complexes with fewer electron withdrawing groups on the arene ring, the electrochemically oxidized species rapidly decomposes, i.e.



where k_3 is very large. Such decompositions have been shown to lead to several types of products in other alkyls ligand containing Fp complexes,²²



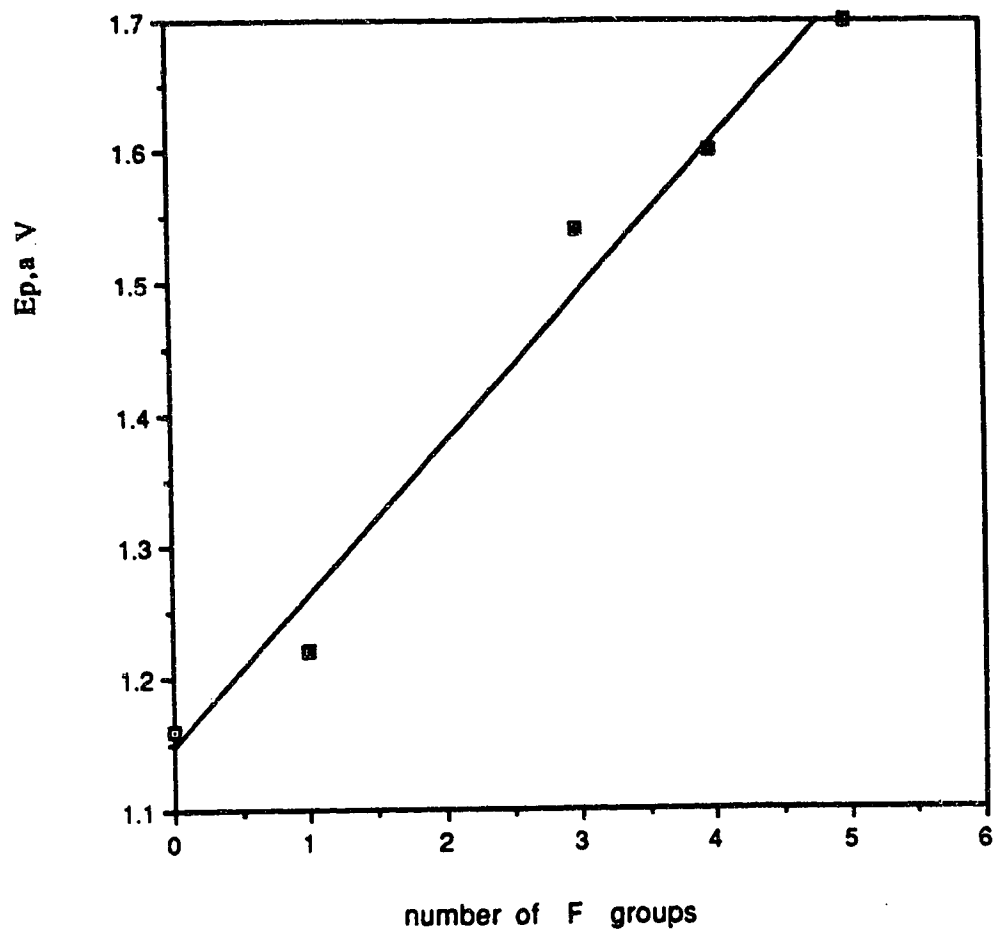


Figure 3.4 $E_{p,a}$ vs number of F groups on the arene ring.

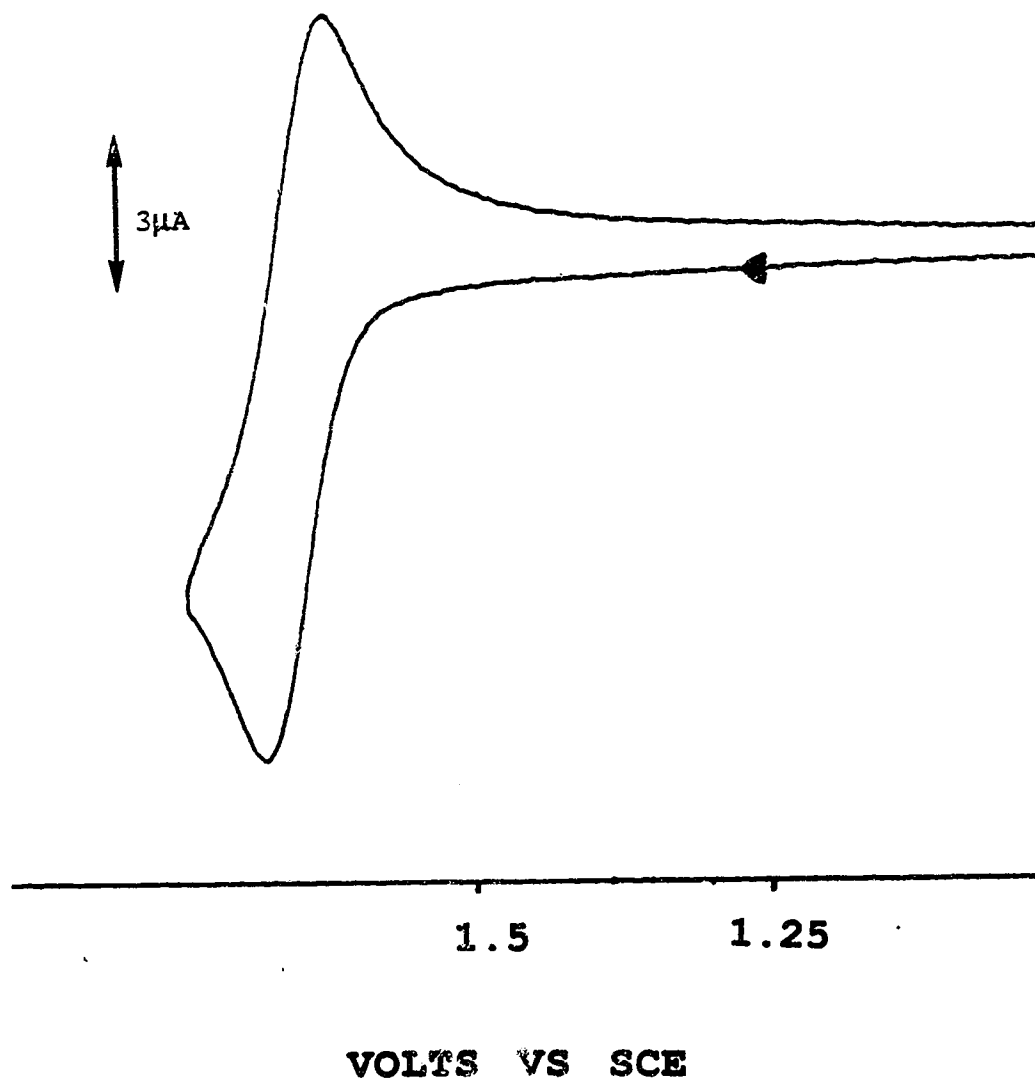


Figure 3.5 Cyclic voltammogram of $\text{C}_6\text{F}_5\text{Fp}$, 6, at scan rate of 0.4V/s

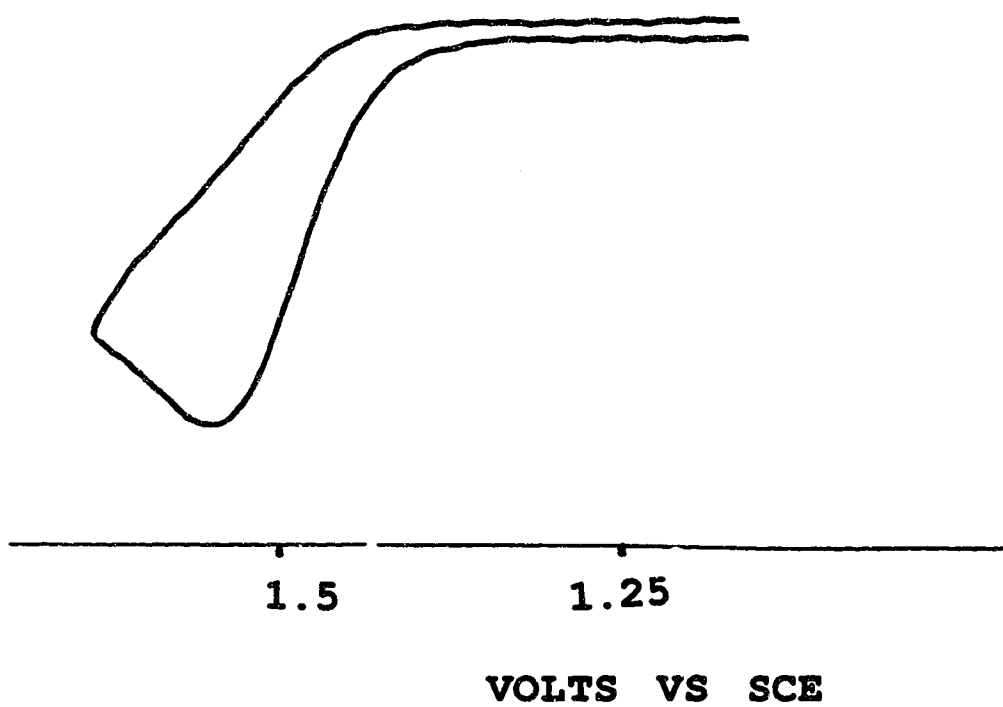


Figure 3.6 Cyclic voltammogram of $C_6H_2F_3Fp$ at scan rate of 0.1

The oxidation reactions, especially for those complexes with fewer than four F groups on the arene ring, were usually followed by extensive electrode coating and any subsequent waves became ill-defined, and were not studied in detail. Thus a second oxidation wave expected for compound 2, 1,3-C₆H₄Fp₂ could not be positively identified.

Diffusion control for those processes which exhibited some degree of electrochemical reversibility was established by the linearity of plots of $i_{p,c}$ vs (scan rate)^{1/2}, over at least one order of magnitude for each complex (a representative plot is shown in Figure 3.7). It has been shown^{7,8,23} by coulometry that related complexes undergo one electron oxidations. We established the single electron nature of the oxidations of these complexes by comparison of limiting currents and ΔE_p values with those obtained for equimolar solutions of ferrocene.^{23,24} Generally, we observed that the peak to peak separations (ΔE_p) of the cyclic voltammogram in all these complexes were greater than 58 mV, however, they were similar to the ΔE_p values for ferrocene recorded under the same conditions (usually in the range $58 < \Delta E_p < 70$ mV). Similar observations have been made by other workers, and such deviations from the predicted ΔE_p values have been attributed to the effects of uncompensated solution resistance in the cells which results in slow electron transfer kinetics.²⁵ Thus, we believe that electrochemical reversibility was exhibited by these compounds.

A reaction between AgPF₆ and compound 10, C₅NF₄Fp, was carried out in an attempt to oxidize the compound chemically. However, even though Ag⁺ is a good oxidant, no electron transfer was observed, i.e.

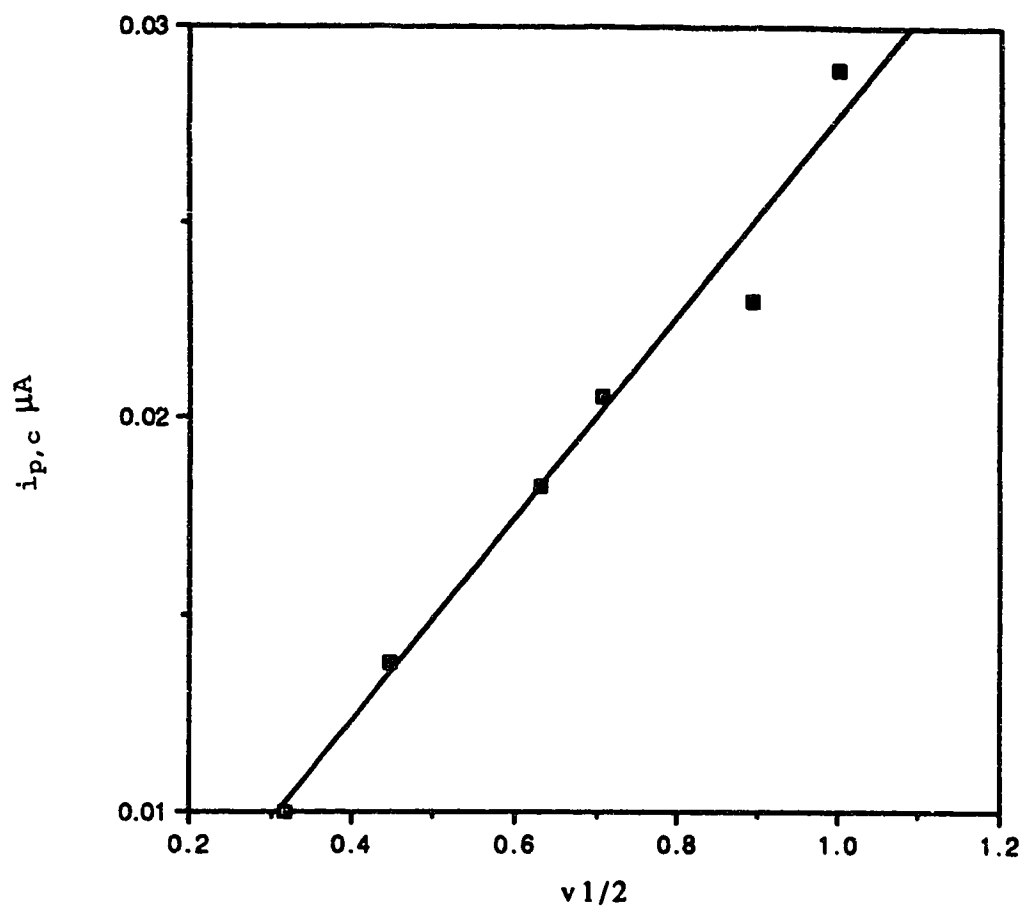
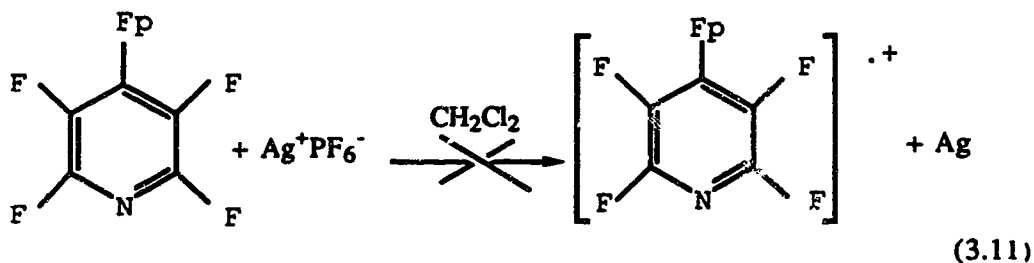
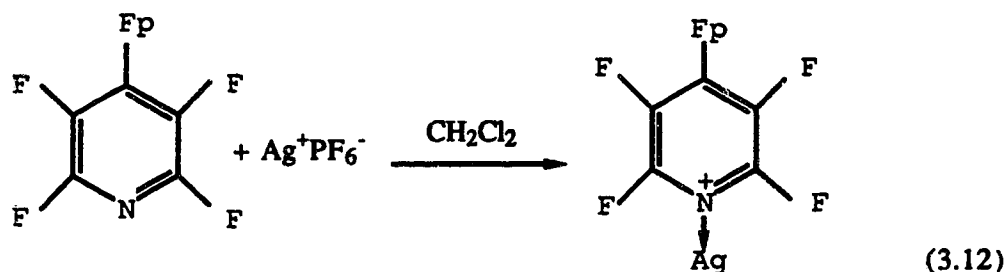


Figure 3.7 Current vs square root of scan rate for compound 10.



Rather, the addition of AgPF_6 appeared to result in a coordination of the Ag^+ cation to the aza group, thus:



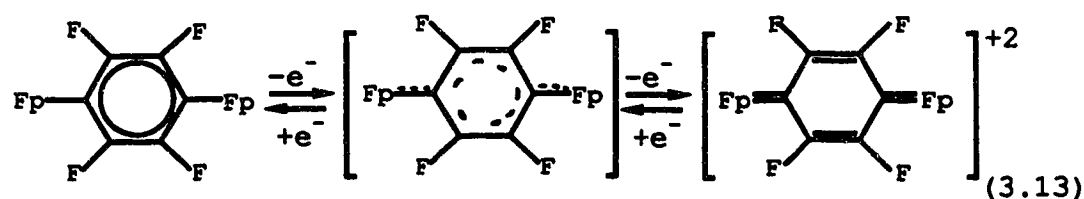
As stated in the Introduction, we have earlier reported that ^{13}C NMR evidence indicates that in the phenylene bridged complexes the strongest interaction between the two metal centres linked by the phenylene bridge occurs when the two metal centres are arranged *para* to each other rather than when they are placed *meta* to one another. We were interested in confirming this result *via* cyclic voltammetry. As mentioned earlier, those complexes which are not polyfluorinated all displayed chemically irreversible oxidations and such reactions usually led to extensive coating of the electrodes. Thus, to avoid these difficulties, the perfluorinated complexes 7 (1,4- $\text{C}_6\text{F}_4\text{Fp}_2$) and 8 (1,3- $\text{C}_6\text{F}_4\text{Fp}_2$) were studied to determine the extent of metal-metal interaction as a function of substitution geometry.

Both complexes showed double oxidation waves which are fairly well separated from each other (i.e., $\Delta E_{1/2} = 280$ mV for compound 7 (1,4-C₆F₄Fp₂) and 200 mV for compound 8 (1,3-C₆F₄Fp₂) see Figures 3.8 and 3.9). According to the models developed by Savéant, Bard and Anson,²⁶ the fact that these complexes exhibit two clearly separated one electron waves, as shown by their respective cyclic voltammograms, can be accounted for only if it is assumed that the redox sites interact with one another, with the magnitude of this difference in the wave to wave separations, $\Delta E_{1/2}$, directly reflecting the degree of interaction of the two metal centres. Thus, in complex 7 (1,4-C₆F₄Fp₂) the two metal centres interact more strongly than in complex 8 (1,3-C₆F₄Fp₂). This result clearly shows that the electronic interaction between the two metal centres is largely through-bond, since the reverse pattern would have been observed if the interaction were largely through-space.

Indeed, the magnitudes of $\Delta E_{1/2}$ for these complexes compare favourably with those reported for related complexes with homogeneous redox centres containing a pyrazine bridge. (e.g., [(NH₃)₅M]₂(μ -Pz) (M = Fe, Ru and Os), [W(CO)₂(PR₃)₃]₂(μ -Pz), Pz = pyrazine).²⁷ It has generally been observed^{24b} that the $\Delta E_{1/2}$ values for compounds from a particular transition metal triad appear in the order 3d < 4d < 5d, a phenomenon attributed to the better π -bonding ability of the metals as the triad is descended. Indeed, the observed $\Delta E_{1/2}$ value for compound 7 is comparable to those observed for ruthenium complexes. This is further evidence of the excellent π -interactions mediated by these phenylene bridges..

A characteristic feature of those complexes which have very strong coupling between the two metal centres is the lowering of the first oxidation

potential and an increase in the second oxidation potential,^{3i,4d,24} moreover, the first oxidation is often observed to be completely reversible.^{26b} Our observations are consistent with the above general trends, thus for compound 7, the first oxidation occurs at 1.35 V compared to 1.36 V for the 1,3-isomer (8). Similarly, the second oxidation potential for the 1,4 complex 7 occurs at 1.63 V compared to 1.56 V for the 1,3 complex 8 consistent with the expected decrease and increase of the first and second oxidation potentials respectively for such a complex with strong electronic coupling between two redox centres. The 1,4 complex (7), also exhibits better chemical reversibility than does the 1,3 complex (8) see table 2. Furthermore, the first oxidation of compound 7 was observed to be much more electrochemically reversible than by the second, indicating that a greater structural change accompanies the second oxidation. This is consistent with the expected bonding changes upon oxidation, i.e.



Also observed for complex 7 at lower scan rates is a post wave peak of very high intensity, (see Figure 3.10). This peak is characteristic of an adsorption peak, and overlaps with the return peak for the first oxidation. At higher scan rates, (>1.0 V/sec) this peak disappears, as expected.

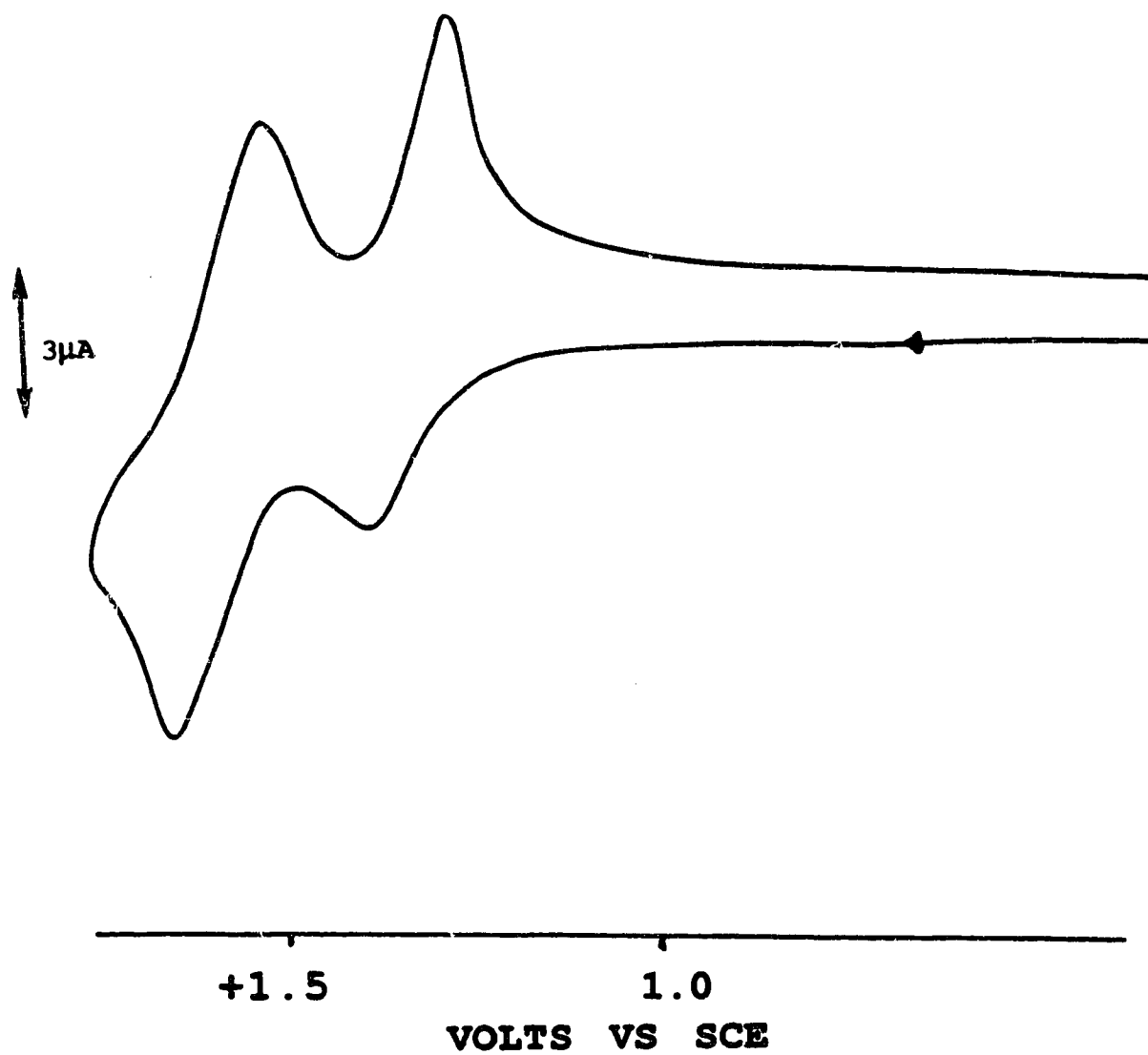


Figure 3.8 Cyclic voltammogram of 1,4-C₆F₄Fp_{2,7}, at scan rate of 1.0V/s.

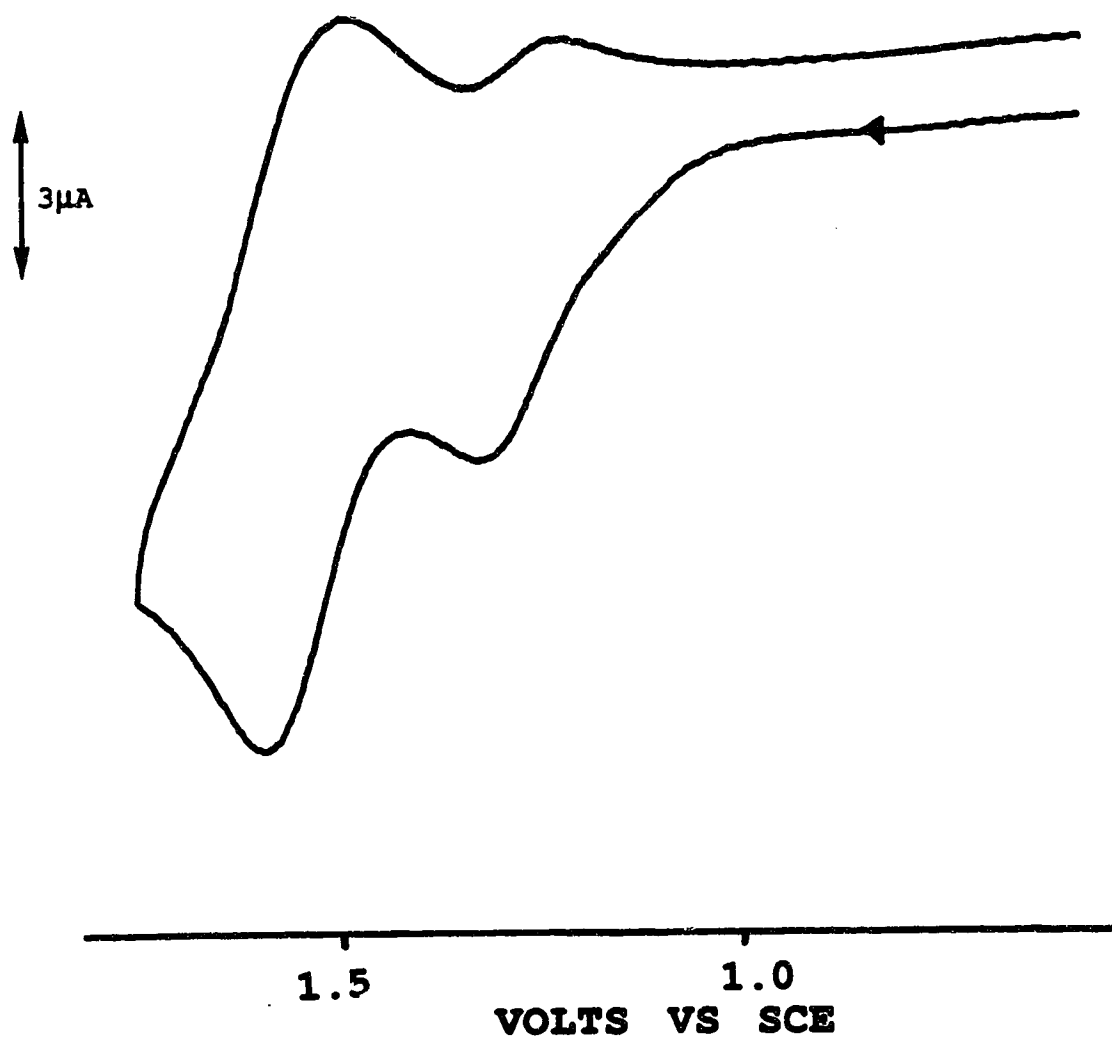


Figure 3.9 Cyclic voltammogram of 1,3-C₆F₄Fp₂. 8, at scan rate of 0.5V/s.

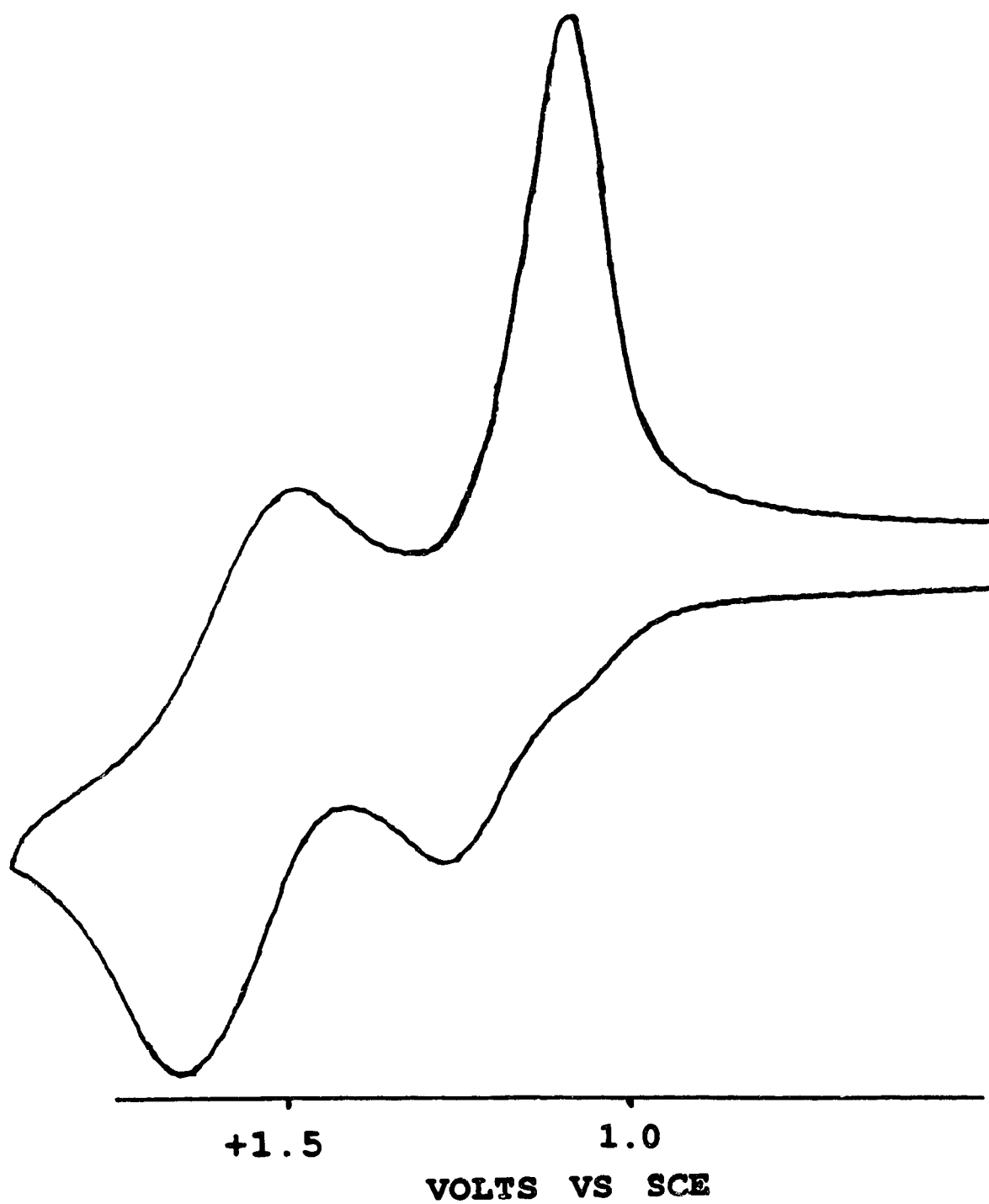


Figure 3.10 Cyclic voltammogram of 1,4-C₆F₄Fp_{2.7}, at scan rate of 0.5V/s. showing adsorption wave.

The X-ray crystal structure of compound 6, C_6F_5Fp , has also been determined. Selected views of ORTEP plots of the structure are shown in Figures 3.10 and 3.11, selected bond lengths and angles, torsional angles and least squares planes are shown in Tables 3.3 to 3.6. The $CpFe(CO)_2$ fragment is as expected, with the iron atom carrying a symmetrically bonded $\eta^5-C_5H_5$ group as well as two linear CO groups. Thus, the expected three-legged piano stool arrangement around iron is observed. The Fe-C (phenyl) bond length is 1.994(3)Å, and is within the range reported for other complexes having *formal* Fe-C(sp²) single bonds (1.94-2.03Å)²⁸ and those of cationic Fp-carbene complexes having *formal* Fe-C(sp²) double bonds (1.91-2.00Å).²⁹ Thus the Fp-arene bond may have multiple bond character, as expected. The internal C-C-C bond angle at the *ipso*-carbon at 113.0(2)° is in the range reported for other pentafluorophenyl complexes of transition metals (the reported range is between 109.0 to 121.2).³⁰

Two important features of this structure is the planarity of the phenyl ring and its perpendicular orientation towards the Fp mirror plane (see Fig. 3.11), contrary to its expected orientation (see Chapter 2 of this thesis for more details on the unusual orientations of the phenyl ring in these complexes).

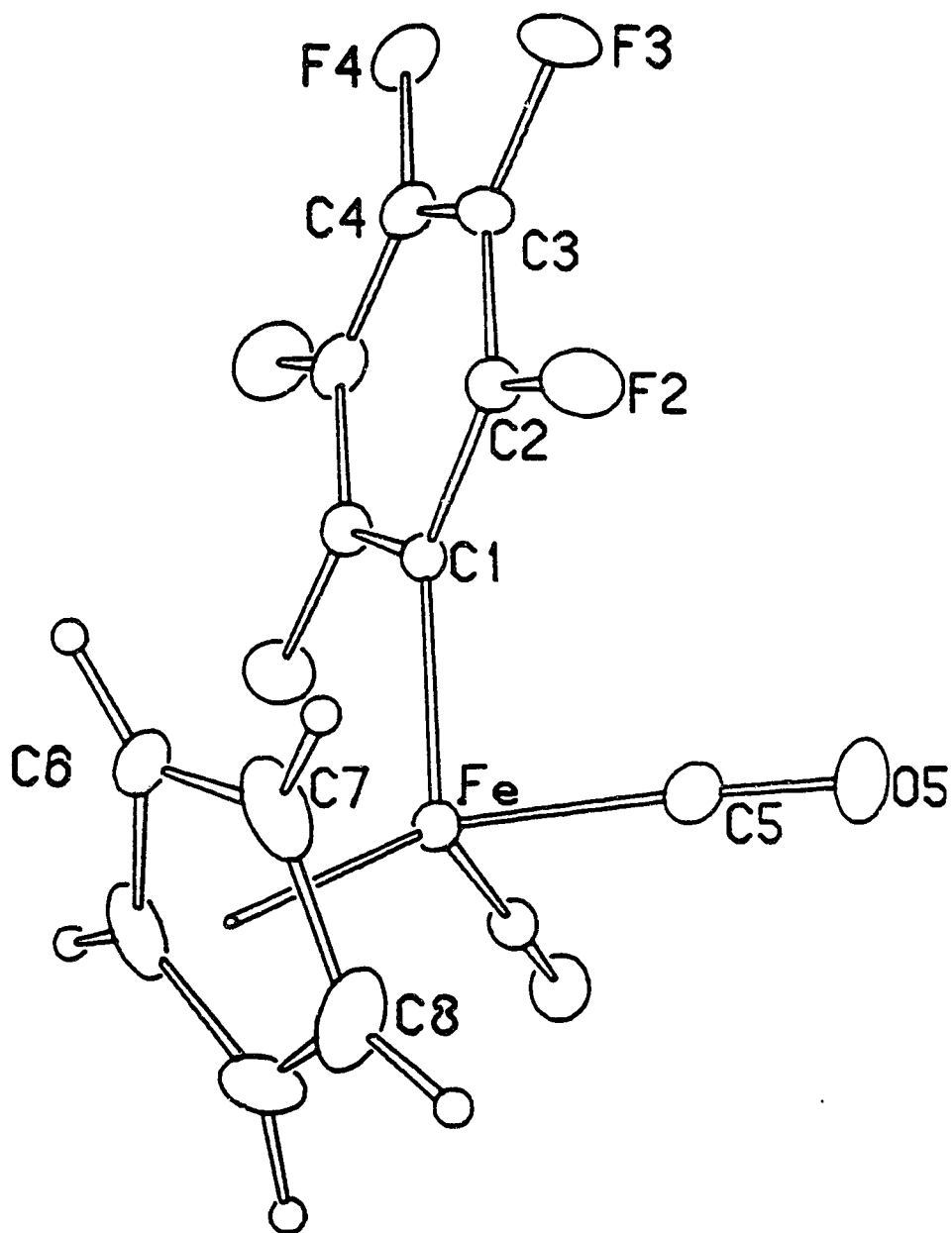


Figure 3.11 ORTEP plot of the complex $[\text{CpFe}(\text{CO})_2]\text{C}_6\text{F}_5$, 6.

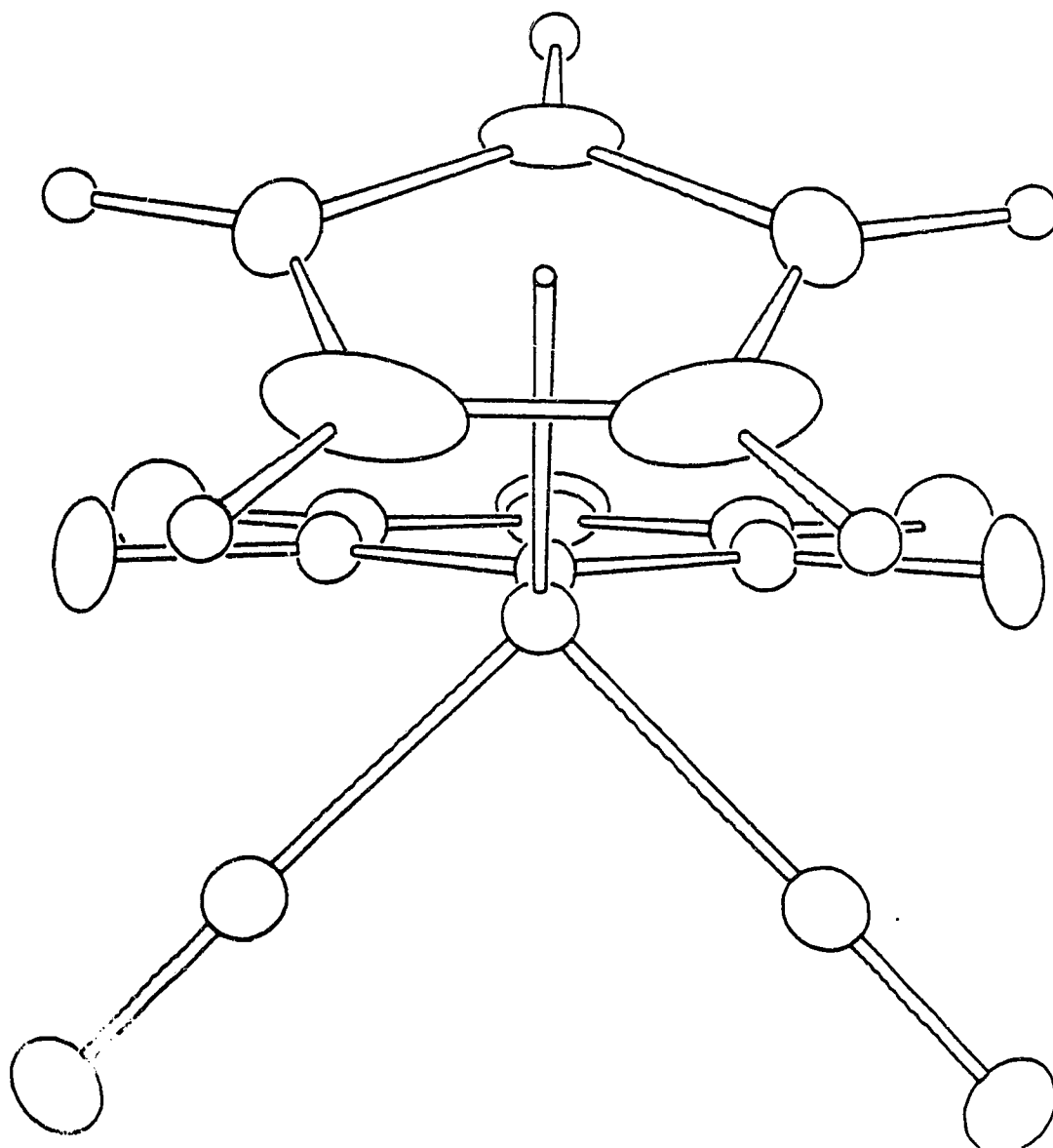


Figure 3.12 ORTEP plot of the complex $[\text{CpFe}(\text{CO})_2]\text{C}_6\text{F}_5$, 6, view down Fe1-C1.

Table 3.3 Selected bond lengths in $[\text{CpFe}(\text{CO})_2]\text{C}_6\text{F}_5$, 6.

Atom1	Atom2	Length
Fe	C1	1.994 (3)
Fe	C5	1.772 (3)
Fe	C6	2.096 (3)
Fe	C7	2.088 (3)
Fe	C8	2.075 (3)
C1	C2	1.387 (3)
C2	C3	1.380 (3)
C3	C4	1.363 (3)
C5	O5	1.140 (3)
C6	C7	1.388 (4)
C7	C8	1.395 (5)
C8	C8	1.337 (1)
C2	F2	1.358 (3)
C3	F3	1.352 (3)
C4	F4	1.339 (4)

Table 3.4 Selected interatomic angles in [CpFe(CO)₂]C₆F₅, 6.

Atom	Atom2	Atom3	Angle
C1	Fe	C5	92.24 (10)
C5	Fe	C5'	91.56 (11)
Fe	C1	C2	123.51 (14)
C2	C1	C2'	113.0 (2)
C1	C2	C3	124.2 (2)
C1	C2	F2	119.5 (2)
C3	C2	F2	116.3 (2)
C2	C3	C4	119.9 (3)
C2	C3	F3	120.2 (3)
C4	C3	F3	119.9 (2)
C3	C4	C3'	118.8 (3)
C3	C4	F4	120.6 (2)
C7	C6	C7'	108.6 (3)
C6	C7	C8	106.5 (3)
C7	C8	C8'	109.2 (2)

Table 3.5 Weighted least squares planes in [CpFe(CO)₂]C₆F₅, 6.

Plane	Coefficients ^b				Defining Atoms with Deviations ^c			
1	5.5751	-0.1415	-8.2379	0.7112				
					C6	C7	C8	
					<u>Fe</u>	-1.730	<u>H6</u>	0.010
					<u>H7</u>	0.000	<u>H8</u>	0.013
2	6.9559	0.1565	-1.3937	2.6891				
					C1	0.000(3)	C2	0.000(3)
					C3	0.000(3)	C4	0.000(4)
Dihedral Angles ^d								
Planes	Angle							
1 - 2	31.3							

^aThe weights are generated from the estimated standard deviations of the atomic coordinates. The plane is determined from an algorithm derived by Hamilton, *Acta Cryst.*, 14,185 (1961).

^bCoefficients are of the form $ax + by + cz - d = 0$, where x , y , and z are fractional crystallographic coordinates.

^cDisplacements from the least-squares plane are given in Angstroms, with the estimated standard deviations given in parentheses. Those atoms which are underlined were not included in the definition of the least-squares plane.

^dIn degrees.

Table 3.6 Torsional angles in $[\text{CpFe}(\text{CO})_2]\text{C}_6\text{F}_5$, 6.

Atom 1	Atom 2	Atom 3	Atom 4	Angle
C5	Fe	C1	C2	44.90 (0.28)
C6	Fe	C1	C2	-89.27 (0.26)
C7	Fe	C1	C2	-55.13 (0.29)
C8	Fe	C1	C2	-55.02 (0.40)
C1	Fe	C5	O5	158.71 (5.05)
C6	Fe	C5	O5	-113.35 (5.02)
C7	Fe	C5	O5	-94.76 (5.05)
C8	Fe	C5	O5	-55.69 (5.06)
C1	Fe	C8	C7	-0.17 (0.74)
C5	Fe	C8	C7	-99.60 (0.23)
Fe	C1	C2	C3	179.92 (1.30)
Fe	C1	C2	F2	-0.54 (0.43)
C8	Fe	C7	C6	116.48 (0.33)
C1	C2	C3	C4	0.04 (1.31)
C1	Fe	C6	C7	120.39 (0.21)
C1	C2	C3	F3	179.08 (0.32)
C5	Fe	C6	C7	30.22 (0.32)
F2	C2	C3	C4	-179.51 (0.45)
C8	Fe	C6	C7	-38.72 (0.25)
F2	C2	C3	F3	-0.48 (0.39)
C1	Fe	C7	C6	-63.62 (0.22)
C2	C3	C4	F4	178.44 (0.32)
C1	Fe	C7	C8	179.90 (0.45)
F3	C3	C4	F4	-0.60 (0.55)
C5	Fe	C7	C6	-159.58 (0.22)
Fe	C6	C7	C8	61.23 (0.24)
C5	Fe	C7	C8	84.94 (0.25)
C6	C7	C8	Fe	-61.91 (0.27)

REFERENCES

1. Some of the work described in this Chapter has been presented in a poster format, i.e. 72nd Canadian Chemical conference, 1989, Victoria, B.C. *Abstr.* 348.
2. (a) Mikkelsen, K.V.; Ratner, M.A. *Chem. Rev.* 1987, 87, 113. (b) Keppeler, U.; Schnieder, O.; Stöffer, W.; Hannack, M. *Tetrahedron Lett.* 1984, 25, 3679. (c) Metz, J.; Schnieder, O.; Hannack, M. *Inorg. Chem.* 1984, 23, 1005. (d) Hannack, M.; *Mol. Cryst. Liq. Cryst.* 1984, 105, 133. (e) Datz, A.; Metz, J.; Schneider, O.; Hannack, M. *Synth. Met.* 1984, 9, 31. (f) Metz, J.; Hannack, M. *J. Am. Chem. Soc.* 1983, 105, 828. (g) Meyer, T.J.; *Prog. Inorg. Chem.* 1975, 19, 1. (h) Vergamini, P.J., Kubas, G.J. *Prog. Inorg. Chem.* 1976 21, 261. (i) Lemoine, P. *Coord. Chem. Rev.* 1982, 47, 55. (j) Geiger, W.E.; Connelly, N.G.; *Adv. Organomet. Chem.* 1985, 24, 87.
3. See for example: (a) Carter, F.L. *Molecular Electronic Devices*, Ed.; Marcel Dekker: New York; 1982. (b) Carter, F.L. *Molecular Electronic Devices II*; Ed.; Marcel Dekker: New York; 1987. (c) Mort, J.; Pfister, G. *Electronic Properties of Polymers*, John Wiley & Sons: New York; 1982.
4. (a) Jutzi, P.; Siemeling, U.; Müller, A.; Bögge, H. *Organometallics* 1989, 8, 1744. (b) Lockmeyer, J.R.; Rauchfuss, T.B.; Rheingold, A.L. *J. Am. Chem. Soc.* 1989, 111, 5733. (c) Weitellier, S.; Launay, J.P.; Spangler, C.W. *Inorg. Chem.* 1989, 28, 758. (d) Bowyer, W.J.; Geiger, W.E., Boekelheide, V. *Organometallics* 1984, 3, 1079. (e) Richardson, D.E.; Taube, H. *Inorg. Chem.* 1981, 20, 1278. (f) Grentz, C., Taube, H. *J. Am. Chem. Soc.* 1973, 95, 1086.

5. (a) Hunter, A.D.; Szigety, A.B. *Organometallics*, 1989, 8, 1118.
(b) Richter-Addo, G.B.; Hunter, A.D.; Wichrowska, N. *Can. J. Chem.* 1989, 41. (c) Richter-Addo, G.B.; Hunter, A.D. *Inorg. Chem.* 1989, 28, 4063.
6. See for example: (a) Liu, H-Y.; Golovin, M.N.; Fertal, D.A.; Tracey, A.A.; Eriks, K.; Giering, W.P.; Prock, A. *Organometallics* 1989, 8, 1454.
(b) Miholova, D.; Vleck, A.A. *J. Organomet. Chem.* 1982, 240, 413.
(c) *ibid.*, *Inorg. Chem. Acta* 1980, 43, 43. (d) Demisomovich, L.I.; Polovyanyuk, I.V.; Lokshin, B.V.; Gubin, S.P.; *izv. Akad. Nauk SSSR, Ser. Khim.* 1971, (Engl. translation, 1964). (e) Demisomovich, L.I.; Gubin, S.P.; Chapovskii, Y.A. *izv. Akad. Nauk SSSR, Ser. Khim.* 1967, (Engl. translation, 2378).
7. Philp, R.H.; Reger, D.L.; Bond, A.M. *Organometallics* 1989, 8, 1714.
8. Bitcon, C.; Whiteley M.W. *J. Organomet. Chem.* 1987, 336, 385.
9. Nicholson, R.S. *Anal. Chem.* 1966, 1406.
10. (a) Perrin, D.D.; Armarego, W.L.F.; Perrin, D.R. *Purification of Laboratory Chemicals*, 3rd ed. Pergamon: New York; 1987.
(b) Shriver, D.F.; Dredzon, M.A. *The manipulation of air sensitive compounds*, 2nd ed., John Wiley & Sons: New York, 1986.
11. (a) King, R.B.; Eisch, J. *J. Organomet. Synth.* 1965, 1, 114; (b) *ibid.*, 1965, 1, 151.
12. Wash grade solvent.
13. Bruce, M.I.; Stone, F.G.A. *J. Chem. Soc. (A)* 1966, 1837.
14. Legzdins, P.; Wassink, B. *Organometallics* 1984, 3, 1811.
15. Holloway, J.D.L.; Geiger, W.E. *J. Am. Chem. Soc.* 1980, 101, 2038.
16. Gagne, R.R.; Koval, C.A.; Lisensky, G.C. *Inorg. Chem.* 1980, 19, 2854.

17. (a) *International table for X-ray crystallography* Kynoch: Birmingham; 1969 1., (b) Walker, N.; Stuart, D. *Acta Crystallogr.* 1983, A39, 158. (c) The computer program and diffractometer program used include the Enraf-Nonius *Structure Determination Package, Version 3* (1985, Delft, The Netherlands) adapted for a SUN Microsystems 3/160 Computer, and several locally written programs by Dr. R.G. Ball.
18. (a) Pickett, C.J.; Pletcher, D. *J. Chem. Soc., Dalton Trans.* 1975, 8791. (b) Dessy, R.E.; Stary, F.E.; King, R.B.; Waldrop, M. *J. Am. Chem. Soc.* 1966, 88, 471. (c) Legzdins, P.; Wassink, B.; Einstein, F.W.B.; Jones, R.H. *Organometallics* 1988, 7, 477.
19. Brandsma, L. *Preparative Polar Organometallic Chemistry*, Vol. I, Springer Verlag: Berlin Heidelberg; 1987.
20. (a) Bruce, M.I. *J. Chem. Soc. (A)* 1968, 1459. (b) Buckingham, A.D.; Petcher, E.; Stone, F.G.A. *J. Chem. Phys.* 1962, 36, 124.
21. Lukehart, C.M. *Fundamental Transition Metal Organometallic Chemistry*, Brooks/Cole: Monterey; 1985, p29.
22. See Magnuson, R.H.; Zulu, S.; Tsai, M. M.; Giering, W.P. *J. Am. Chem. Soc.* 1980, 102, 6887 and work cited therein.
23. (a) Lee, M.T.; Foxman, B.M.; Rosenblum, M. *Organometallics* 1985, 4, 539. (b) Caylon, H.R.; Chisholm, M.H. *J. Am. Chem. Soc.* 1989, 111, 8921.
24. Morrison, W.H.; Kroschorud, S.; Henrickson, D. *Inorg. Chem.* 1973, 1998.
25. Gallaha, R.W.; Keene, F.R.; Meyer, T.J.; Sahon, D.J. *J. Am. Chem. Soc.* 1977, 1064.
26. (a) Ammar, F.; Saveant, J.M. *J. Electroanal. Chem.* 1973, 47, 215. (b) Flanagan, J.B.; Margel, S.; Bard, A.J.; Anson, C.F. *J. Am. Chem. Soc.* 1978, 100, 4248.

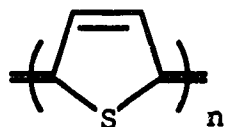
27. Bruns, W.; Kaim, W. *J. Organomet. Chem.* **1990**, *390*, C45. and work cited therein
28. For structures of CpFe(CO)L aryls see (a) Adrianov, V.G.; Sergeeva, G.N.; Streuchkov, Y.T.; Aninov, K.N.; Kolobova, N.E.; Beechastnov, A.S. *Zh. Strukt. Kim.* **1970**, *11*, 168 (Engl. translation, 163). (b) Lehmuksi, H.; Mehler, G.; Benn, R.; Rufinska, A.; Schroth, G.; Kruger, C.; Raabe, E. *Chem. Ber.* **1987**, *120*, 1987. (c) Semion, V.A.; Struchkov, Y.T. *Zh. Strukt. Khim.* **1969**, *10*, 85 (Engl. translation, 80).
29. For structures of Fp-R (where R is sp^2 hybridized) see: (a) Churchill, M.R.; Wormald J. *Inorg. Chem.* **1969**, *8*, 1936. (b) Ferede, R.; Noble, M.; Cordes, A.W.; Allison, N.T.; Lay, J. Jr. *J. Organomet. Chem.* **1988**, *399*, 1. (c) Bruce, M.I.; Liddell, J.J.; Snow, M.R.; Tiekink, E.R.T. *J. Organomet. Chem.* **1988**, *354*, 103. (d) Dhal, L.F.; Doedena, R.J.; Huble, W.; Nielson, J. *J. Am. Chem. Soc.* **1966**, *88*, 446. (e) Kolobova, N.E.; Rozaantava, T.V.; Struchkov, Y.T.; Betaanov, A.S.; Bakmutov, V.I. *J. Organomet. Chem.* **1985**, *292*, 247.
- 30 Jones, P.G. *J. Organomet. Chem.* **1988**, *345* 405

CHAPTER 4

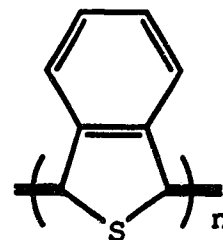
(η^5 -CYCLOPENTADIENYL)IRON DICARBONYL COMPLEXES CONTAINING
 TERMINAL AND BRIDGING FUSED HETEROCYCLIC LIGANDS: SYNTHESIS AND
 X-RAY CRYSTAL STRUCTURE OF
 2-[(η^5 -CYCLOPENTADIENYL)IRON DICARBONYL]-3-CHLOROQUINOXALINE.

INTRODUCTION

Organic polymers containing aromatic cores such as polythiophene, polypyrrole, poly(*p*-phenylene), polyaniline, etc., have been shown to exhibit useful electroconductive and photoconductive properties. During the studies on the conducting behaviour of these species, it has sometimes been found useful to modify the structure of the aromatic cores in order to enhance these desirable properties. For example, incorporating a benzene ring into a quinoid thiophene to give poly(isothianaphthalene), PITN, has been shown² to result in the lowering of the conduction band gap (E_g) of the polymer by about one half.

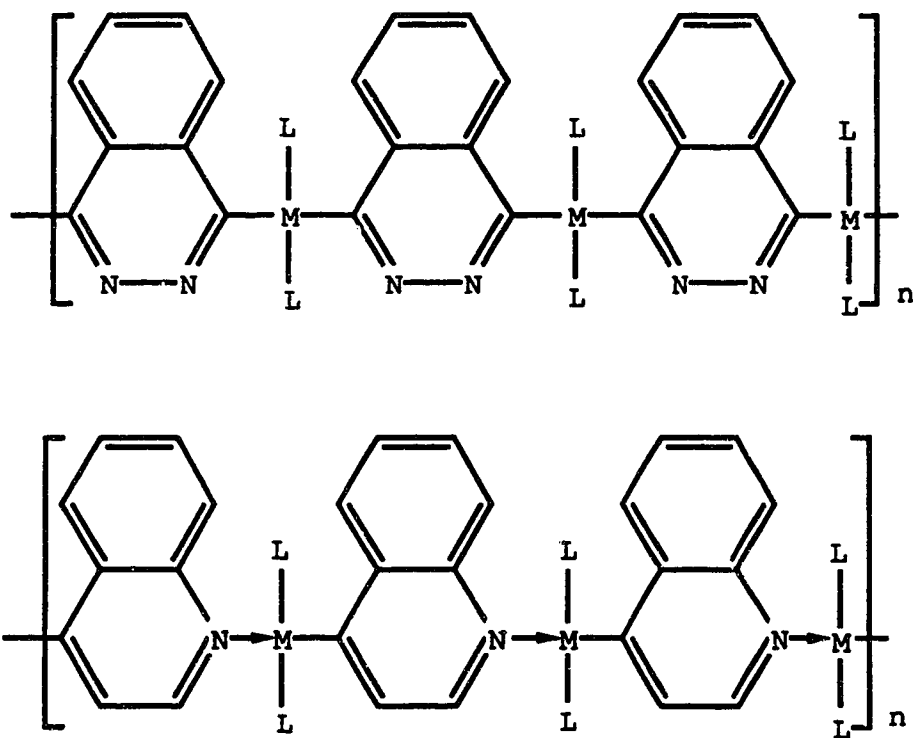


$$(E_g) = 2\text{eV}$$



$$(E_g) = 1\text{eV}$$

In the earlier Chapters, we discussed our attempts to prepare low molecular weight model compounds for organometallic heteroarene bridged complexes. To obtain, at least potentially, some of the benefits observed in going from organic heterocyclic to condensed heterocyclic polymers, we were interested in preparing a series of organometallic polymers containing related condensed (fused) ring bridging ligands, e.g.



In this Chapter the preliminary studies on the syntheses and characterization of model compounds bearing such linkages, including the X-ray crystal structure of a terminally bonded quinoxaline complex is reported.

EXPERIMENTAL SECTION

Unless otherwise noted, all reactions and subsequent manipulations were performed under anaerobic and anhydrous conditions. General procedures routinely employed in this study have been described in Chapters two and three of this thesis.

Synthesis of 2-((η^5 -cyclopentadienyl)Irondicarbonyl)-3-Chloroquinoxaline, 1Cl.

An orange solution of NaFp (4.9 mmol) in THF (75 mL) prepared as usual was cooled to $\sim -78^\circ\text{C}$. The substrate, 2,3-dichloroquinoxaline (0.98 g, 4.9 mmol) was added in one portion to the stirred solution and the temperature of the reaction mixture was maintained at $\sim -78^\circ\text{C}$ for 1 h. The cooling source was then removed and the solution allowed to warm up to room temperature over 3 h. The solution was taken to dryness *in vacuo* and then the product was purified by column chromatography (Florisil packed 2.5x14 cm column) in air. The first (purple) band was eluted with CH_2Cl_2 /hexane (1:1) and showed ν_{CO} bands (in THF) at 1994 (s), 1975 (s) and 1784 (s) cm^{-1} and was discarded as these bands are characteristic of the Fp₂ starting material. The second (yellow) band eluted with CH_2Cl_2 was identified as the desired product. The eluant was concentrated and crystallized to yield 39% (0.64 g, 1.9 mmol) of orange crystals of $\text{C}_{15}\text{H}_9\text{ClFeN}_2\text{O}_2$, 1Cl.

Anal. Calcd for $\text{C}_{15}\text{H}_9\text{ClFeN}_2\text{O}_2$: C, 52.90; H, 2.66; N, 8.23. Found: C, 53.00; H, 2.77; N, 8.21. IR (CH_2Cl_2) ν_{CO} 2034 (s) and 1983 (s) cm^{-1} . ^1H NMR ($(\text{CD}_3)_2\text{SO}$) δ 5.25 (s, 5H, C_5H_5), 7.58, 7.69 (m, 2H, H_6 & H_7), 7.82, 7.89 (m, 2H, H_5 & H_8).

$^{13}\text{C}\{^1\text{H}\}$ NMR ($(\text{CD}_3)_2\text{SO}$) δ 87.31 (s, 5C, C_5H_5), 127.37, 127.73, 128.05 & 129.09 (s, 4C, C_5 , C_6 , C_7 , & C_8), 137.46, 141.71 (s, 2C, C_9 & C_{10}), 158.57 (s, C-Cl); 189.86 (s, C-Fe); 214.90 (s, C-O). Low resolution mass spectrum m/z 340 (P^+).

Synthesis of 2,3-bis{(η^5 -cyclopentadienyl)Irondicarbonyl}-Quinoxaline, 2.

An orange solution of NaFp (10.1 mmol) in THF (90 mL) prepared as usual was cooled to $\sim -78^\circ\text{C}$. The substrate, 2,3-dichloroquinoxaline (1.00 g, 5.0 mmol) was added in one portion to the stirred solution and the temperature of the reaction mixture was maintained at $\sim -78^\circ\text{C}$ for 1 h. An IR spectrum of the solution at this stage showed carbonyl peaks at 2030 (s), 1994 (sh), 1976 (s), 1954 (sh) and 1784 (s) cm^{-1} . The cooling source was removed and the solution was allowed to warm up to ambient temperature over 3 h, and an IR spectrum showed a new peak at 1932 cm^{-1} as a shoulder peak. An air cooled reflux condenser was attached to the flask, and the mixture was refluxed for 2 days. The peak at 1932 cm^{-1} had become more pronounced. The solution was taken to dryness *in vacuo* and the compound purified by column chromatography under an N_2 atmosphere (degassed Florisil-packed column, 2.5x14 cm). The first (reddish) band eluted with CH_2Cl_2 was shown by IR to contain Fp₂ as well as some of the mono-substituted complex $\text{C}_{15}\text{H}_9\text{ClFeN}_2\text{O}_2, 1\text{Cl}$. The second (yellow) band eluted with CH_2Cl_2 was shown to be the mono-substituted complex by comparison with an authentic sample (the exact amount of the mono-substituted complex was not determined, but was estimated to be about 25%). The third (dark red) band eluted with THF was the desired product. This last eluent was taken to dryness *in vacuo* and then dissolved in CH_2Cl_2 (30 mL). The mixture was filtered and the filtrate was again taken to dryness. The resulting solid was washed with cold (-90°C) heptane (4x5 mL) and dried

in vacuo to yield 26% (0.64 g, 13.3 mmol) of the dark red product, $C_{22}H_{14}Fe_2N_2O_4 \cdot 2$.

Anal. Calcd for $*C_{22}H_{14}Fe_2N_2O_4 \cdot 1/2CH_2Cl_2$: C, 51.52; H, 2.83; N, 5.34. found: C, 52.06; H, 3.01; N, 5.63. IR (CH_2Cl_2) ν_{CO} 2038 (s), 1992 (s) and 1928 (s) cm^{-1} ; 1H NMR ($(CD_3)_2SO$) δ 4.84 & 5.22, (s (5+5)H, C_5H_5), 7.63 & 7.79 (m, 2H, H_6 & H_7) (see Fig. 3), 7.93, 7.98 (m, 2H, H_5 & H_8). $^{13}C\{^1H\}$ ($(CD_3)_2SO$) δ 82.86 & 87.61 (s, (5+5)C, C_5H_5), 126.51, 126.63, 130.29 & 131.06 (s, 4C, C_5 , C_6 , C_7 & C_8), 138.54, & 143.96 (s, 2C, C_9 & C_{10}), 211.27, 213.97 (s, 2C, C_2 & C_3), 214.12, 219.16, 289.90 (s, 4C, $C-O$). Low resolution mass spectrum m/z 482 (P^+).

* This complex was not obtained in a completely analytically pure form however its isomeric purity was ascertained from its spectroscopic data. As mentioned in Chapter two, the crystals obtained from these species often contained solvated CH_2Cl_2 and tend to desolvate to varying degrees upon exposure to vacuum or upon sitting under an inert atmosphere.

Isolation of a hydrogen-substituted byproduct, from the purification procedure for compound 2.

In an attempt to purify the di-substituted product, 2, *via* column chromatography, elution of the desired product was not complete due to an error in packing. The di-substituted complex was left on the column exposed to vacuum for 2 days and the chromatography was then completed with two major bands being eluted. The first purple band was identified by IR as containing mainly the Fp2 starting material as well as some traces of the mono-substituted complex, 1C1. The second major (dark purple) band contained a new product whose IR spectrum showed carbonyl bands in CH_2Cl_2 at 2028 (s),

1973 (s) cm^{-1} . Analysis of the material by MS showed that one of the Fp groups had been replaced by a H atom. (The compound is henceforth referred to as the hydrogen-substituted complex 1H). The compound was further purified by chromatography to exclude all the Fp₂ starting material. Subsequent to this, the compound was obtained by deliberately pumping air through a column containing the disubstituted compound, 2. Purification was carried out as above. The compound was never obtained in analytically pure form and was analyzed only spectroscopically.

IR (CH_2Cl_2) ν_{CO} 2028 (s), 1973 (s) cm^{-1} . ^1H NMR ($(\text{CD}_3)_2\text{SO}$) δ 5.2 (br), 7.9. (br). $^{13}\text{C}\{^1\text{H}\}$ NMR ($(\text{CD}_3)_2\text{SO}$) δ 86.47 (s 5C C_5H_5), 126.44, 127.13, 128.21, & 128.71 (s, 4C, C_5 , C_6 , C_7 & C_8), 138.12, & 144.37 (s, 2C, C_9 & C_{10}), 156.30 (s, C-H), 188.24 (s, C-Fe), 214.93 (C-O). Low-resolution mass spectrum m/z 306 (P^+).

Attempted Synthesis of 2 from 1Cl.

An orange solution of NaFp (1.5 mmol) in THF (50 mL) prepared as usual was cooled to $\sim -78^\circ\text{C}$. The substrate $\text{C}_{15}\text{H}_9\text{ClFeN}_2\text{O}_2$, 1Cl, (0.51 g 1.5 mmol) prepared as earlier described was added in one portion to the stirred solution, and the reaction mixture was maintained at $\sim -78^\circ\text{C}$ for 2 h. An IR spectrum of the reaction mixture at this point showed no carbonyl peak at 1932 cm^{-1} , which is characteristic of the desired product. The cooling source was removed and the reaction mixture was allowed to warm up to room temperature over 1 h. A reflux condenser was then attached to the flask and the mixture was refluxed for a total of 48 h. Over the 48 h period, only a small shoulder peak at 1934 cm^{-1} had appeared, the reaction was discontinued.

Reaction of NaFp with 1,4-dichlorophthalazine.

An orange solution of NaFp (10.1 mmol) in THF (90 mL) prepared as usual was cooled to -78°C . The substrate 1,4-dichlorophthalazine (2.00 g, 10.1 mmol) was added in one portion to the stirred solution and the temperature of the reaction mixture was maintained at -78°C for 4 h. An IR spectrum of the sample taken after 15 min showed peaks at 2032 (s), 2013 (s), 1994 (sh), 1974 (s), 1953 (s), 1785 (w) and 1687 (w) cm^{-1} . After 4 h an IR spectrum of the mixture showed peaks at 2032(s), 2013 (w), 1994 (sh), 1974 (s), 1955 (sh), 1785 (w) and 1687 (w) cm^{-1} . The solution was allowed to warm up to room temperature over 2 h, then taken to dryness *in vacuo*. An IR spectrum of the reddish sample in CH_2Cl_2 only showed peaks at 1994 (s), 1954 (s) and 1785 (s) cm^{-1} characteristic of Fp_2 dimer. The low resolution mass spectrum of a sample of the crude product showed a parent peak at m/z 354 and other peaks due to successive loss of 4 CO ligands (i.e Fp_2), while no peak was observed at m/z 340, the parent ion of desired product, nor were any peaks due to the successive loss of CO from this compound observed.

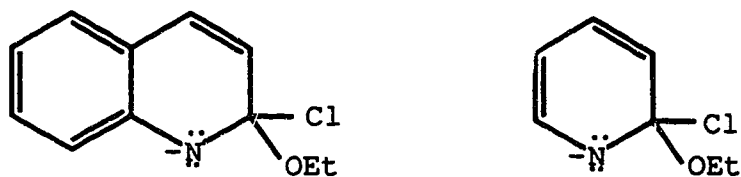
A similar reaction was carried out using two mole equivalents of Fp^- to one mole equivalent of substrate, with similar results as above; i.e., the IR spectrum of the reaction mixture after 20 min showed peaks at 2027 (sh), 2013 (s), 1994 (s), 1974 (sh), 1953 (s) and 1785 (s) cm^{-1} . The IR spectrum of a sample in CH_2Cl_2 at the end of the reaction only showed peaks 1994 (s), 1954 (s) and 1785 (s) cm^{-1} . Likewise, low resolution MS of the sample did not show any peaks at 482, the parent ion for the desired disubstituted product, nor were there any peaks due to successive loss of CO ligands observed.

X-ray crystal structure determination of C₁₅H₉ClFeN₂O₂, ICl.

All data collection and analysis was done by Dr. B.D. Santarsiero of this department. An orange crystal of C₁₅H₉ClFeN₂O₂ (approximate dimensions of 0.36x0.42x0.55 mm) was selected from a batch grown from CH₂Cl₂ (see above). Crystal data: C₁₅H₉ClFeN₂O₂, F_w = 340.55, monoclinic space group P2₁/c (No14),^{3a} a = 15.291(3)Å, b = 6.561(2)Å, c = 14.541(4)Å, β = 106.891(21)°, V = 1395.9Å³, Z = 4, D_c = 1.620 g cm⁻³, MoKα radiation (λ = 0.71073Å), μ(MoKα) = 12.75 cm⁻¹. The X-ray diffraction data (6207 reflections) were collected at ~-20°C on an Enraf-Nonius CAD4 diffractometer by the ω-2θ scan method (ω scan width = 1.00 + 0.347 tan θ). The structure was solved by examination of Patterson and Fourier maps, and adjusted by full-matrix least-squares refinement. Hydrogen atoms were placed in idealized positions by assuming C-H bond length of 0.95Å and the appropriate sp² and sp³ geometries. These atoms were then included in the calculations with fixed, isotropic Gaussian parameters 1.2 times that of the attached atom and constrained to ride on that atom. The data were corrected for absorption (and other systematic errors) using a scheme based on the absorption surface (Fourier filtering) method of Walker and Stuart.^{3b} The refinement converged to a final GOF of 1.81 and R of 0.051 with anisotropic Gaussian displacement parameter for all non-hydrogen atoms. The Enraf-Nonius SDP program package^{3c} was used.

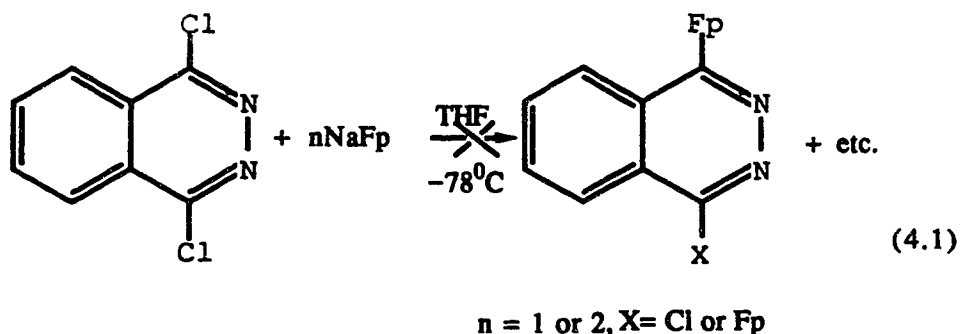
Characterization of The Complexes

It is known that fused bicyclic heteroaromatic compounds containing halides on the N-heterocyclic ring are generally more highly activated towards nucleophilic reactions than the related non-fused compounds. For example, 2-chloroquinoline reacts with sodium ethoxide about 300 times faster than 2-chloropyridine.⁴ This difference in reactivities can be explained by considering the energy difference between the starting material and the intermediate anion in both cases:

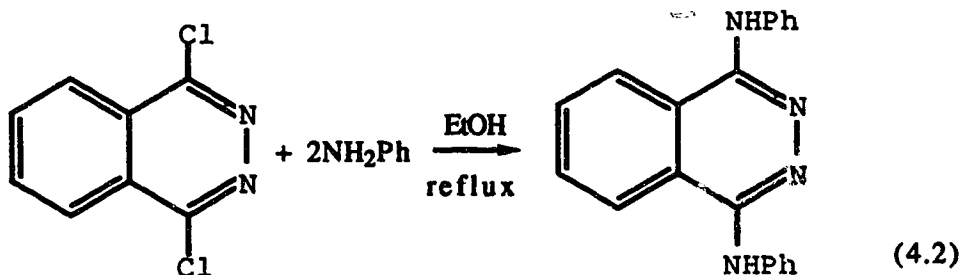


Since the sum of the aromatic resonance energies of benzene and pyridine is expected to be appreciably more than the aromatic resonance energy of quinoline, it is obvious that the loss in aromatic resonance energy on going from pyridine to its intermediate anion will be more than the corresponding loss on going from quinoline to its intermediate. Note that the intermediate anion from quinoline contains an unperturbed benzene ring. The Fp^- anion is also known to be a powerful nucleophile,⁵ thus we proceeded to synthesize our target compounds *via* direct nucleophilic displacement of a halide on the ring by the Fp^- nucleophile.

We were disappointed to find that we could not isolate our desired product(s) from the reaction(s) between the Fp^- nucleophile and 1,4-dichlorophthalazine, i.e.



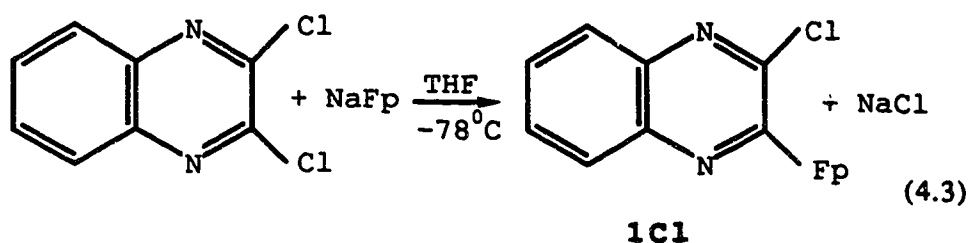
The infrared spectral evidence suggests that a reaction between the two reagents takes place at low temperature ($\sim -78^\circ\text{C}$) giving after 4 h a light red solution with carbonyl absorptions (in THF) at 2032 (s), 2013 (w), 1994 (sh), 1974 (s), 1953 (sh), 1785 (w) and 1685 (w) cm^{-1} . However, this complex peak pattern vanishes when the solution is kept at room temperature for about two hours. The new IR spectrum displayed only bands at 1994 (s), 1954 (s) and 1785 (s) cm^{-1} which is the characteristic νCO pattern of the Fp_2 dimer starting material. It is well known⁶ that organic nucleophiles such as NH_2^- , OEt^- , etc., readily displace both Cl groups in the compound 1,4-dichlorophthalazine, e.g.



However, some of the resultant products are known to be unstable.⁶ We believe from the IR evidence that the reaction of the substrate with Fp^-

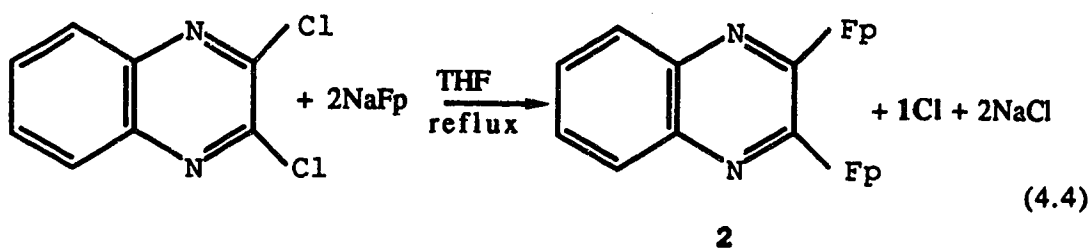
anion proceeded as expected but that the derived product(s) decomposed at ambient temperatures and thus were not isolated.

The related diazine, 2,3-dichloroquinoxaline, on the other hand has been shown to yield more stable substitution products.⁶ Not surprisingly therefore, the reaction between one equivalent each of Fp^- anion and 2,3-dichloroquinoxaline proceeded very smoothly, yielding the desired mono-substituted product, **1Cl**, i.e.



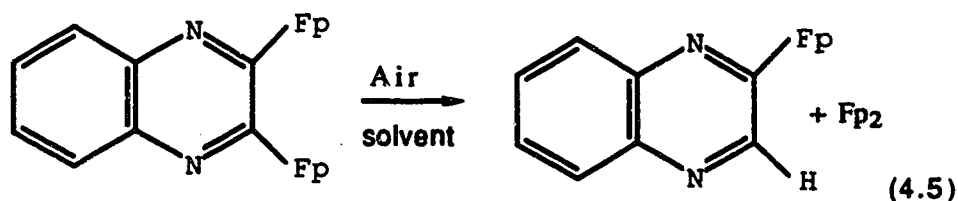
This product crystallizes readily from CH_2Cl_2 solution giving a remarkably stable crystalline compound in moderate (39%) yield.

The reaction of two equivalents of Fp^- with the substrate under more forcing conditions resulted in the formation of an additional product, the di-substituted species, **2**, i.e.



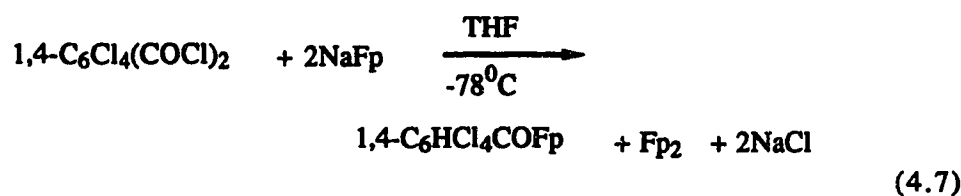
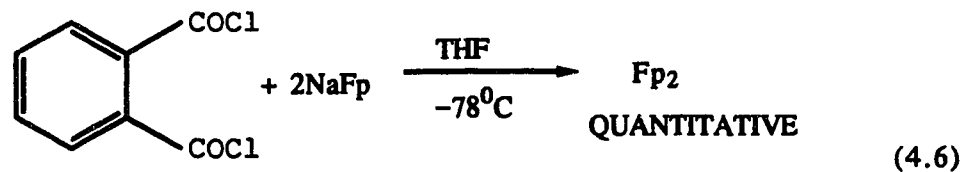
This di-substituted complex is less stable towards air and heat than is **1Cl**.

When this product was exposed to air on a chromatographic column packed with Florisil, a decomposition reaction occurred which gave rise to the formation of a new complex wherein one of the Fp groups had been replaced by a H atom, 1H, i.e.,



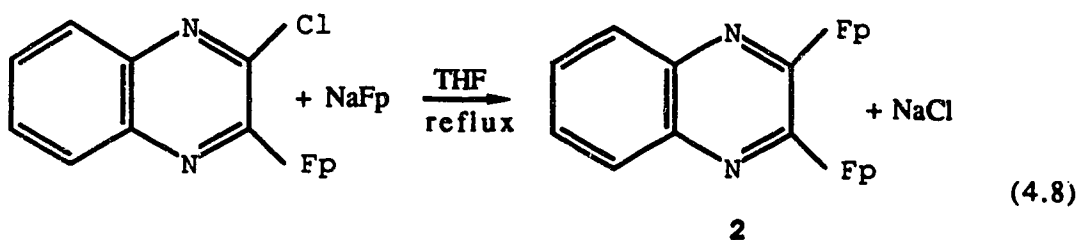
This product was only partially characterized and was not obtained in an analytically pure state.

The fact that we could synthesize and isolate the di-substituted complex was intriguing, since previous attempts to synthesize related *ortho*-substituted complexes (and other sterically crowded complexes) were unsuccessful, e.g.⁷

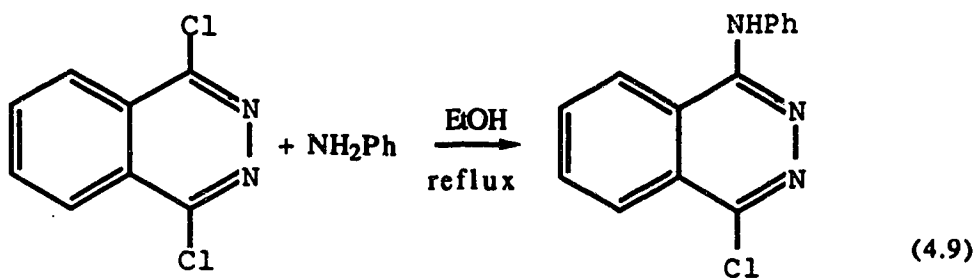


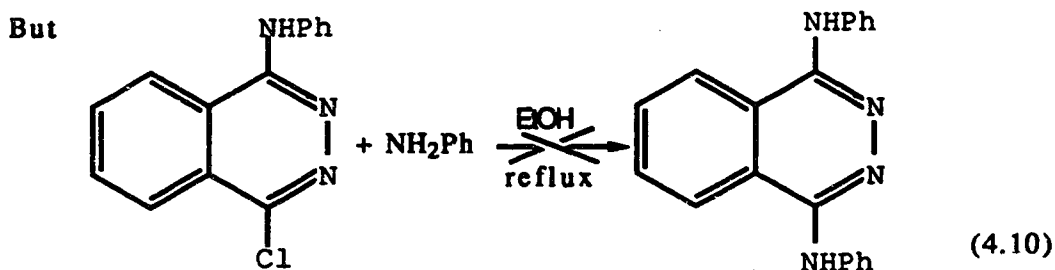
We believe that our inability to prepare these and related species arises from the steric crowding in such complexes.⁷

Attempts to increase the yields of the di-substituted complex *via* stepwise substitution of Cl group by Fp, using equations 4.3 and 4.8 were only partially successful as described in the Experimental section.



The reason(s) for the retardation of the reaction on going *via* the stepwise route is not entirely clear, but similar observations have been made earlier using organic nucleophiles.^{6a} Thus, whereas the reaction of two moles of aniline with one mole of 1,4-dichlorophthalazine proceeded smoothly to yield the desired disubstituted product as shown in equation 4.2, attempts to synthesize this disubstituted compound *via* stepwise substitution with one mole each of reactants under identical conditions for each step was unsuccessful, i.e.





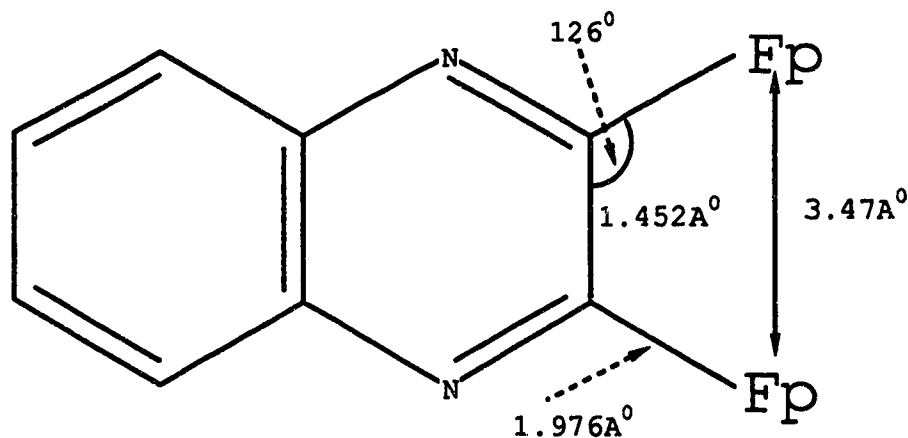
Characterization of the Complexes.

The nuclearities of the complexes were identified by their elemental analysis and mass spectra. Thus, the mono-substituted complex, 1Cl, showed a parent ion, P^+ , at m/z 340 and other peaks at 312 and 284 due to the successive loss of the two CO groups, and each of these peaks displayed the characteristic isotopic pattern expected of compounds containing a single Cl group (with its two isotopes in a 3 to 1 ratio). The di-substituted complex, 2, showed a parent ion peak, P^+ , at m/z 482 with other peaks at 454, 426, 398 and 370 due to the successive loss of four CO groups. Compound 1H showed a P^+ at m/z 306 and other characteristic peaks at 278 and 250.

The identity of the mono-substituted complex, 1Cl, was further confirmed by determination of its X-ray crystal structure. ORTEP plots of selected views of the complex are reproduced in Figures 4.1-4.3. Selected bond lengths and angles, torsion angles and least-squares planes are reported in Tables 4.1-4.4 respectively. The iron centre has the expected three-legged piano-stool geometry. Thus, iron carries a normal symmetrically bonded η^5 -C₅H₅ group, as well as two linear CO groups having Fe-C and C-O bonds (1.765(3)Å, 1.769(3)Å and 1.139(3)Å, 1.143(4)Å, respectively) in the ranges expected for Fp complexes. The quinoxaline ring is bonded to the iron atom at the 3-position to form the third leg of the piano-stool arrangement. The Fe-C

(quinoxaline) bond length of 1.976\AA is in the same range as reported for related complexes having formal $\text{Fe-C}(sp^2)$ single bonds ($1.94\text{-}2.03\text{\AA}$)⁸ and also within the range of those reported for cationic Fe-carbene complexes having formal $\text{Fe-C}(sp^2)$ double bonds ($1.91\text{-}2.00\text{\AA}$).⁹ Again,¹⁰ this is consistent with our proposal that these bonds have significant double bond character. Again, we observe that the plane of the quinoxaline ring is oriented perpendicular to the Fp mirror plane (Fig. 4.2) contrary to its expected orientation.¹⁰

The most important structural feature of this complex is the loss of the planarity of the quinoxaline ring as shown in Figure 4.3. The Fp and Cl groups are bent upwards and downwards relative to each other, presumably to minimize steric repulsion. In the process, the quinoxaline ring is twisted to a propeller blade type structure. Extrapolation of this structure to the anticipated structure of the di-substituted complex wherein the two Fp groups subtend approximately equal angles at the *ipso* carbons, as does the Fp in compound 1Cl (i.e. 126.2°), and maintaining the Fe-C quinoxaline bond lengths equal at $1.976(2)\text{\AA}$ as in 1Cl, gives the structure shown below.



This allows us to calculate that the distance between the two metal centres in such a species (3.47Å) would be within the sum of their Van der Waals radii (estimated at 4.0Å).¹¹ Thus, considering the bulkiness of the Fp group, such a complex would be expected to be very sterically crowded and exhibit unusual structural features such as substantially greater quinoxaline ring twisting, or ligand rearrangement to give more closely interacting Fe-centres. Results of the spectroscopic and electrochemical characterization of the complexes (see below) confirm that some such structural distortion is in fact present in the disubstituted complex.

We have studied a wide variety of Fp substituted arenes and Fp substituted heterocyclic complexes and in each case have observed^{7,12} that, as expected, the IR spectra of the complexes in the carbonyl region display two characteristic stretching bands. For the azine complexes in particular, we observe a symmetric band, A', between 2010 and 2050 cm⁻¹ and an anti-symmetric band, A'', 1970 and 2000 cm⁻¹. Indeed, in our earlier studies,¹³ we found that even a complex with two Fp groups in two inequivalent positions, i.e. 2,4-C₅NF₃Fp₂,¹⁰ displays only a single pair of carbonyl bands (ν_{CO} (CH₂Cl₂) 2033 and 1983 cm⁻¹) and that for all of the disubstituted azenes, these occur at energies lower than those of the related monosubstituted complexes i.e. 4-C₅NF₄Fp (ν_{CO} (CH₂Cl₂) 2044 and 1997 cm⁻¹). Both mono-substituted complexes 1Cl and 1H exhibited the expected peak pattern. As would be expected on the basis of the relative electronegativities of the H and Cl substituents, complex 1H contains a more electron rich iron centre, thus it has its peaks at lower frequencies (ν_{CO} (CH₂Cl₂) 2028 and 1973 cm⁻¹) than the analogous complex 1Cl (ν_{CO} (CH₂Cl₂) 2032, 1983 cm⁻¹).

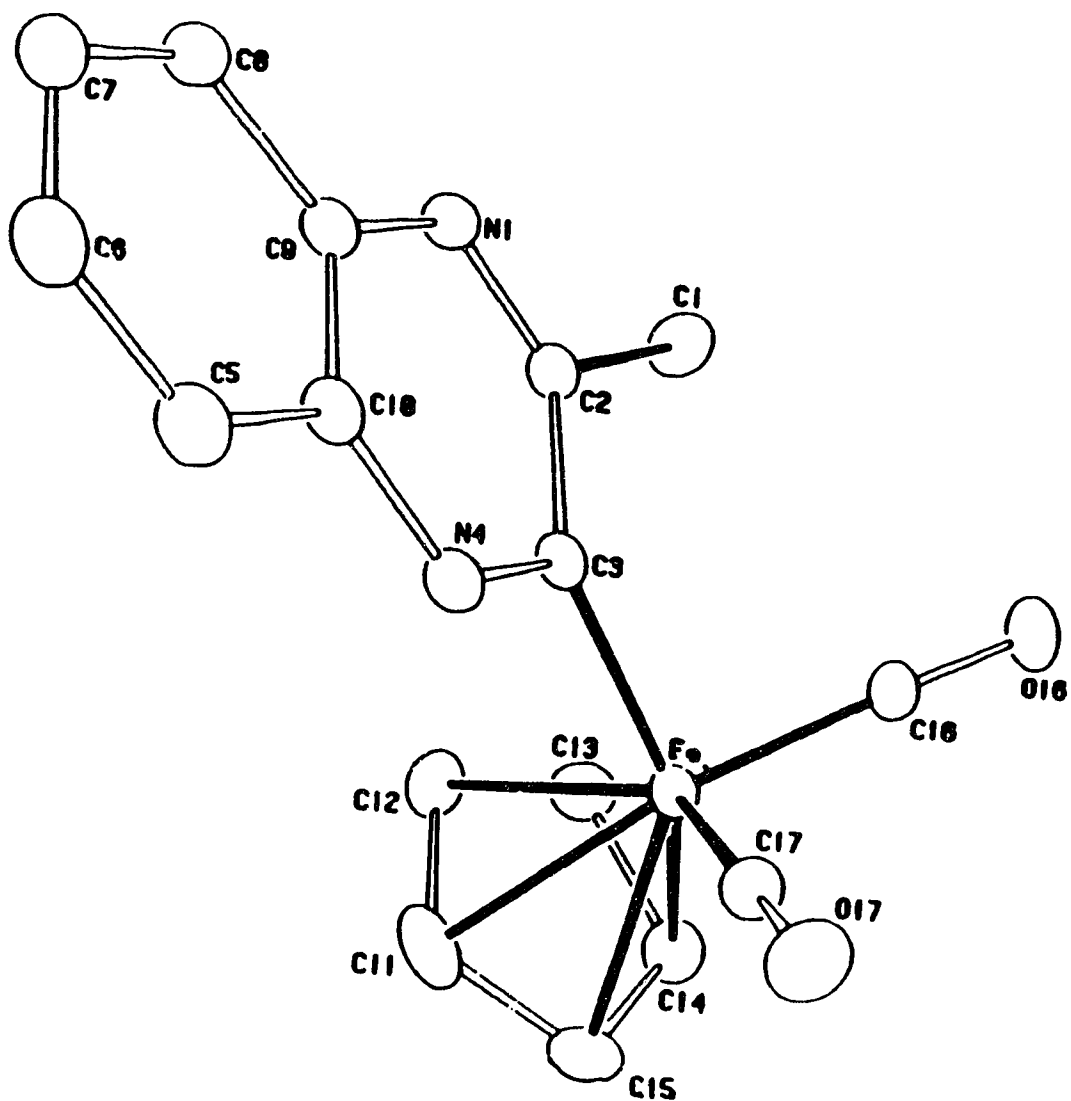


Figure 4.1 ORTEP plot of $[\text{CpFe}(\text{CO})_2]\text{C}_8\text{H}_4\text{N}_2\text{Cl} \cdot \text{Cl}$.

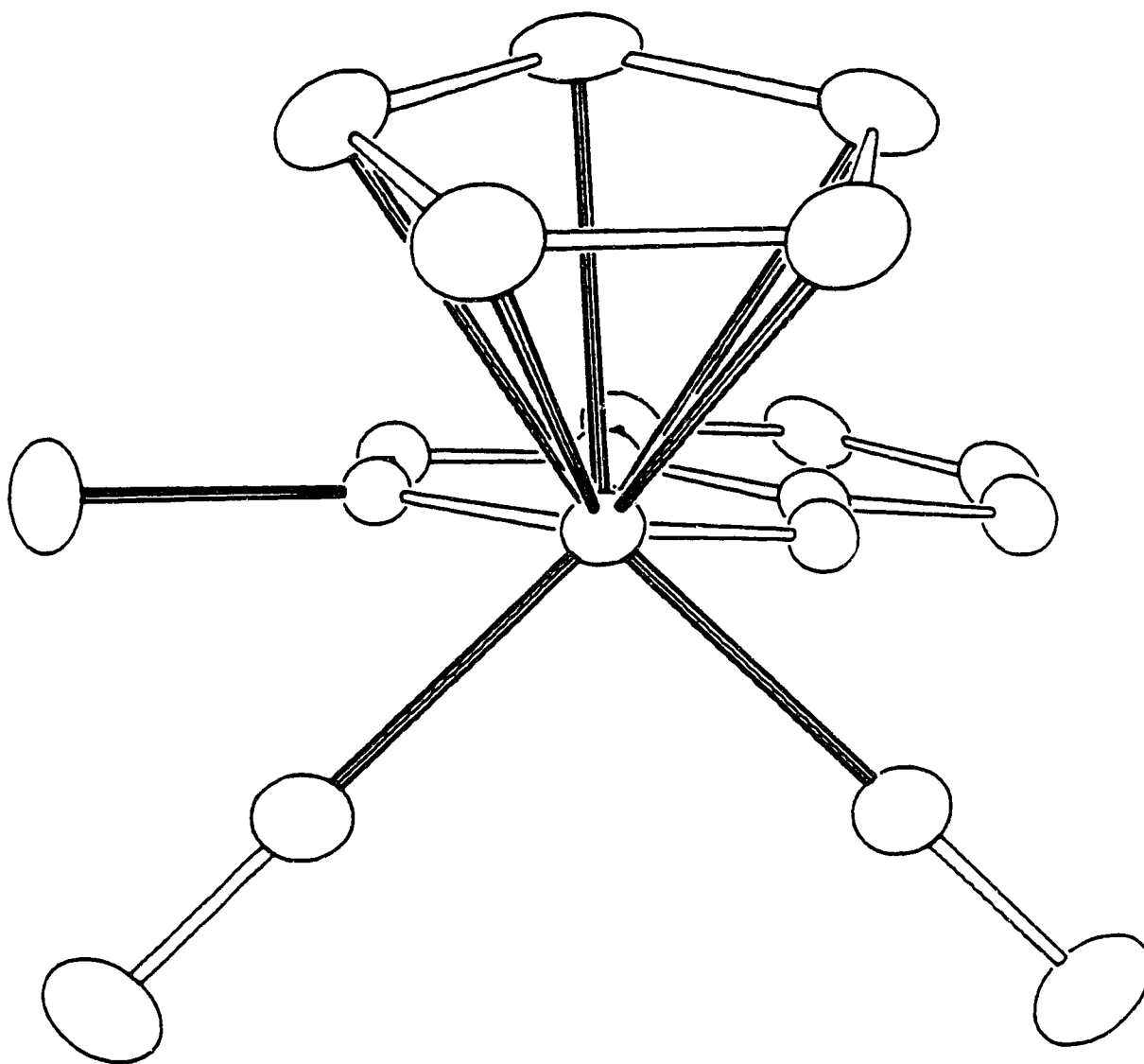


Figure 4.2 ORTEP plot of $[\text{CpFe}(\text{CO})_2]\text{C}_8\text{H}_4\text{N}_2\text{Cl}$, 1Cl, view down Fe-C3.

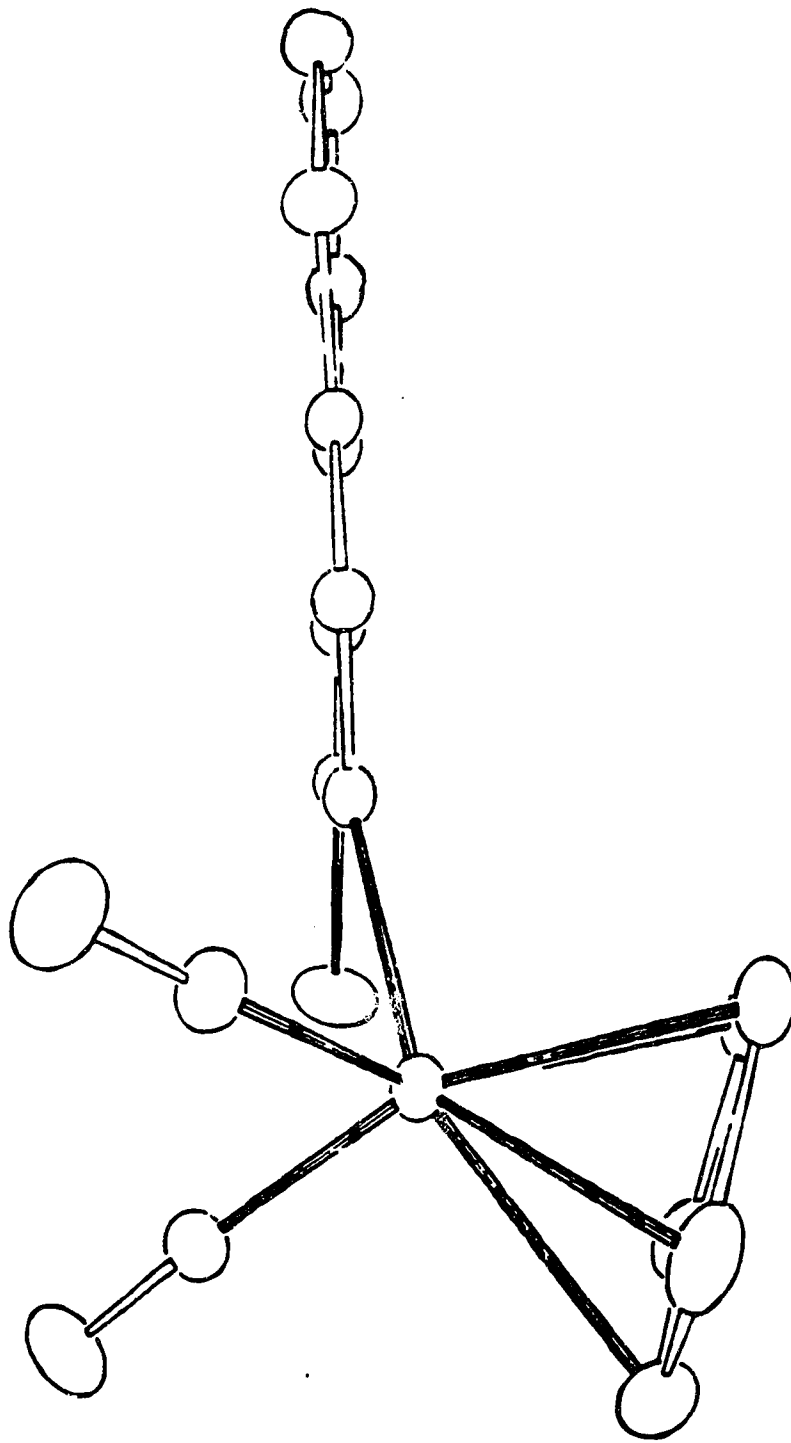


Figure 4.3 ORTEP plot of [CpFe(CO)₂]C₈H₄N₂Cl, 1Cl, showing twist in quinoxaline ring

Table 4.1 Selected bond lengths in $[\text{CpFe}(\text{CO})_2]\text{C}_8\text{H}_4\text{N}_2\text{Cl}$, 1Cl.

Atom1	Atom2	Length	Atom1	Atom2	Length
Fe	C3	1.976 (2)	C5	C6	1.355 (4)
Fe	C11	2.095 (3)	C5	C10	1.416 (4)
Fe	C12	2.107 (3)	C6	C7	1.405 (5)
Fe	C13	2.106 (3)	C7	C8	1.369 (4)
Fe	C14	2.123 (3)	C8	C9	1.406 (3)
Fe	C15	2.116 (3)	C9	C10	1.400 (4)
Fe	C16	1.765 (3)	C11	C12	1.409 (5)
Fe	C17	1.769 (3)	C11	C15	1.430 (4)
C1	C2	1.750 (2)	C12	C13	1.394 (4)
N1	C2	1.289 (3)	C13	C14	1.412 (4)
N1	C9	1.371 (3)	C14	C15	1.388 (5)
C2	C3	1.452 (3)	C16	O16	1.139 (3)
C3	N4	1.317 (3)	C17	O17	1.143 (4)
N4	C10	1.370 (3)			

Table 4.2 Selected interatomic angles in $[\text{CpFe}(\text{CO})_2]\text{C}_8\text{H}_4\text{N}_2\text{Cl}$, 1Cl.

Atom1	Atom2	Atom3	Angle	Atom1	Atom2	Atom3	Angle
C3	Fe	C11	99.26 (10)	C11	C12	C13	108.1 (2)
C3	Fe	C12	84.44 (10)	C12	C13	C14	108.4 (3)
C3	Fe	C13	108.56 (10)	C13	C14	C15	108.3 (2)
C3	Fe	C14	147.03 (11)	C14	C15	C11	107.9 (3)
C3	Fe	C15	138.63 (10)	C15	C11	C12	107.3 (3)
Fe	C16	O16	176.9 (2)	Fe	C17	O17	179.2 (2)
Fe	C3	C2	126.2 (2)	Fe	C3	H4	117.9 (2)
C3	Fe	C16	95.68 (11)	C3	Fe	C17	87.84 (11)
C16	Fe	C17	93.22 (12)				
C2	C3	H4	115.4 (2)	C3	H4	C10	120.5 (2)
C6	C5	C10	120.1 (3)	C5	C6	C7	120.7 (3)
C6	C7	C8	120.4 (3)	C7	C8	C9	119.6 (3)
H1	C9	C8	120.0 (3)	H1	C9	C10	119.7 (2)
C8	C9	C10	120.0 (2)	H4	C10	C5	119.7 (3)
H4	C10	C9	121.2 (2)	C5	C10	C9	119.0 (2)
C2	H1	C9	116.5 (2)	C1	C2	H1	114.4 (2)
C1	C2	C3	119.0 (2)	H1	C2	C3	126.5 (2)

Table 4.3 Weighted least squares planes in $[\text{CpFe}(\text{CO})_2]\text{C}_8\text{H}_4\text{N}_2\text{Cl}$, 1Cl.

Plane	Coefficients ^b				Defining Atoms with Deviations ^c			
1	0.7214	-6.3975	2.8139	1.0457	<u>C11</u>	-0.007(3)	<u>C12</u>	0.008(3)
					<u>C13</u>	-0.006(3)	<u>C14</u>	0.003(3)
					<u>C15</u>	0.003(3)		
					<u>Fe</u>	-1.737	<u>C16</u>	-2.771
					<u>C17</u>	-2.790	<u>C3</u>	-2.667
2	-3.7652	-4.5109	-8.4642	-2.7661	<u>Fe</u>		<u>C16</u>	
							<u>C17</u>	
					<u>O16</u>	0.061	<u>O17</u>	-0.013
					<u>N1</u>	-4.167	<u>C2</u>	-2.916
					<u>C3</u>	-1.966	<u>N4</u>	-2.471
					<u>C1</u>	-2.364	<u>C11</u>	0.519
					<u>C12</u>	-0.121	<u>C13</u>	0.636
					<u>C14</u>	1.772	<u>C15</u>	1.711
3	3.5903	-5.6223	5.3912	-0.0234	<u>N1</u>	-0.021(2)	<u>C2</u>	-0.032(2)
					<u>C3</u>	0.030(2)	<u>N4</u>	0.019(2)
					<u>C5</u>	-0.050(3)	<u>C6</u>	-0.034(3)
					<u>C7</u>	0.040(3)	<u>C8</u>	0.032(3)
					<u>C9</u>	0.008(2)	<u>C10</u>	-0.007(2)
					<u>Fe</u>	0.356	<u>C1</u>	-0.120
					<u>C16</u>	-0.939	<u>C17</u>	-0.708
					<u>O16</u>	-1.760	<u>O17</u>	-1.392
Dihedral Angles ^d								
Planes	Angle	Planes	Angle	Planes	Angle			
1 - 2	59.3	1 - 3	18.9	2 - 3	77.4			

^aThe weights are generated from the estimated standard deviations of the atomic coordinates, and the plane is determined from an algorithm derived by Hamilton, *Acta Crystallogra.*, 14, (1961).

^bCoefficients are of the form $ax + by + cz - d = 0$ where x , y , and z are fractional crystallographic coordinates.

^cDisplacements from the least-squares plane are given in Angstroms, with the estimated standard deviation given in parentheses. Those atoms which are underlined were not included in the definition of the least-squares plane.

^dIn degrees.

Table 4.4 Torsional angles in [CpFe(CO)₂][C₈H₄N₂Cl, 1Cl.

Atom 1	Atom 2	Atom 3	Atom 4	Angle	Atom 1	Atom 2	Atom 3	Atom 4	Angle
C16	Fe	C3	C2	53.78 (0.22)	Fe	C3	N4	C10	-170.49 (0.18)
C16	Fe	C3	N4	-134.73 (0.19)	C2	C3	N4	C10	1.91 (0.33)
C17	Fe	C3	C2	146.81 (0.22)	C3	N4	C10	C5	-178.48 (0.22)
C17	Fe	C3	N4	-41.71 (0.20)	C3	N4	C10	C9	1.50 (0.35)
C3	Fe	C16	O16	178.34 (4.46)	C10	C5	C6	C7	0.69 (0.48)
C17	Fe	C16	O16	90.19 (4.47)	C6	C5	C10	N4	-177.95 (0.26)
C3	Fe	C17	O17	28.67 (18.64)	C6	C5	C10	C9	2.07 (0.41)
C16	Fe	C17	O17	124.25 (18.64)	C5	C6	C7	C8	-3.15 (0.45)
C9	N1	C2	C1	-178.16 (0.18)	C6	C7	C8	C9	2.74 (0.42)
C9	N1	C2	C3	2.24 (0.37)	C7	C8	C9	N1	-178.95 (0.29)
C2	N1	C9	C8	-179.50 (0.36)	C7	C8	C9	C10	0.05 (1.72)
C2	N1	C9	C10	1.49 (0.35)	N1	C9	C10	N4	-3.42 (0.36)
C1	C2	C3	Fe	-11.97 (0.30)	N1	C9	C10	C5	176.57 (0.24)
C1	C2	C3	N4	176.37 (0.18)	C8	C9	C10	N4	177.58 (0.23)
N1	C2	C3	Fe	167.62 (0.20)	C8	C9	C10	C5	-2.44 (0.37)
N1	C2	C3	N4	-4.05 (0.36)					

Surprisingly, the di-substituted complex, **2**, shows three rather than the expected two peaks in the carbonyl stretching frequency region, at 2038, 1992 and 1929 cm^{-1} , in CH_2Cl_2 . The two peaks at higher energy in **2** are in the range found for other Fp-azines. However, they are at higher energy than those of compound **1Cl** (see above). It would be expected that the simple replacement of Cl on compound **1Cl** by a Fp substituent would render the quinoxaline ring, and thus the Fe centres in **2** even more electron rich than in the mono-substituted analogue, **1H**, thus giving lower ν_{CO} values. This is the opposite of what we observe. The third carbonyl band in this compound at 1928 cm^{-1} appears in an extremely unusually position for a terminal carbonyl for a Fp-X complex. The lowest reported carbonyl bands for such an aryl or azine complex are at 2013 and 1958 cm^{-1} for $\text{C}_6\text{H}_3\text{Fp}_3$ ⁷. Given the relative electron poorness of the Fp-azine complexes, such a band position is incompatible with a simple terminal carbonyl on Fp and is perhaps better considered as some sort of bridging carbonyl ligand. For comparison, the bridging carbonyl band in Fp_2 is observed at 1774 cm^{-1} in CH_2Cl_2 .

The ^{13}C and ^1H NMR data for both mono-substituted complexes are as expected. For example, the singlet at δ 5.25 ppm for compound **1Cl** is assignable to the cyclopentadienyl ligand and is found in the usual region (5.20-5.35 ppm) for Fp-azines.¹¹ The ^1H signals of the quinoxaline protons for this complex (see Fig.4.5) appear as an ACEG spin system indicating that all four protons are chemically inequivalent, as expected for this asymmetric geometry.

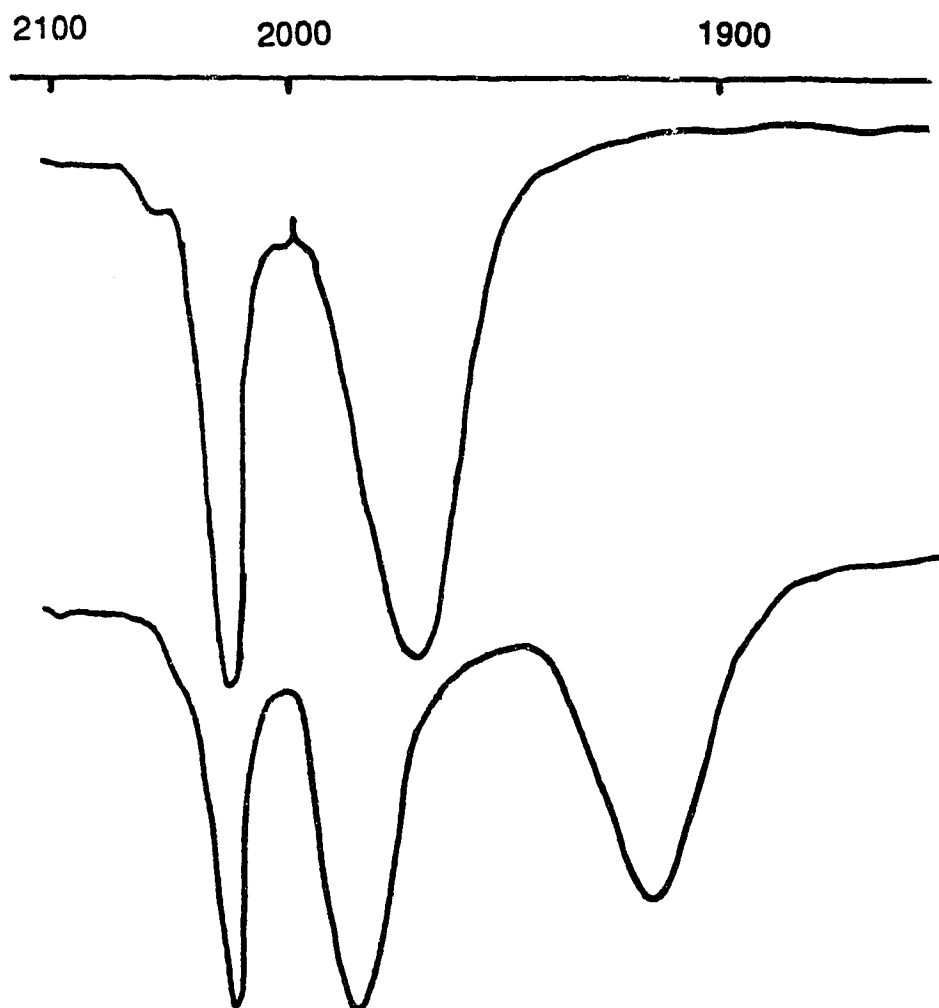
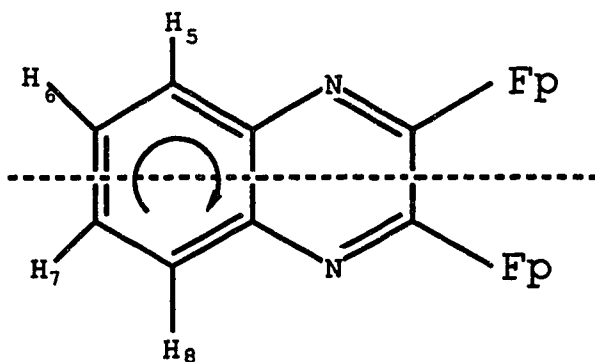


Figure 4.4 IR spectra of 1C1 (top) and 2 (bottom), in the carbonyl region.

The ^{13}C NMR data for both mono-substituted complexes are again as expected. Thus, each has a signal assignable to the cyclopentadienyl carbons and a second signal attributable to the carbonyl carbons. Again, these occur in the usual regions for Fp-azines (i.e., 86.6-87.9 and 210-220 ppm for Cp and CO, respectively). As expected from the asymmetric structure and the ^1H NMR data, one observes eight other carbon signals attributable to the eight different carbons in the quinoxaline ring.

On the other hand, the ^1H and ^{13}C NMR spectra for the disubstituted complex, **2**, (Figures 4.6 and 4.8 respectively) were most unexpected. Assuming that the two Fp groups were chemically equivalent, then one would expect that the complex has a mirror plane of symmetry or a two-fold axis of rotation along the centre line of the quinoxaline ring.



Thus, one would expect to observe only two proton signals for the quinoxaline protons and one signal for the ten equivalent cyclopentadienyl protons. One would also observe four signals for the quinoxaline ring

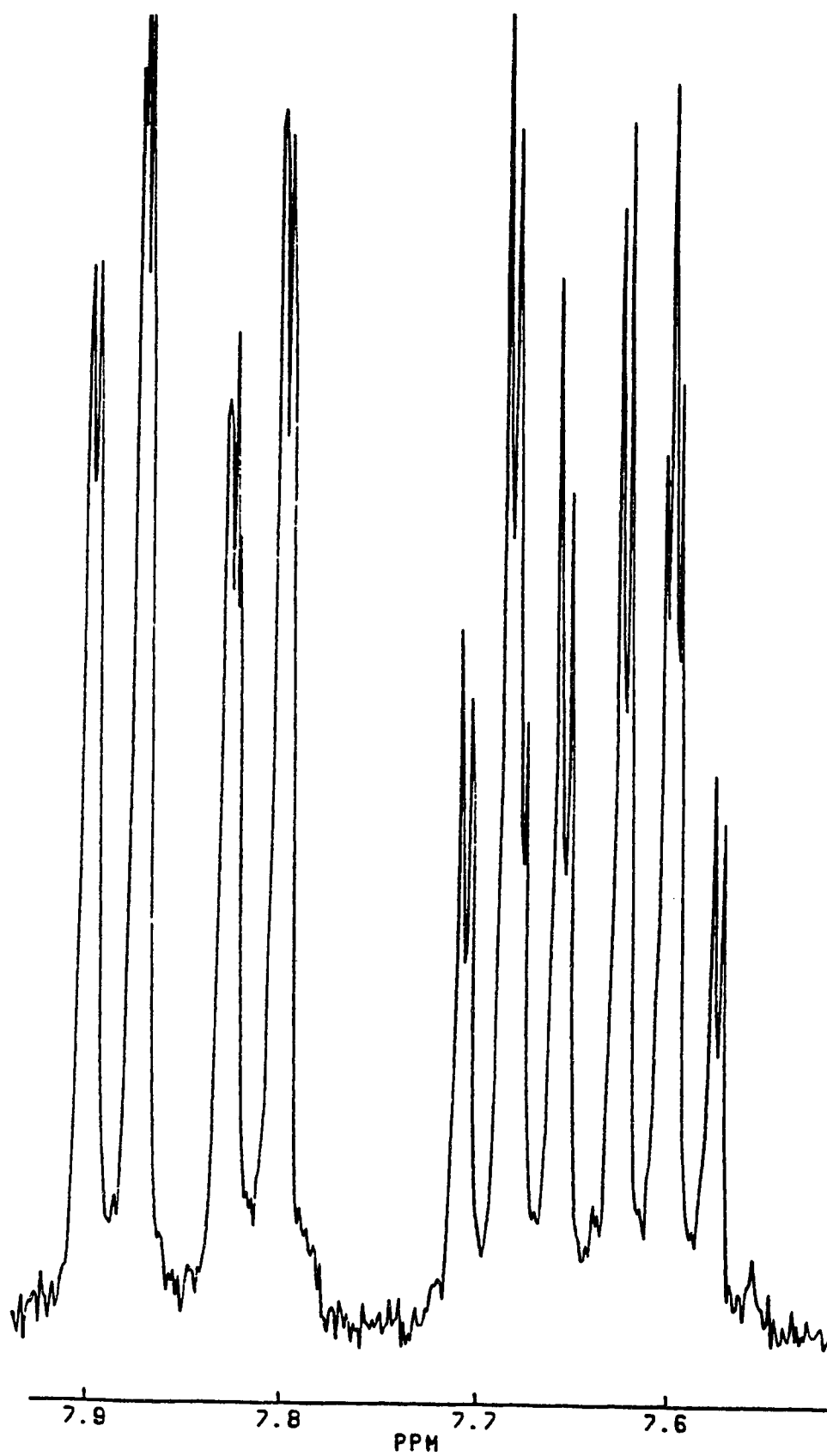


Figure 4.5 ^1H NMR spectrum of 1Cl showing the quinoxaline region.

carbons, one for the ten cyclopentadienyl carbons and one (or possibly two with hindered rotation) for the four carbonyl carbons. Surprisingly, a totally different kind of spectral pattern is observed in both the ^1H and ^{13}C NMR spectra.

The ^1H NMR spectrum shows two signals attributable to the cyclopentadienyl protons, one at a position normally observed for such complexes (i.e., at 5.22 ppm) and the other at a much higher field position (4.74 ppm) than we have observed previously. Similarly, in the ^{13}C NMR spectrum two signals attributable to the cyclopentadienyl ring are observed, one peak (87.81 ppm) occurring in the region usually observed for related complexes and the other peak at 82.85 ppm is shifted approximately 5 ppm upfield from the position normally observed for Fp-X type complexes.

We have now synthesized and characterized over sixty Fp substituted complexes in our laboratories (including those in which the Fp-phenyls are further complexed to a $\text{Cr}(\text{CO})_3$ fragment). In all of these complexes, the ^1H signal of the cyclopentadienyl protons appear at 5.2 ± 0.2 ppm, while the ^{13}C signal of the cyclopentadienyl carbons appear at 87.0 ± 0.8 ppm (all signals observed in $(\text{CD}_3)_2\text{SO}$ as solvent with TMS as reference). Thus, the ^1H and ^{13}C spectra of compound 2 indicate that an unusual type of cyclopentadienyl ligand is present.

The ^{13}C NMR signals attributable to the carbonyl carbons are also unusual. There are two signals observed at 214.96 and 219.16 ppm, in the region usually observed for terminal carbonyl carbons of Fp-azine complexes (*vide supra*). In addition, a very low field signal is observed at 289.90 ppm, a region normally associated with bridging carbonyl carbons (e.g., for Fp_2 the bridging carbonyls are observed at 290 ppm). This strongly

indicates that there is some type of a bridging carbonyl ligand in this complex as the IR data presented above also suggests.

Finally, we observed that the ^1H signals attributable to the quinoxaline protons have multiplicities similar to those of the mono-substituted complexes and can be described as an ACEG spin system representing four inequivalent types of protons. The following were also observed: The ^{13}C spectrum shows asymmetry related to that observed in the ^1H spectrum, thus, there are eight other signals assignable to eight different carbons on the quinoxaline ring, again showing that the mirror plane or two-fold axis of symmetry does not exist for this complex, hence that the two iron centres are inequivalent. Also, $^1\text{H}[H]$ experiments (Fig. 4.8) indicate that the signals arise from a single compound, while variable temperature NMR (-78 to 58°C) showed no evidence for nonrigidity.

We have also characterized the mono-substituted complex 1Cl and the di-substituted complex, 2, by studying their electrochemical oxidation *via* cyclic voltammetry. The mono-substituted complex, 1Cl, exhibited chemical irreversibility upon oxidation at a potential of 1.35 V ($E_{p,a}$). This was as expected, since we have generally observed that all Fp-azine complexes that we have studied in which the Fp group(s) is (are) substituted adjacent to the ring nitrogen atom(s), e.g.,

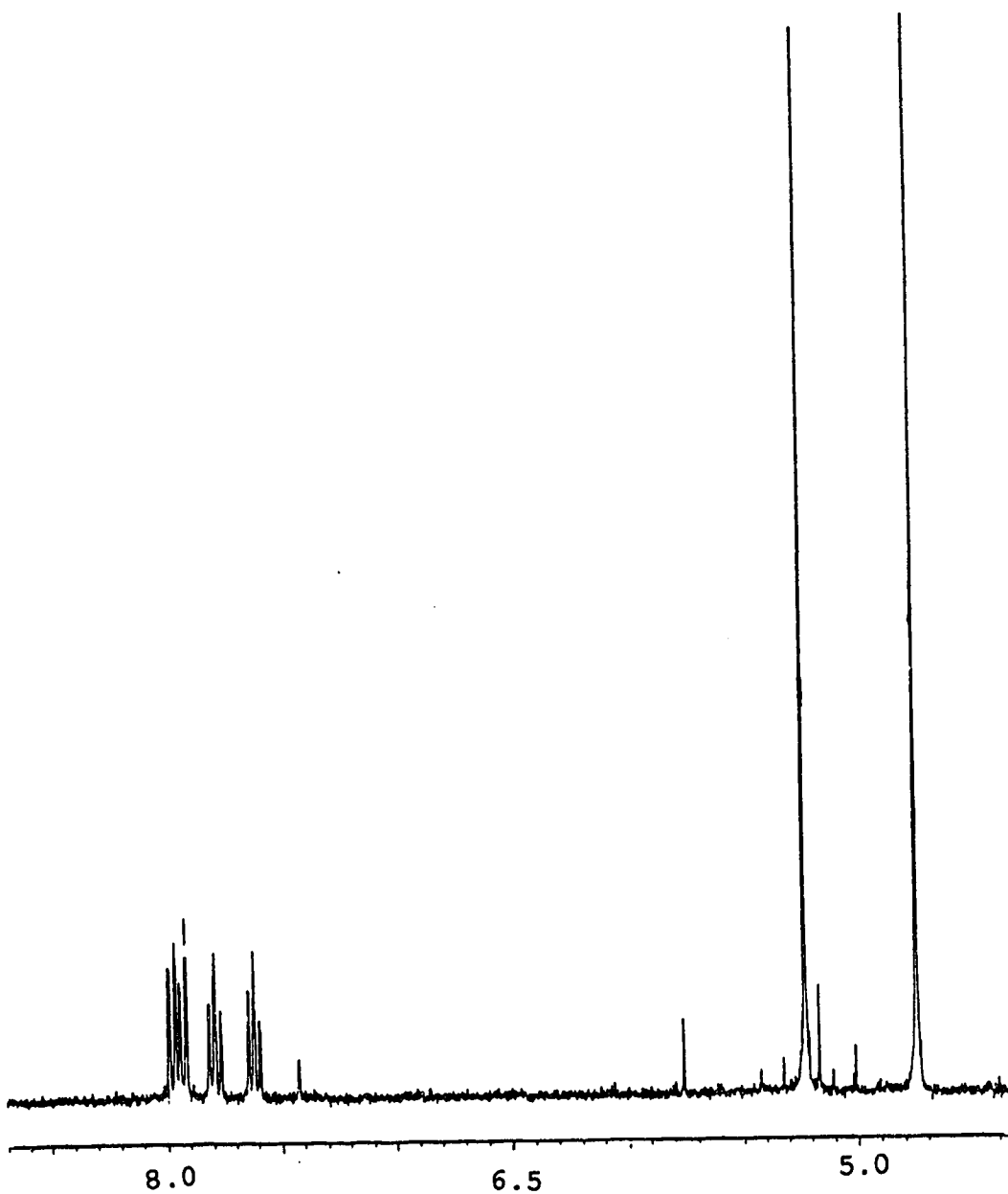


Figure 4.6 ^1H NMR spectrum of **2** showing the C_5H_5 and quinoxaline regions

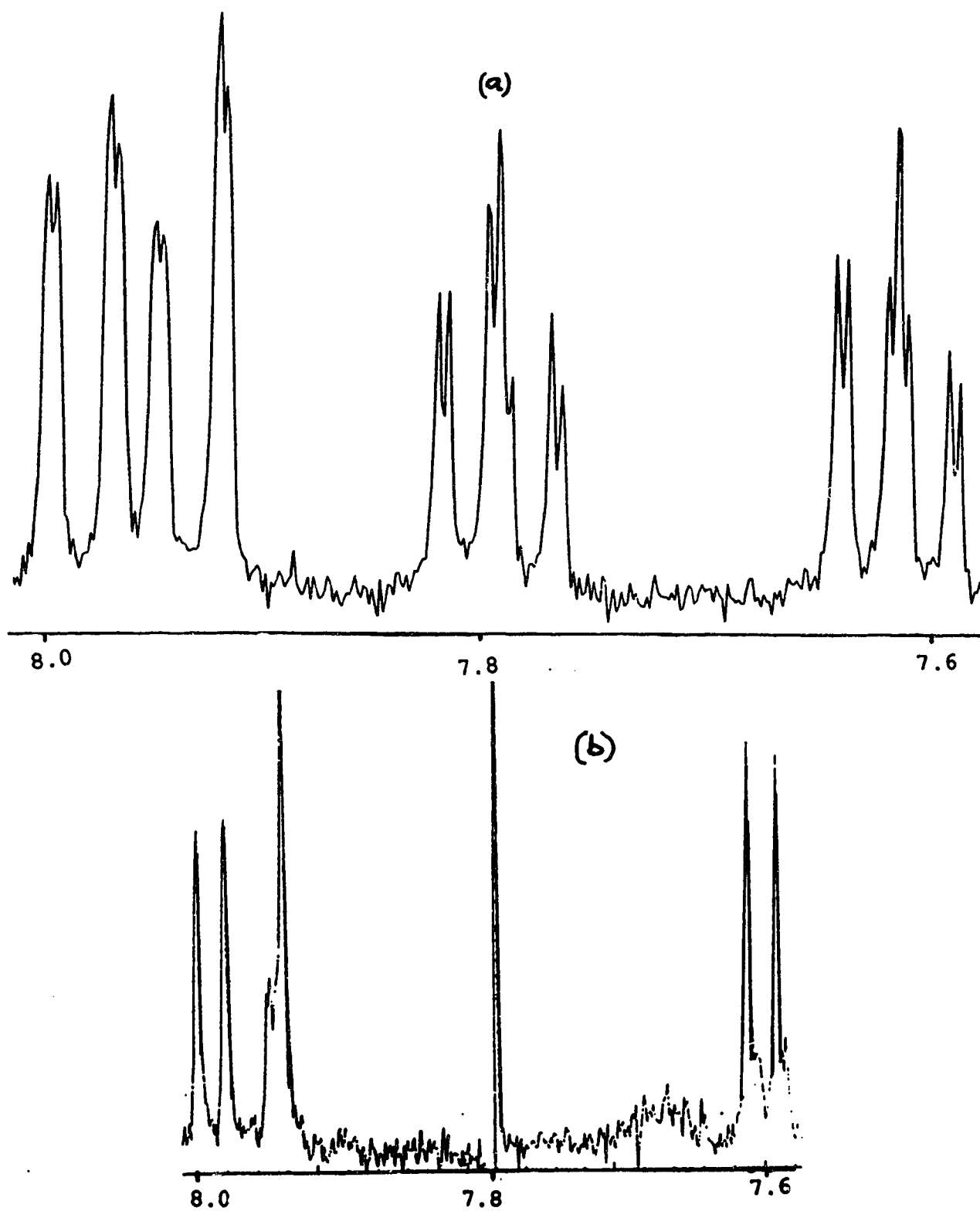


Figure 4.7 (a) ^1H NMR spectrum of **2** showing quinoxaline region. (b) irradiating the signal at δ 7.8 ppm

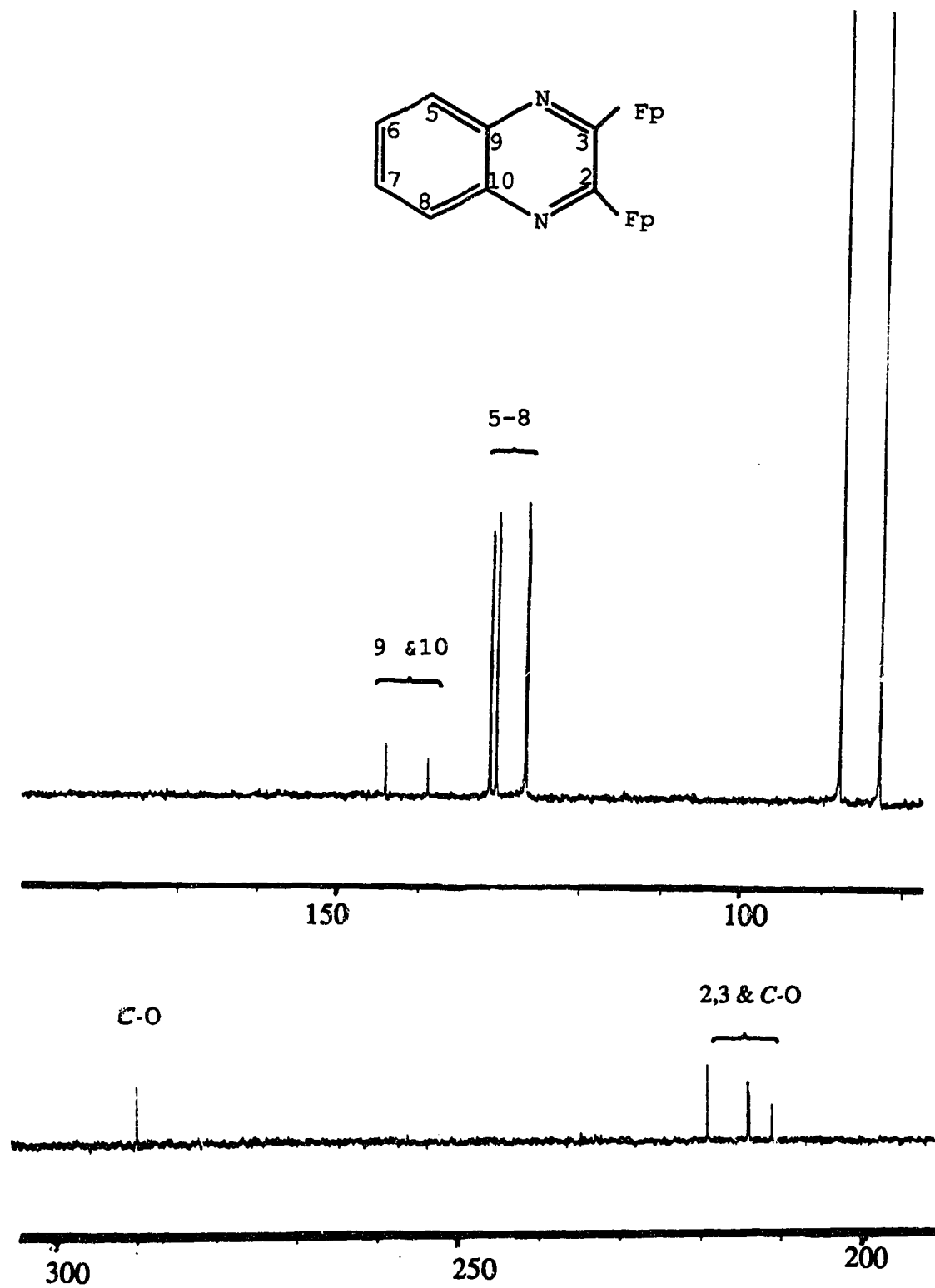


Figure 4.8 ^{13}C NMR spectrum of 2.

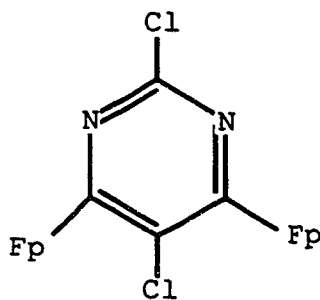
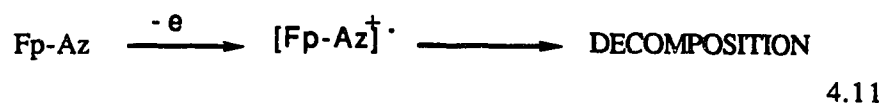


exhibit total electrochemical irreversibility (no return peaks) at scan rates up to 10 V/sec.¹³ We postulate that instability and thus chemical irreversibility of the radical cations generated in such oxidations, i.e.,



may be connected to migration of the $[\text{Fp}]^+$ group to the nitrogen atom, followed by subsequent product decomposition.

Surprisingly, the di-substituted complex showed some degree of reversibility (see Fig. 4.9) even at low scan rates. Thus, at a scan rate of 1.0 V/sec the ratio $i_{p,c}/i_{p,a}$ is 0.94 (for complete chemical reversibility, $i_{p,c}/i_{p,a} = 0.96$ is the accepted standard). Moreover, on scanning to higher potentials, we observed a second oxidation peak which was less well defined. The unusually low first oxidation potential (0.34 V compared to 1-1.98 V for other Fp-azines we have studied)¹⁴ and the very large wave to wave separation for the two oxidations ($\Delta E_{1/2} = 660$ mV, see Chapter 3 of this thesis) indicates substantial Fe-Fe interaction in this complex.¹⁴

These novel data for compound 2 can be summarized as follows;

- (a) steric crowding around the quinoxaline ring
- (b) bridging carbonyl(s)

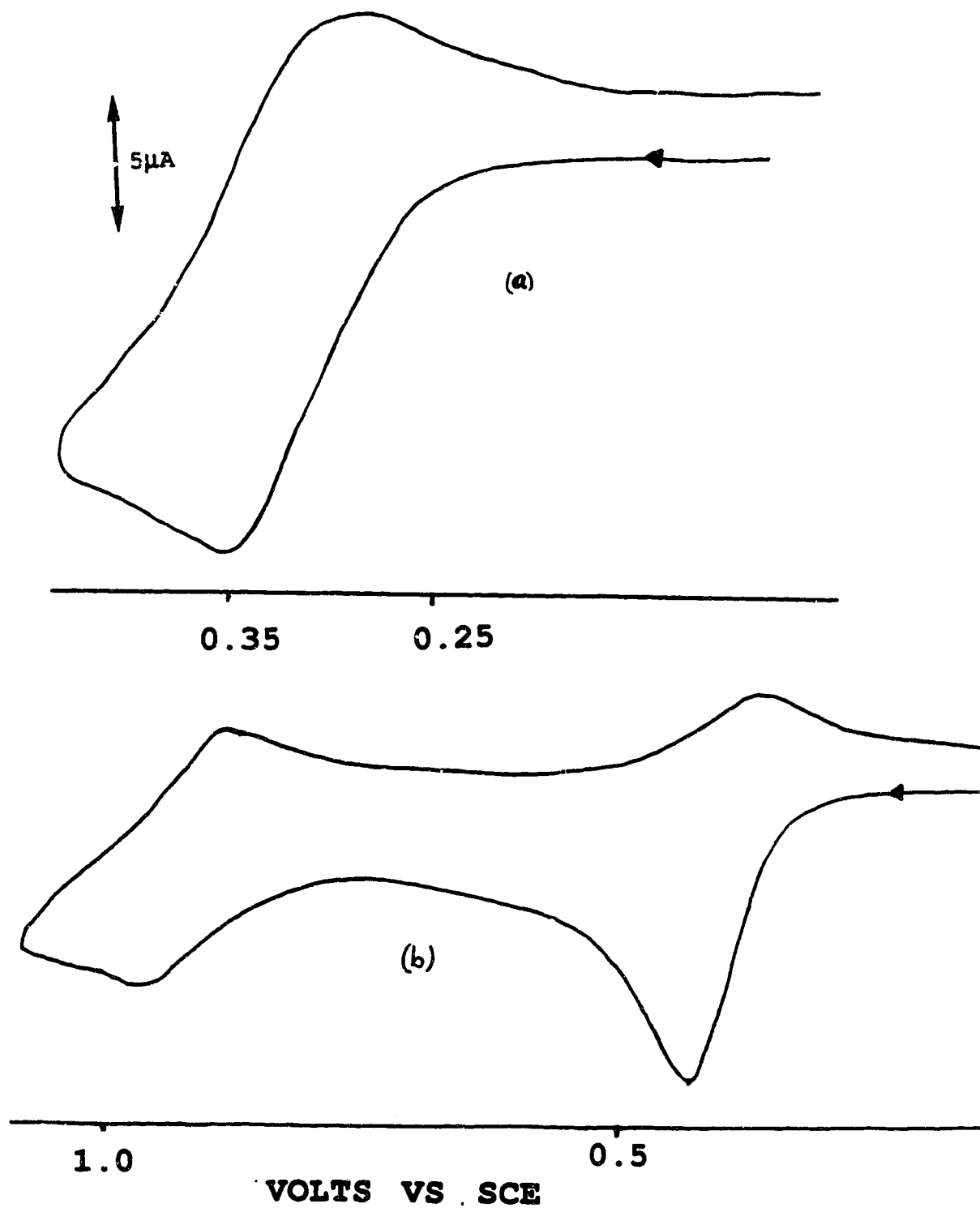
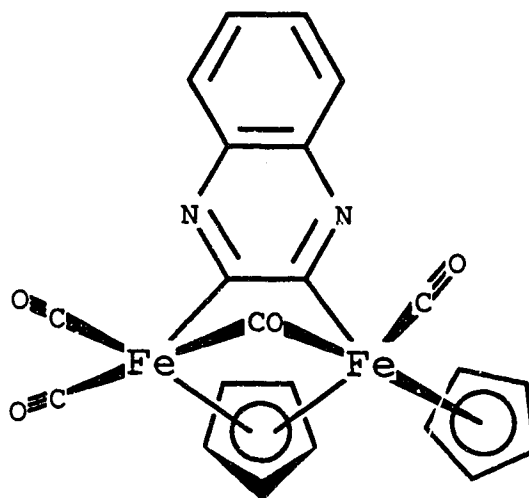


Figure 4.9 Cyclic voltammograms of 2 showing (a) First oxidation wave (b) Scanning to higher potentials.

(c) two Fe centres which are inequivalent and having one unusual C_5H_5 ligand

(d) electrochemical coupling of Fe centres.

To explain these structural features, we propose that compound 2 may have a structure similar to that shown below.



Thus, the bridging carbonyl accounts for the very low field ^{13}C signal and the low energy ν_{CO} band. The bridging cyclopentadienyl group accounts for the unusual cyclopentadienyl 1H and ^{13}C NMR signals. Precedence for such bridging cyclopentadienyl ligands have previously been reported for Pd and Pt complexes.¹⁵ The increase in the shielding observed^{15b} for the Cp protons in the NMR spectra of these complexes is similar to those observed in compound 2.

Finally, the structural difference between the two Fe centres would account for the observed inequivalence of the quinoxaline protons, and the eight quinoxaline carbon atoms. Obviously, the exact structure and bonding of this unusual species remains to be ascertained. Efforts to do this

by synthesizing and hopefully obtaining X-ray structural data on related quinoxaline derivatives are currently under way in our research group.

1. Much of the work reported in this Chapter has previously been presented in a conference i.e. 73rd Canadian Chemical conference, July 1990, Halifax, Nova Scotia *Abstr.* 623IN-F14.
2. Prasad, P.N.; Ulrich, D.R. *Non-linear Electroactive Polymers*, Plenum: York; 1988.
3. (a) *International Tables for X-Ray Crystallography 1969*, vol 1 Kynoch: Birmingham. (b) Walker, N.; Stuart, D. *Acta Crystallogr.* 1983, 158, A39. (c) The computer programs used in this determination include the Enraf-Nonius Structure Determination Package, Version 3, 1985, Delft, The Netherlands. adapted for a SUN microsystems 3/160 computer, and several locally written programs by Dr. R.G. Ball.
4. Joule, J.A. and Smith, G.F. *Heterocyclic Chemistry* 2nd ed. Van Nostrand Reinhold: New York; 1978.
5. (a) Dessy, R.E.; Pohl, R.L.; King, R.B. *J. Am. Chem. Soc.* 1966, 88, 5121.. (b) Henderson, S.; Henderson, R.A.; *Adv. in Phys. Org. Chem.* 1987, 23, 7. (c) Artanskina, G.A.; Mil'chenko, A.Y.; Beletskaya, I.P.; Reutov, D.A. *J. Organomet. Chem.* 1968, 311, 199
6. (a) Haworth, R.D.; Robinson, S. *J. Chem. Soc.* 1948, 777. (b) Weissberger, A. *The Chemistry of Heterocyclic Compounds; Condensed Pyridazine, and Pyrazine Rings*, Interscience: New York; 1953, P178 & P203. (c) Lockhart, D.; Turner, E. E. *J. Chem. Soc.*, 1937, 424.
7. Hunter, A.D.; Szigety A.B. *Organometallics*, 1989, 8, 2670
8. For structures of CpFe(CO)L acyls see (a) Adrianov, V.G.; Sergeeva, G.N.; Streuchkov, Y.T.; Aninov, K.N.; Kolobova, N.E.; Beechastnov, A.S. *Zh. Strukt. Khim.* 1970, 11, 168, (Engl. translation, 163). (b) Lehmkuhi, H.;

- Mehler G.; Benn, R.; Rufinska, A.S; Chroth, G.; Kruger, C.; Raabe, E. *Chem. Ber.* **1987**, 120. (C) Semion, V.A.; Struchkov, Y.T. *Zh. Strukt. Khim.*, **1969**, 10, 85 (Engl. translation, 80)
9. For structures of Fp-R (where R is sp^2 hybridized) see (a) Church, M. R.; Wormald, J. *Inorg. Chem.* **1969**, 8, 1936. (b) Ferede, R.; Noble, M.; Cordes, A.W; Allison, N.T.; Lay, J. *J. organomet. Chem.* **1988**, 399, 1. (c) Bruce, M.I.; Liddell, J.J.; Snow, M.R.; Tiekens, E.R.T. *J. Organomet. Chem.* **1988**, 354, 103. (d) Dahl, L.F.; Doedena, R.J.; Huble, W.; Nielson, J. *J. Am. Chem. Soc.* **1966**, 88, 446. (e) Kolobova, N.E.; Rozaantava, T.V.; Struchkov, Y.T.; Betaanov, A.S.; Bakmutov, V.I. *J. Organomet. Chem.* **1985**, 292, 247.
- 10 See Chapter two of this thesis for more complete discussion of the orientational preferences.
- 11 (a) In Nagle, K.J. *J. Am. Chem. Soc.* **1990**, 112, 4741, the Vander Walls radius of Fe atoms is given as 2.03 Å. (b) The Vander Walls radius of the CpFe(CO)₂ fragment can be estimated as being equal to its covalent radius plus 0.75 (e.g. in Fp-C₆F₅, the value is $\sim 1.25 + 0.75 = 2.00$ Å), see Chapter two of this thesis.
- 12 (a) Hunter, A.D. and MacLernon, J.C. *Organometallics* **1989**, 8, 2679. (b) Richter-Addo G.B.; Hunter, A.D.; Wichrowska, N. *Can. J. Chem.* **1990**, 68, 41. (c) Hunter, A.D. *Organometallics* **1989**, 8, 1118.
- 13 Chukwu, R.; Hunter, A.D. *unpublished observations*.
- 14 Layton, R.H.; Chisolm, M.H. *J. Am. Chem. Soc.* **1989**, 111, 8923.
- 15 See for example (a) Werner, H. *J. Organomet. Chem.* **1980**, 200, 273. (b) Werner, H.; Kraus, H-J. *Chem. Ber.* **1980**, 113, 1072. (c) Werner, H.;

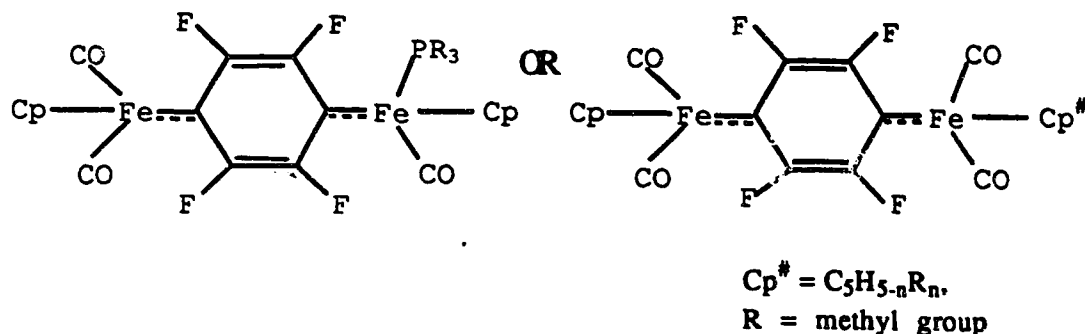
Kraus, H-J. *J. Chem. Soc. Chem. Commun.* 1979 814. (d) Werner, H.;
Kuhn, A.; Tunc, D.J. *Chem. Ber.* 1977, 110, 1763.

CHAPTER 5

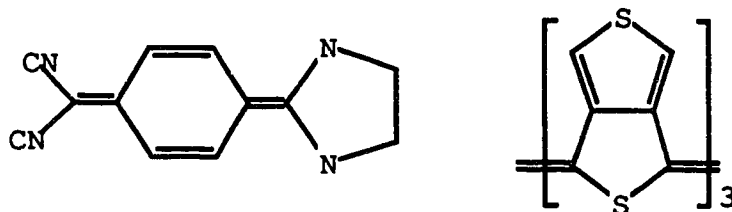
GENERAL DISCUSSION AND PROJECTIONS

Work presented in this thesis further highlights the versatility of the Fp fragment in aromatic substitution reactions. Thus, this fragment is a very appropriate starting material for the preliminary studies on various model compounds for organometallic polymers having the types of linkages of interest, namely: metal to ring carbon s bonds. As results presented in the previous Chapters indicate, variation of the bridging ligands can be readily achieved thus enabling the facile studies of the long-range indirect metal-metal interactions in such model compounds. Moreover, the electron richness (and nucleophilicity) of the Fp fragment can be readily varied by either replacing the CO groups with more electron rich groups such as PR₃ groups or by changing to Cp ligands containing various numbers of methyl substituents.¹

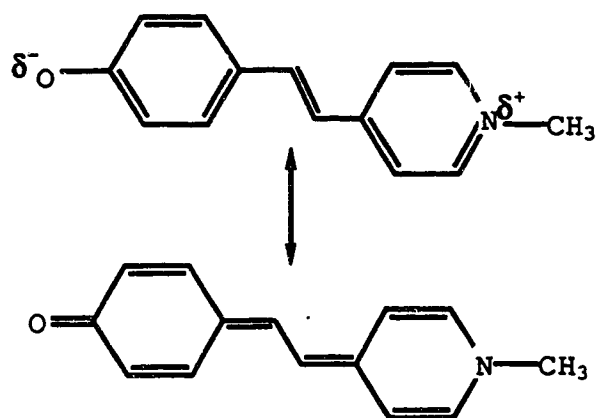
Such readily achievable variations in the electron richness of the ligands and metal centres can lead to an enhancement of the "quinoidal" characteristics of the 1,4-complexes and hence may give rise to large electrical polarizabilities.



The phenomenon of electrical polarizability has been shown to be of fundamental importance in nonlinear optical behaviour of organic materials.^{2,3} Thus, the nonlinear optical behaviour of complexes of the type DCNQ [2-(4-dicyanomethylenecyclohexa-2,5-dienylidene)-imidazolidine] and thieno(3,4)-thiophene trimer have been associated with the quinoidal structures of these compounds.³



The novel complex reported in Chapter 3, in which a silver cation is attached to a pyridine ring nitrogen atom is also of considerable interest, as several organic compounds containing similar linkages are known to exhibit nonlinear optical behaviour. A comparison can be made between this complex and related pyridine chromophores represented by the example shown below.



All the complexes containing heterocyclic ligands could readily be adapted to form complexes related to the above, including novel organometallic polymers containing both metal to arene σ bonds and metal to arene dative bonds (an example of which was recently reported)⁴ but with two different metal centres (e.g. an early/late transition metal mixture). As stated in the introductory Chapter of this thesis, the heteroaromatic complexes could also be of considerable interest in biological chemistry. Hence the observed regioselectivity in the synthesis of these complexes is heartwarming.

Results from the electrochemical studies in conjunction with the spectroscopic and x-ray crystal studies on these complexes confirm the expected inter-relation between energies of the frontier molecular orbitals of the arene/heteroarene ligands, as well as the geometric orientation of the complexes, and the extent of the metal-ligand, and consequently metal-ligand-metal electronic interactions in these types of complexes. Although we observed that the complexes in which two metal centres are oriented in a 1,4- manner showed considerably better metal-metal electronic communication than their 1,3- analogues, other results indicate that the 1,3-

species (which would form more readily processable polymers) may also be reliable conducting polymer models.

The disubstituted complex reported in Chapter 4 appears to exhibit interesting structural features hence determination of its structure by X-ray crystallography is important.

REFERENCES

1. Hunter, A.D.; Szigety, A.B. *Organometallics* 1989, 8, 2670.
2. Prasad, P.N.; Ulrich, D.R. *Nonlinear Optical and Electroactive Polymers*, Plenum: New York; 1988
3. Kuzmany, H.; Mehring, M.; Roth, S. *Electronic Properties of Conjugated Polymers III*, Springer-Verlag: Heidelberg; 1989.
4. Farizzi, F.; Sunley, G.J.; Wheeler, J.A.; Adams, H.; Bailey, N.A.; Montlis, P.M. *Organometallics* 1990, 9, 131.